Materials Advances

ROYAL SOCIETY OF CHEMISTRY

REVIEW

View Article Online
View Journal | View Issue

Cite this: *Mater. Adv.*, 2021, 2, 4966

On the evolution of sulfonated polyphenylenes as proton exchange membranes for fuel cells

Michael Adamski, Nicolas Peressin and Steven Holdcroft *

The recent expansion in proton exchange membrane (PEM) research has been commensurate with the growth of PEM fuel cell research. Perfluorosulfonic acid (PFSA) ionomer materials remain the technological membrane of choice for PEMFCs because of their robustness, versatility of use, and widespread commercial availability. PFSAs, however, are far from ideal: they are prepared from fluorine-based chemicals that are under increasing environmental scrutiny, they are inherently expensive to prepare and dispose of, their ionic conductivity is limited, and they are highly permeable to gases. Numerous classes of ion-containing polymers have been investigated as potential replacements over the past decades, but PFSA remains the incumbent technology because hydrocarbon-based solid polymer electrolyte membranes are perceived to lack the oxidative stability of their fluorine-containing counterparts. A new era of hydrocarbon PEM research has recently emerged with an emphasis on the hydrocarbon membrane's inherent lower gas permeability and unanticipated stability in fuel cell applications. Of the various classes of polymer derivatives that hold promise, sulfonated polyphenylenes, devoid of heteroatom linkages in the main chain, are leading candidates. The absence of heteroatom linkages in the polymer backbone is not without penalty: their synthesis is challenging and processing restricted due to their rigid-rod character, coupled with the requirement to attach acid bearing groups in high concentration. This review focuses exclusively on the evolution of sulfonated polyphenylenes, from intractable rigid rods to architecturally-controlled, sterically-encumbered sulfo-phenylated polyphenylenes, with an emphasis on synthesis, precise molecular control, structure–property relationships, and ultimately, wide-scale adoption in fuel cells.

Received 11th June 2021,
Accepted 12th July 2021

DOI: 10.1039/d1ma00511a

rsc.li/materials-advances

Holdcroft Research Group, Department of Chemistry, Simon Fraser University, Burnaby, British Columbia V5A 1S6, Canada. E-mail: holdcrof@sfu.ca

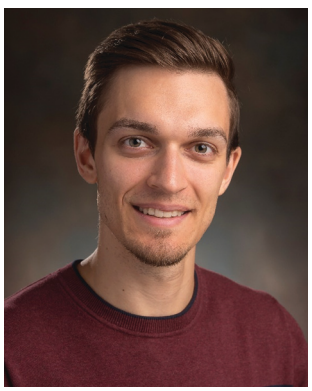

Michael Adamski

Mike is an experienced, award-winning chemist and materials scientist with a broad knowledge in design, development, and application of novel polymer electrolytes for electrochemical energy technologies such as hydrogen fuel cells. He received his PhD in 2019 (Simon Fraser University, BC, Canada). He was awarded the Governor General's Gold Medal for graduate research and the Macromolecular Science & Engineering Division Award of the CIC. Mike continues his efforts with industrial and academic partners to improve and commercialize ground-breaking ion-exchange membrane and polymer solutions for clean energy technologies including fuel cells, hydrogen production, and energy storage applications.

Nicolas Peressin

Nicolas received his BSc from the University of British Columbia (UBC) and his MSc from Simon Fraser University (SFU) in 2020. While at SFU, Nicolas studied structure–property relationships in state-of-the-art polymer electrolyte membrane materials. He has extensive experience in synthetic chemistry and materials science working in multiple areas of academia, industry, and government agency. After obtaining his graduate degree, Nicolas joined Ballard Power Systems Inc. (Canada) as an applied scientist, where he continues to pursue his interest in clean energy technologies.

1 Introduction

Proton exchange membranes (PEMs) have been the focus of appreciable scientific and industrial R&D for several decades, due in-part to their applicability as selective solid-state ion transport media in low temperature (<100 °C) electrochemical energy devices such as hydrogen fuel cells, water electrolyzers, and redox flow batteries.[1–4] In this realm, materials based on perfluorosulfonic acid (PFSA) ionomers such as Nafion, and thinner, reinforced derivatives, are commonplace.[5] Progress has been made in understanding how these materials function,[5–7] which has helped define fundamental principles for low temperature polymer electrolyte membranes, particularly those employed in fuel cells: (i) the material must be electrically insulating to serve as a solid electrode separator within electrochemical cells; (ii) it must be highly conductive to protons to promote their transport; (iii) it must possess a low permeability to gases (*e.g.*, H_2 and O_2); (iv) it must effectively transport water to mitigate simultaneous flooding and dehydration of gas diffusion electrodes; (v) it must be mechanically and chemically stable because its degradation leads to fuel cell failure.[1] These requirements are highlighted in Fig. 1.

Despite comprehensive investigation and ubiquitous application,[5,8] the fundamental structure of PFSAs has remained largely unchanged for over 50 years (Fig. 2),[9–12] and is inherently challenging. There is a growing concern surrounding environmental implications of perfluorinated chemical use.[3,13–15] Disposal of Nafion, for instance, is limited to landfills or incineration in small quantities under highly specialized conditions.[16] There are no manufacture-recommended recycling options.[16] Due to demanding synthetic procedures that rely on controlled substances, preparation of such materials is limited to a few establishments globally. Material costs are consequently high and impinge on the broad commercialization of fuel cells, for example,[17] which is predicted to reach millions of fuel cell (FC) vehicles world wide by 2050. In addition, PFSAs are synonymous with high reactant gas permeabilities, which may lead to fuel cell inefficiencies, promotion of their degradation, and limitations in durability.[3,13]

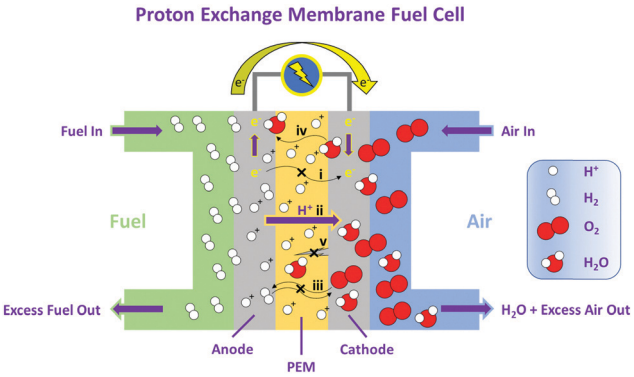

Fig. 1 Schematic of a hydrogen fuel cell. See text for explanation of symbols i–v.

In order to address shortcomings associated with PFSA-based PEMs, significant research has been devoted to alternative hydrocarbon-based, fluorine-free materials.[3,8,11] Numerous classes of polymers and countless derivatives of these polymers have been investigated over the past decades. The height of this activity occurred in the 1990s, with the collective goal of replacing PFSA to extend PEMFC operation to 120 °C. A vast amount of research into structure–property relationships during this time greatly advanced the field and led to many examples of highly-conductive proton exchange membranes.[11,18,19] Particular emphasis was placed on aromatic polymer backbones due to the inherent thermochemical resilience associated with sp^2 linkages (aryl–aryl and aryl–heteroatom) compared to labile sp^3-based linkages (methylene and methenyl) found in early sulfonated polystyrene research.[20,21] Diverse synthetic strategies not limited

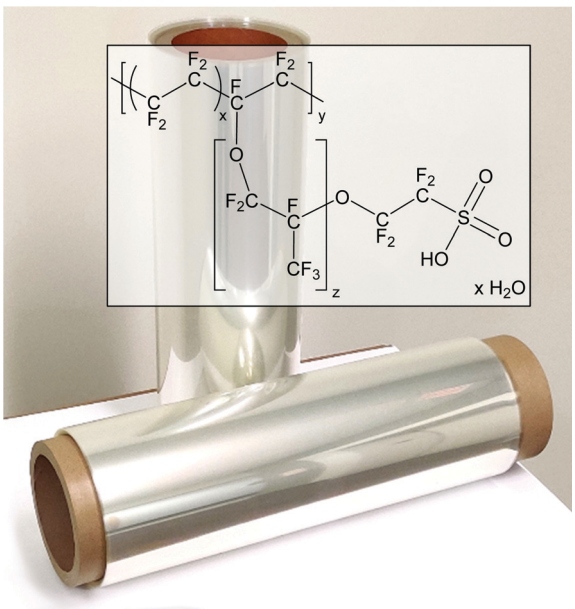

Fig. 2 Representative chemical structure and roll of a Nafion® membrane.

Steven Holdcroft

Dr Steven Holdcroft is a Professor of Chemistry at Simon Fraser University, Canada, and former Chair of the Department. He holds a Tier 1 Canada Research Chair in Electrochemical Materials. He has authored/co-authored more than 300 peer-reviewed articles on ionic polymers, electrochemistry, energy conversion devices, and conjugated polymers. He serves on the Editorial Advisory Board of Chemistry of Materials and Energy and Environmental Science. He is a Fellow of the Chemical Institute of Canada and past President of the Canadian Society for Chemistry.

by perfluorinated reagents led to numerous classes of proton-conducting sulfonated polyarylenes with differing backbone architectures: poly(arylene ether ketone)s,[11,14,22] poly(arylene ether sulfone)s,[11,22–24] poly(benzimidazole)s,[11,14,25] poly(arylene sulfone sulfide)s,[18,26–28] and poly(phenylene)s.[29–32] A persistent criticism of hydrocarbon-based polymer membranes, however, is that they lack the oxidative stability of their PFSA counterparts; research into hydrocarbon-based PEMS eventually dwindled, caused in-part by the emerging interest and available funding for the discovery of anion exchange membranes.

2 Scope of this review

In recent years, renewed interest in fluorine-free alternatives to PFSAs has arisen. This, for two reasons: (i) the growing concern of fluorine-containing precursors and the daunting prospect of generating vast quantities of waste perfluorinated membranes, and (ii) their high permeability to gases – leading to hydrogen and oxygen crossover – which, amongst other reasons, exacerbates the degradation of fuel cells. A new era of PEM research has thus emerged, with emphases on proton-conducting polymers that provide greater stability to long-term use in commercial fuel cells, and on materials that can be synthetically scaled up and integrated into state-of-the-art commercial fuel cell stacks. Of the various classes of polymer derivatives to hold promise, sulfonated polyphenylenes, devoid of heteroatom linkages in the main chain, have emerged as leading candidates.

This review focuses exclusively on the evolution of fluorine-free, sulfonated polyphenylenes with an emphasis on synthesis and structure–property relationships. For overviews on hydrocarbon PEM materials, in general, including ionic polyaromatics containing heteroatoms in the main chain, the reader is directed to any number of excellent reviews on the topic.[14,15,33] For comprehensive summaries on current understanding and states-of-the-art of PFSA-based materials, the reader is directed to recent reviews by A. Kusoglu and A. Weber,[5] and M. Zatoń *et al.*[6] This review does not include the growing field of research focused on anion exchange membranes, for which comprehensive reviews also exist.[34–36]

For clarity and comparison, we categorize the diverse number of sulfonated polyphenylene (SPP) variants into generalized classes: (i) linear, (ii) kinked, (iii) side-chain sulfonated, (iv) post-sulfonated phenylated, and (v) pre-sulfonated phenylated, as shown in Table 1.

Commercialization of sulfonated polyphenylenes (SPP)s has been several decades in the making, starting with the early work of G. Goldfinger on linear poly(*p*-phenylene)s,[74,75] and W. Ried,[76–78] as well as J. K. Stille,[79–81] on phenylated polyphenylenes in the late 1940s to early 1970s, to the first ever reported post-sulfonation of a phenylated polyphenylene in 1972,[82] through to reinforced SPPs produced by Ionomr Innovations, Inc., announced in 2020,[83,84] as illustrated in the timeline shown below (Fig. 3).

This review is structured in the following manner. First, we provide a brief introduction of aspects considered in designing proton exchange membranes for fuel cells. This includes their morphology,[5,23,85–87] proton conductivity,[3] ion exchange capacity (IEC), water uptake, water permeation,[88–90] chemical stability,[12] gas permeability,[91] and mechanical properties.[92–95] Details of these topics are found in the literature and are therefore given only rudimentary attention here. Secondly, we delve into the classes of sPP listed in Table 1, highlighting their synthetic underpinnings and diversity of derivatives within a class. Thirdly, we compare representatives of a given class listed in Table 1 – including positive and negative attributes of their syntheses and selected physical properties. Lastly, we provide an outlook for the future, describing potential future derivatives of sPPs, and a path forward for their large-scale production, adoption, and commercialization.

3 Aspects to consider for proton exchange membranes

Polymer sequence, distribution, and morphology

Molecular structures of acidic polymers designed for proton exchange membranes typically comprise of a hydrophobic polymer backbone with pendant hydrophilic acid groups. The incompatibility of these two distinct moieties, especially when hydrated, drives the system to phase segregate into respective domains at nanoscale.[23,96–98] Both the structure of the polymer backbone and the number and placement of acid groups greatly impacts the morphology of acid-bearing polymers and their membranes.[99] At low relative humidity (RH), the absorption of water into the hydrophilic acid domains leads to the formation of hydrated ion clusters that are dispersed throughout the hydrophobic polymer matrix, akin to inverted micellar domains.[100–102] As additional water is absorbed (upon increasing RH), the micelles swell, extend, and connect. With sufficient hydration, a percolation network of connected hydrophilic channels within the polymer membrane is created,[96] which is responsible for proton transport.[3,23,103,104] Hydrophobic, non-conductive domains play an equally important role by opposing the osmotic pressure that would cause the polymer membrane to unduly swell, or dissolve entirely.

PFSA ionomers have been available for over 50 years, and their morphology has been the subject of continuous research and debate.[105–107] Small and wide-angle X-ray and small angle neutron scattering, and molecular modeling are common techniques used to probe polymer morphology. Scattering measurements involve the detection of a scattered incident beam of known wavelength upon interaction with a material's electronic (X-ray) or nuclear (neutrons) structure.[5] The intensity of the scattered beam is recorded as a function of the scattering wave vector, q, which is related to the scattering angle and the incident wavelength.[5] Scattering techniques are able to investigate structural information ranging from large scale structural features at low q, to inter- and intra-crystalline atomic spacing at high q. The most commonly used scattering information comes from a single, broad ionomer peak at intermediate q values, corresponding to the spacing between hydrophilic water-domains on the order of nanometers.[5] Using scattering techniques, it is possible to evaluate crystallinity,

Table 1 Generalized structures of linear, kinked, branched, and phenylated sulfonated polyphenylenes (PPs)

Category	Generalized structures	Representative references
Linear sulfonated PPs	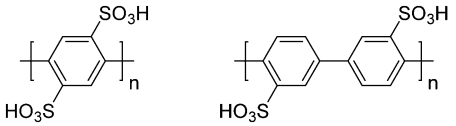	29 and 37–44
Kinked sulfonated PPs	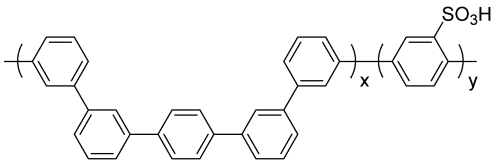	32 and 45–48
Side-chain sulfonated PPs[a]	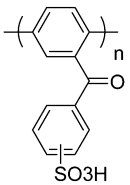	49–63
Post-sulfonated phenylated PPs[b]	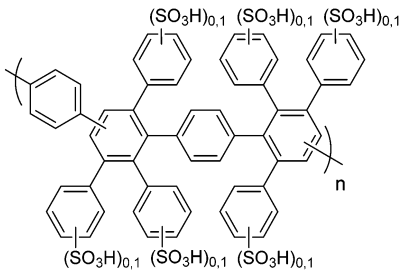	30, 64 and 65
Pre-sulfonated phenylated PPs[b]	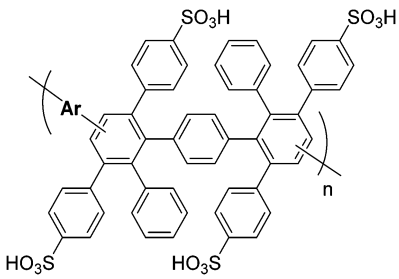	31 and 66–73

[a] Side-chain sulfonated PPs are also commonly referred to as sulfonated poly(benzophenone)s. [b] Also referred to as sulfo-phenylated polyphenylenes.

domain spacing, and water/ionic clustering within polymer matrices. X-ray studies reveal that Nafion® contains larger and more well-connected hydrophilic channels than hydrocarbon-based materials (*e.g.*, sulfonated poly(arylene ether ketone)s),[23,96,108] due to enhanced hydrophilic/hydrophobic phase separation.[108]

Ion exchange capacity and acid strength

The IEC of a polymer membrane notably impacts its ability to generate hydrophilic channels, including the thresholds at which isolated and interconnected water-rich domains form.[96,99] IEC governs membrane water uptake and total water

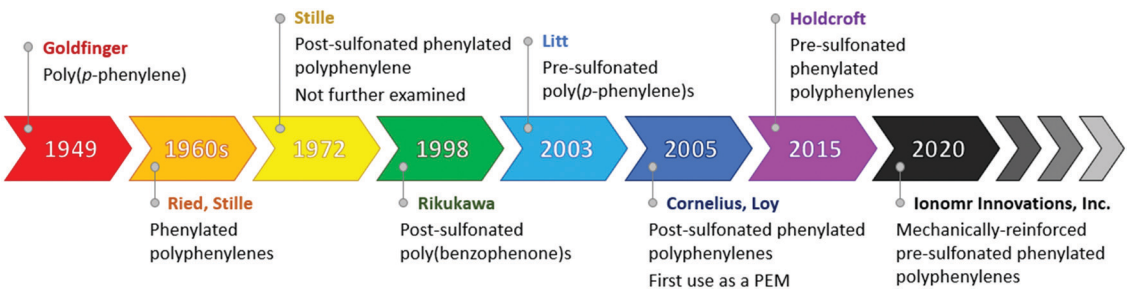

Fig. 3 Timeline for evolution of sulfonated polyphenylenes.[28–30,36,71–79] Corresponding authors from each publication are named.

content. A polymer containing a greater number of acidic functional groups exhibits more pronounced hydrophilicity and absorbs more water upon hydration.[23,99] Water content within membranes influences the tortuosity of formed hydrophilic channels, impacts the overall dissociation of acidic functional groups, as well as the analytical acid concentration in the membrane.[23,99,109] These parameters collectively influence proton conductivity. Consequently, a multi-faceted relationship exists between the structure of the polymer backbone, its degree of functionalization, membrane morphology, and physicochemical and electrochemical properties.[1,23,99]

Similarly, the nature of the acidic functional group plays a role in governing the properties of proton exchange membranes. In this review, only sulfonic acid groups are considered because they represent by far the most common means of acid-functionalization in low temperature (<100 °C) polymer electrolyte membranes. However, a clear difference exists between super acidic sulfonic acid groups found in PFSAs ($pK_a \sim -6$) and aryl sulfonic acid groups found in polyaromatic hydrocarbon-based PEMs ($pK_a \sim -1$).[96,99] For example, in a series of syndiotactic polystyrenes,[110] and poly(arylene ether sulfone)s,[111] functionalized with either arylsulfonic acid or alkyl perfluorosulfonic acid functional groups, the super acidic PFSA groups exhibited increased dissociation of the proton, and enhanced ionic character and better solvation of the sulfonate, compared to arylsulfonic acid groups.[110,111] This in turn provided membranes with higher proton conductivity under reduced relative humidity, despite possessing a lower IEC, and was attributed to the way water is distributed within the PEMs, and how it is affected by membrane morphology as well as strength of the acidic functional groups.[23,112] S. Smedley *et al.*[112] showed that a greater number of water molecules interact with each ionic head group in PFSA-sulfonate functional groups *versus* aryl-sulfonates but that the PFSA-SO_3^-–H_2O hydrogen bond is weaker.

The discrepancy in conductivity between PFSA-based PEMs *versus* polyarylene PEMs is partly due to differences in functional group acidity, which results in differing membrane properties that must be considered when comparing materials from both categories. For example, the IEC of a commonly used PFSA reference material, Nafion 211, is 0.95–1.01 meq. g^{-1}, which affords *ex situ* proton conductivity values up to $\sim$110 mS cm^{-1} at 95% RH and 80 °C,[109] but to achieve similar protonic conductivity, hydrocarbon-based PEMs must typically employ $\geq 2\times$ the acid functionalization (IEC $\sim$2.0 meq. g^{-1}).[11,42,65,66,97,113–115] While this may be lowered by employing block copolymerization strategies to maximize the hydrophilic–hydrophobic phase segregation within a material,[23,116–118] literature reports of highly conductive, fluorine-free PEMs possessing low acid content (IEC $\approx$ 1.0 meq. g^{-1}) are exceptionally rare.

Water content

Water uptake in proton exchange membranes is critical to their function, and is related to the IEC, polymer backbone and microstructure, and dependant on the phase-separated morphology. Aspects of water content are often quantified as water uptake and water content (wt%), volumetric expansion (vol%), and hydration number λ (mol H_2O/mol SO_3^-).[119] These parameters are inter-related. Water uptake generally increases with IEC, with increasing hydrophilicity of the hydrophobic domain, and with reduced chain entanglement or reduced interconnection of hydrophobic domains. The latter may be a consequence of limited aggregation of the hydrophobic domains and/or low molecular weight of the polymer.[120]

PEMs swell more in liquid water than in saturated water vapor at identical temperatures. In the unique case of liquid water and saturated water vapor where the activity of water is 1, Nafion membranes, for example, absorb more water when immersed in the former,[121] a phenomenon known as "Schröeder's paradox".[122] The origin of this is due to differences in surface morphology of the membrane in contact with liquid water *versus* water vapor.[122] Water vapor sorption is a complex multistep process involving the interaction of hydrophilic acid groups, and the response of the hydrophobic domains to osmotic pressure. Absorption from the vapour is non-linear and sigmoidal with increasing water activity. Water vapor sorption data is more representative of fuel cell operating conditions and can be examined using the Park model,[123–125] which comprises three types of sorption: Langmuir-, Henry-, and clustering-type sorption, which contribute to low, mid, and high water activity regimes, respectively (see Fig. 4).

Proton conductivity

Proton conduction within hydrated PEMs occurs *via* combination of three mechanisms. The vehicular mechanism represents proton transport by movement of larger molecular "vehicles" through hydrophilic channels, in the form of hydrated protons (*e.g.*, $H_5O_2^+$, $H_7O_3^+$, *etc.*).[3,23,103,104] The Grotthus mechanism represents proton transport *via* structural diffusion through the bulk aqueous phase, wherein protons are "passed" *via* continuous formation and breaking of hydrogen bonds with surrounding water molecules and clusters.[3,23,103,104] A surface transport mechanism involves transport of protons between anionic $-SO_3^-$ head groups located along the walls of the hydrophilic channels.[3,23,103,104] It is generally believed that the Grotthus and vehicular mechanisms are more facile and yield appreciable ionic

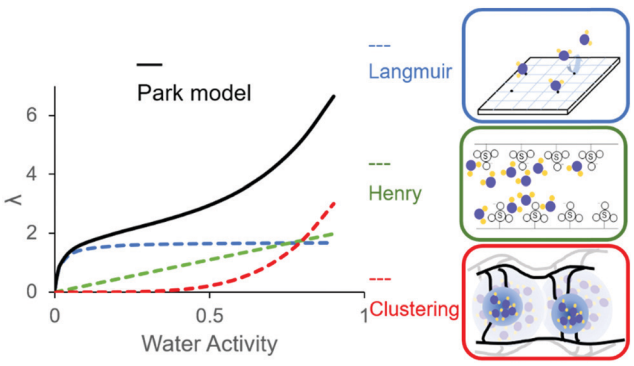

Fig. 4 Park model for water absorption with increasing water activity. Reprinted from *J. Membr. Sci.*, 610, Y. Wu *et al.*, "Water transport through hydrocarbon-based proton exchange membranes", #118276, Copyright (2020), with permission from Elsevier.[125]

conduction compared to the surface mechanism, but are more dependent on hydration, becoming insignificant under reduced relative humidity.[3,23,103,104]

Both the activity (a_{H^+}) and mobility (μ_{H^+}) of a proton impact its overall conductivity (σ_{H^+}), as per the Nernst–Einstein relationship, eqn (1), where F is the Faraday constant.[23,97] In the context of PEMs, this relationship is modified because conditions found within membranes are not adequately represented by a traditional view of free ions in solution. Instead of proton activity (a_{H^+}), the value for a membrane's analytical acid concentration, [SO_3H], is commonly used.[23,97] This parameter is typically calculated from experimentally-obtained values of a given membrane's acid content, or ion exchange capacity (IEC), and water content, and assumes complete dissociation of sulfonic acids. It more suitably accounts for the numerous differences which may exist between distinct materials, such as the degree of dissociation of the acid functional groups (*e.g.*, aryl *versus* perfluorinated sulfonic acid groups), and number of water molecules per acidic functional group (λ).[23,97] Likewise, instead of proton mobility (μ_{H^+}), an effective proton mobility (μ'_{H^+}) is determined from experimentally-obtained parameters.[23,97] It accounts for the various factors which impact ionic mobility within a membrane, such as the distribution and uniformity of ionic functional groups, as well as the overall tortuosity of proton conducting hydrophilic channels.[23,97] With these considerations in mind, proton conductivity of a PEM may be described using eqn (2).[23,97]

$$\sigma_{H^+} = F(a_{H^+})(\mu_{H^+}) \quad (1)$$

$$\sigma_{H^+} = F([SO_3H])(\mu'_{H^+}) \quad (2)$$

Molecular modeling, including molecular dynamics simulations, coarse-grained modeling, and density functional theory, are used for describing the complex morphology and proton transport within polymeric systems. For instance, simulations of a PEM in changing hydration conditions may provide researchers with information regarding sulfonic acid dissociation behavior, the threshold at which a percolated hydrophilic network is formed, as well as its tortuosity, and hence valuable insights to proton conductivity.[65,126] A large body of molecular modelling work on PFSA ionomers exist in the literature; for further information we direct the reader to a recent review on this topic.[5] These techniques have also been applied to sulfonated, sterically-encumbered polyaromatics (*e.g.*, polyphenylenes,[32,65,72,126,127] polyimides,[128] and polybenzimidazoliums),[129] and to assess chemical stability of hydrocarbon-based systems.[130]

Water transport

Water transport is intimately linked to a membrane's water content and in the context of fuel cells, to the operating conditions and current density of a particular fuel cell system because of electro-osmotic drag (EOD),[119] which is the transport of water associated with the transport of protons from anode to cathode. The number of water molecules carried per proton is defined by the electro-osmotic drag coefficient, N_d. In most cases, N_d increases with hydration state of the membrane. EOD is offset by the generation and build-up of water at the cathode as a result of the oxygen reduction reaction. Water transport through a membrane therefore involves a complex interplay of processes, as illustrated in Fig. 5, including the rate of water transport from the anode to the cathode by electro-osmotic drag (J_{EOD}), and the rate of water permeation (J_{WP}) from cathode anode due to the oxygen reduction reaction. Both J_{EOD} and J_{WP} vary with current density, and both increase with increasing water content of the PEM. Poor water management or an inability for the PEM to transport water can lead to dehydration of the anode or flooding of the cathode, both of which have deleterious consequences on fuel cell performance.

Numerical modelling studies are often undertaken to understand water transport processes involved in *ex situ* and *in situ* water transport measurement outputs. These involve a wide range measurements at different time- and length-scales and include:[5] steady-state permeation under a controlled chemical potential gradient as driving force;[131] transient water diffusion determined by dynamic vapor sorption (DVS);[132] self-diffusion using pulsed-field gradient spin-echo nuclear magnetic resonance spectroscopy,[133,134] or quasi-elastic neutron scattering (QENS);[135] and indirect measurements such as time-resolved SAXS/SANS,[89,90] or FTIR-ATR.[135,136] Steady-state water permeation, which measures the molar water flux though the membrane under a specific chemical potential difference of water, is achieved by controlling the water concentration on both sides of the membrane. Steady-state water permeation is a crucial facet of a PEM pertaining to its ability to regain an even distribution of water when subject to a water concentration gradient, such as when in a fuel cell.[125,137,138] Moreover, steady state permeation allows differentiation of liquid–vapor permeation (LVP), where one side of the membrane is in contact with liquid water while the other side is facing water vapor under regulated relative humidity, from liquid–liquid permeation (LLP), where both sides of the membrane are exposed to liquid water, and an external hydraulic pressure is applied to one side as the driving force.

Chemical stability

Chemical degradation of PEMs in fuel cells has been a central issue ever since their inception. Degradation is caused by *in situ* generation of free radicals which chemically attack weak linkages in the polymer chain. Hydroxyl ($HO^\bullet$), hydroperoxyl ($HOO^\bullet$), and hydrogen ($H^\bullet$) radicals have been detected, but it is the first two of these that are generally regarded as the most prominent reactive species involved in the degradation process.[139] There is no consensus on the mechanisms of formation of these radicals, but the decomposition of H_2O_2 within fuel cells is assumed to play a role,[140] and membrane thickness influences the rate of H_2O_2 formation,[141] from which it is inferred that gas crossover (H_2 and O_2) leads to the formation of H_2O_2. Hydrogen peroxide may also be formed electrochemically through the two electron oxygen reduction reaction,[142] or *via* reaction of H_2 and O_2 on a Pt catalyst.[143]

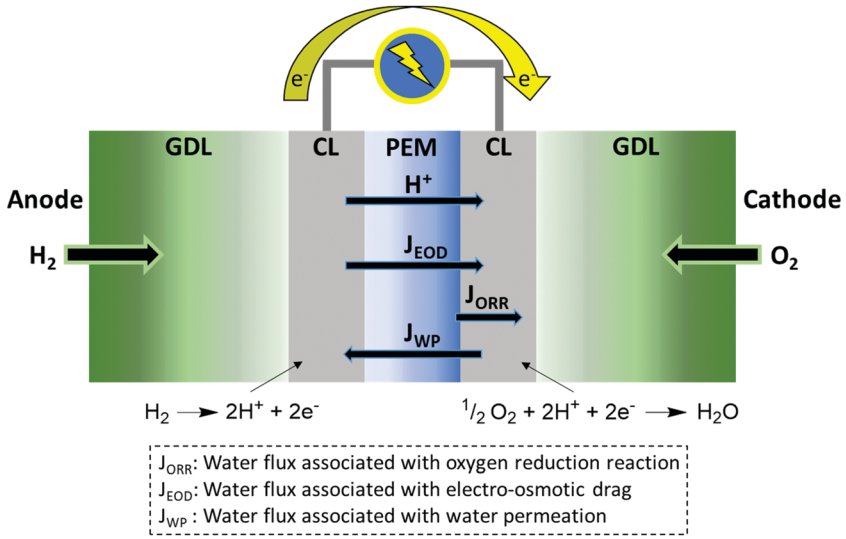

Fig. 5 Water transport within a proton exchange membrane fuel cell.

The degradation of perfluorinated PEMs in fuel cells occurs over the course of thousands of hours of operation, rendering study of degradation impractical under standard operating conditions. Thus, *in situ* accelerated stress tests (AST) have been devised in order to accelerate PEM degradation and progress the understanding of key durability issues within fuel cells,[144] while Fenton's reagent tests are typically used as an *ex situ* degradation method to provide insight into the degradation pathways and chemical labilities of PEMs.[145] Fenton's reagent tests are also used as quick and inexpensive screening tests for novel PEMs; the radicals generated are in high concentration, and hence degradation processes are easily detectable within practical experimental durations (*e.g.*, hours to days), but questions remain concerning the applicability of Fenton's reagent tests to the understanding of membrane degradation in operating fuel cells.[68,139,146,147]

Gas permeability/impermeability

The ability of a PEM to impede the crossing of hydrogen fuel from anode to cathode and oxygen from cathode to anode is a critical characteristic, because excessive gas crossover leads not only to severe safety issues but also lower cell efficiencies and increases the rates of degradation of the membrane electrode assemblies by allowing the formation of reactive free radicals. Two properties that determine gas permeability are the solubility of the gas in the membrane, and its rate of diffusion in the membrane. The former is governed by Henry's law; the latter, by Fick's law. Common methods for measuring gas permeability through membranes involve either a time-lag after applying a pressure gradient on one side of a membrane,[148] or in the case of oxygen, an electroanalytical method using an electrode placed in contact with the membrane.[149–152] Electrochemical measurements are more suited for determining oxygen mass transport parameters at the catalyst-ionomer interface and for ultra-thin membranes; pressure-gradient methods are better suited for gas crossover through membranes. No matter the method, gas permeability increases with increasing relative humidity because increased water content of the membrane allows for higher rates of gas diffusion.[153,154] Perfluorinated ionomers are known to dissolve relatively high concentrations of non-polar gases such as hydrogen and oxygen. This, coupled with a high rate of gas diffusion within the membranes by virtue of their extensive network of hydrophilic channels, renders PFSAs highly permeable to gases. Fluorine-free membranes, on the other hand, generally dissolve lower concentrations of gas, which can translate up to ten times lower gas permeation.

Durability

Operation targets for PEM FCs are 5000 h for light duty vehicles, 25 000 h for heavy duty vehicles, and 40 000 h for stationary applications.[155] During operation, fuel cells experience a wide variety of operating conditions involving wide swings in current density and internal water gradients which impart mechanical stresses on the PEM. As the IEC of a membrane increases, swelling at elevated hydration and embrittlement during dehydration becomes more prominent. Continuous cycles of swelling/de-swelling impose significant internal mechanical stress on the membrane which will ultimately lead to cracks, pinholes, or tears. Membrane degradation generally fall into categories: mechanical, thermal, and chemical/electro-chemical.[156] Mechanical degradation include cracks and pinholes, and delamination,[91,157,158] which typically results from swelling/deswelling and large pressure differentials. Thermal degradation typically involves decomposition of the membrane itself. Chemical/electrochemical degradation is typically associated with internal formation of free radicals that break down the polymer and leads to thinning and loss of material,[159] a process that is linked in a complex manner to the membrane's water content, water transport, gas permeability, and inherent chemical stability.

Durability is intimately interrelated to mechanical properties of the membrane, which are generally compromised as

membranes are made thinner and thinner in order to lower their resistance to proton transport and water transport. Moreover, rates of gas transport increase with reducing membrane thickness, which amplifies chemical and electrochemical degradation. Membranes can be made stronger by reinforcement, and membranes for commercial long-term use must realistically be reinforced to be considered candidates. The topic of mechanical properties is broad and exhaustive and is not covered in this review. For more information the readers is directed to one of a number of reports.[92,94,95,160–162]

Synthetic aspects

The design process for hydrocarbon-based materials is inherently more diverse and flexible than in the case of perfluorinated counterparts. The syntheses of PFSAs such as Nafion® employ restricted and toxic per- and polyfluoroalkyl substances (PFAS), and are typically synthetically complex and potentially hazardous.[163,164] By contrast, hydrocarbon-based materials such as sulfonated polyphenylenes may be prepared from simple organic starting reagents using a variety of easily accessible and well-established organic chemistry transformations, such as transition metal-catalyzed cross-coupling reactions, (poly)condensation reactions, and Diels–Alder reactions. This opens the possibility for numerous divergent synthetic strategies, and has resulted in preparation of innumerable hydrocarbon-based polymer electrolyte variants.[11,14,18,23,165,166]

While there is a considerable diversity in synthetic strategies available to researchers developing hydrocarbon-based PEMs, materials should be designed with emphases placed not just on performance and novelty of structures, but also on repeatability and scalability. A synthesis with good repeatability will reliably output a PEM with predictable properties, which is important for batch-to-batch consistency in its performance metrics. The nature and feasibility of synthetic procedures changes dramatically when reaction scale is increased from laboratory and research scale (*e.g.*, 0.5–25 g) to proof-of-concept (*e.g.*, 50–500 g) and pilot production scale (*e.g.*, 1–10 kg) batches. Powerful and effective purification strategies such as sublimation and column chromatography become increasingly difficult. Reagent, solvent, and transition metal catalyst costs do not change linearly, which limits the directions that the synthesis of a prospective material can proceed. For instance, the fundamental material input costs of precious metal catalysts such as palladium are not affected by economies of scale, which drives up the overall cost of popular synthetic procedures such as Suzuki and Sonogashira cross-coupling reactions. In addition, the environmental impacts and local regulation statuses of solvents and reagents being used must be considered (*e.g.*, the European Union's Registration, Evaluation, Authorisation and Restriction of Chemicals (REACH) program). A material with adequate performance metrics designed with a scalable and green synthesis would hence be of greater long-term value than one with higher performance but with a challenging synthetic protocol.

In Fig. 6, we illustratively summarize the important aspects to consider in designing proton exchange membranes for fuel cells. A word of caution: many, if not all parameters, are inter-related and

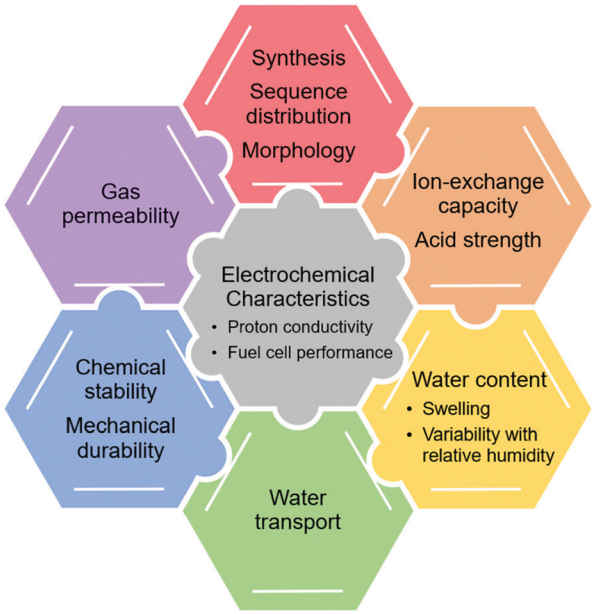

Fig. 6 Attributes for consideration in the design of membranes for proton exchange fuel cells.

inter-dependent. Each parameter needs careful consideration in the context of other parameters. For example, increasing the IEC of a polymer membrane will very likely increase its water content, which in turn may increase its water transport and may or may not increase its proton conductivity, depending on whether lambda and analytical acid concentration increase or decrease. Increasing water content may also increase gas permeability and thus negatively impact chemical stability and/or mechanical durability due to excessive cycles of swelling and deswelling. Increasing a parametric value of one of the parameters will have disparate effects on the polymer membrane's characteristics. Each membrane system requires careful analysis and consideration. In the next section, we attempt to extract similarities and dissimilarities of different sulfonated polyphenylenes, to the extent that is reasonably possible given the diversity of structures, methods, and the research groups reporting them.

4 Sulfonated polyphenylenes

Of all the classes of sulfonated polyarylenes reported to date, the greatest momentum in recent years has been observed in various derivatives of sulfonated polyphenylenes. While this class of materials is more synthetically challenging compared to sulfonated derivatives of poly(arylene ether)s, poly(ether ether ketone)s, and related polymer backbones, they are thermochemical more stable because the backbone comprises of only aryl–aryl bonds. For instance, the bond dissociation energy of a phenyl–phenyl bond, such as that of biphenyl (C_6H_5–C_6H_5 = 479 ± 6 kJ mol^{-1}) is ~35% larger than that of an aryl ether analogue such as diphenyl ether (C_6H_5O–C_6H_5 = 355 ± 6 mol^{-1}).[167] More importantly, the electron-donating effect of the ether-oxygen creates labile electron-rich points on neighboring aryl rings, which

are more susceptible to attack by oxidative species such as HO$^{\bullet}$ radicals.[11,68,168] Oxidative radicals are prevalent in many H_2/O_2 devices and are a primary driving force for *in situ* chemical degradation of a polymer electrolyte membrane. Polymers that are devoid of structural motifs open to such attacks are advantageous for long-term membrane stability.[11,68,168]

Linear poly(*p*-phenylenes)

There are numerous approaches to the preparation of oligo and poly(phenylene)s. Transition metal-catalyzed cross-coupling reactions, for instance, are an excellent means of forming aryl–aryl bonds.[169] This method of polymerization allows precise control over the regiochemistry of the resulting polymer backbone. For example, coupling of *para*-functionalized aromatic monomers results in a strictly *para*-functionalized polymer backbone, or a poly(*para*-phenylene). However, polyphenylenes comprised entirely of *para* linkages are notoriously insoluble in common organic solvents due in-part to their rigid-rod nature.[170–172] The greatest challenge to their direct preparation using transition metal-catalyzed techniques is that they precipitate at low molecular weights, terminating polymerization.[170–173] Strategies such as functionalization of phenylene monomers, and hence polymer backbone, with solubility-enhancing groups have been adopted. For example, J. K. Kallitsis *et al.* prepared poly(*p*-phenylene)s *via* Suzuki cross-coupling of monomers substituted with hexyl chains,[173] yielding soluble polymers with up to 18 phenylene repeat units. A different approach involving a Ni- and Zn-mediated homocoupling of 2′,3′-disubstituted poly(*p*-terphenylene)dichlorides to yield partially phenylated poly(*p*-phenylene)s is also reported,[174] wherein bulkiness of the 2′ and 3′ aryl substituents was attributed to improved polymer solubility. Polymers with degrees of polymerization (DP_n) up to 80 are reported, equivalent to 240 benzene rings.[174]

However, pristine poly(*p*-phenylene)s remain a synthetic challenge.[169] In fact, only recently was a feasible approach to their preparation reported,[172] which involved polymerization of a non-aromatic precursor to initially yield a soluble, non-aromatic polymer from which was thermally generated pristine poly(*p*-phenylene), in a solvent-free environment.[172] Post-functionalization of poly(*p*-phenylene) to its sulfonated analogue has not been reported, likely due to the aforementioned challenges.[175,176]

Sulfonated poly(*p*-phenylene)s have been prepared by M. Litt and coworkers.[29,40,42,43] A pre-functionalization approach was utilized, in which biphenyl monomers containing sulfonic acid-ammonium salts were first synthesized, after which polymerization of the biphenyls was achieved using the copper-catalyzed Ullman reaction. Following ion exchange, the resulting main-chain functionalized acid-bearing poly(*p*-phenylene)s were obtained, as shown in Scheme 1. Both the pre-functionalized hydrophilic monomer and resulting polymers showed improved solubility compared to pristine poly(*p*-phenylene).[29] While this work established sulfonated polyphenylenes as a viable polymeric architecture for PEMs, challenges remained concerning the integrity and mechanical strength of their membranes, which are attributed to the rigid rod-like nature of the poly(*p*-phenylene) backbone.[29,40,42,43]

M. Litt *et al.*[38,39,44] would use their synthetic approach to report on various other poly(*para*-phenylene)s as proton exchange membranes for PEMFCs. The sulfonated polymers **PPDSA**, **PBPDSA**, and **BXPY** (see Fig. 7) were prepared through copper-mediated Ullman coupling reactions between pre-functionalized acid-bearing monomers. Pre-functionalization of monomer units was beneficial because it increased the solubility of the growing polymer chains in polar solvents. However, the reported polymers were soluble in water, so for most practical applications, further research was necessary. An additional series of copolymers based on **PPDSA** and **PBPDSA** were reported, which incorporated cross-linkable aryl groups (*e.g.*, biphenyl) grafted to some (5 to 55%) of the sulfonic acid moieties on the polymer main chain. Thermal cross-linking of these groups yielded insoluble membranes with proton conductivities approaching 200 mS cm^{-1}. However, no information on membrane mechanical properties, water sorption, chemical stability, or *in situ* evaluation was reported.[29,39]

In addition to generating water insoluble PEMs, the research group also looked to use grafts to manage water content, and hence proton conductivity. The authors hypothesized that rigid-rod polymers, such as poly(*para*-phenylene)s, would possess a certain level of intrinsic porosity within membranes, termed "frozen-in" free volume, due to lack of conformational mobility of the rigid chains *versus* more flexible structures such as poly(arylene ether)s,[40] as shown in Fig. 8. It was postulated that incorporating bulky grafts would further increase frozen-in free volume by preventing chains from efficiently packing, which would allow the membranes to retain more water at low environmental humidity (Fig. 8c).[43,44] Many grafting moieties including biphenyl, 2,6-di-*t*-butylphenyl, *t*-butylbenzene, neopentyl benzene, *n*-octylbenzene, and *n*-dodecylbenzene were utilized,

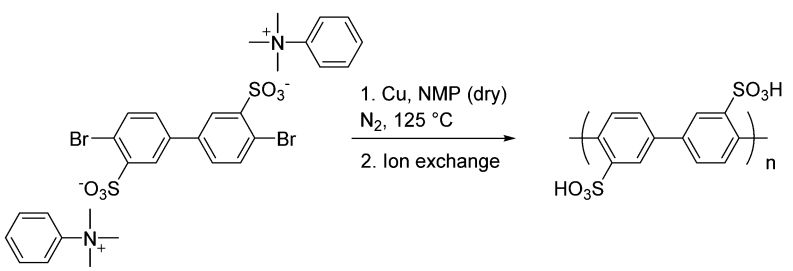

Scheme 1 A representative polymerization of sulfonated poly(*p*-phenylene)s, as reported by M. Litt and coworkers.[29,40,42,43]

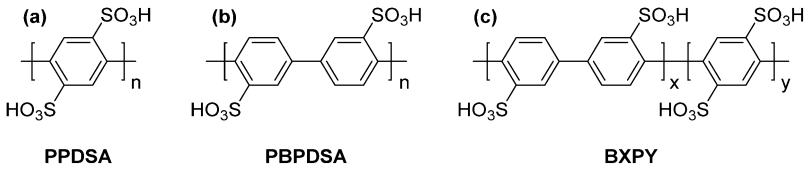

Fig. 7 Chemical structures of the precursor rigid-rod proton conducting membrane polymers: (a) poly(*p*-phenylene 2,5-disulfonic acid) (PPDSA), (b) poly(*p*-biphenylene 3,3′-disulfonic acid) (PBPDSA), and (c) poly[(*p*-biphenylene 3,3′-disulfonic acid)-*co*-(*p*-phenylene 2,5-disulfonic acid)] (BXPY).[44]

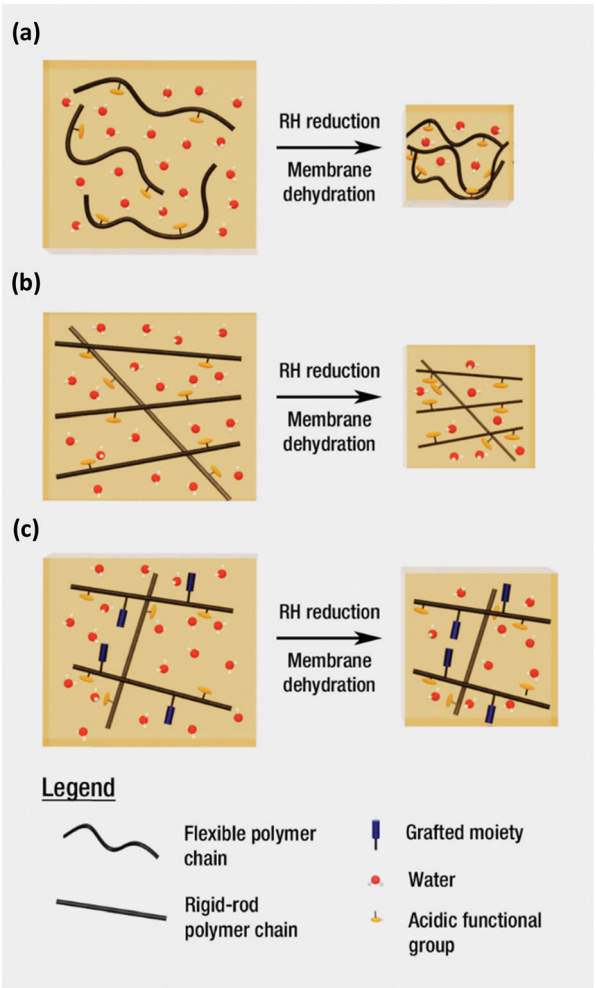

Fig. 8 Schematic representation of the "frozen-in" free volume concept in polymer electrolyte membranes during dehydration, as described by M. Litt and coworkers.[43,44] (a) A polymer containing a flexible backbone, (b) a rigid-rod polymer with restricted reorganization, which retains more hydration within its structure at low relative humidity, and (c) a rigid-rod copolymer with further restricted reorganization and enhanced hydration within its structure, due to bulky grafted moieties.[43,44]

although biphenyl was the sole cross-linking moiety employed. Several grafted and cross-linked poly(*para*-phenylene)s exhibited proton conductivities greatly surpassing Nafion® under both high and low humidity.[41–44] For example, *n*-octylbenzene grafted,[42] and biphenyl cross-linked poly(*para*-phenylene)s,[43] possessed proton conductivities up to 10× greater than Nafion® (*e.g.*, ~100 mS cm^{-1} at 30% RH and ~900 mS cm^{-1} at 95% RH, 80 °C).[44] The high proton conductivity under low relative humidity was attributed to the high frozen-in free volume within the PEMs.[41–44] Unfortunately, poor mechanical properties limited their practical application.[29,42,43] The poor mechanical properties may have been due to the rigid-rod character of the polymer backbone, or the nature of the Ullman reaction, whereby even with pre-functionalized monomers, polymerization is terminated at low molecular weights as polymers precipitate out of the reaction medium.[40,42] For an in-depth overview of sulfonated poly(*p*-phenylene)s, including grafted analogues possessing hydrophobic or cross-linkable moieties, and their characteristic morphologies, the reader is directed to a recent review on the topic.[44]

M. Rikukawa *et al.*[177] reported on a series of side-chain sulfonated poly(*p*-phenylene) diblock copolymers which possessed hexyloxy and (4-sulfophenyl)butoxy side chains **SP1-P2(*m*–*n*)** prepared *via* successive catalyst-transfer polymerization, as shown in Fig. 9. The ratio of hydrophilic to hydrophobic blocks, *m* : *n*, were 28 : 262, 44 : 178, 34 : 141, 44 : 141, 62 : 141, and 74 : 164, with ion exchange capacities ranging between 0.96–2.42 meq. g^{-1}.[177] Microphase separation, probed by atomic force microscopy (AFM), was found to depend on the hydrophobic and hydrophilic block length, as well as their unit ratios. The high IEC block copolymers possessed proton conductivity values comparable to Nafion®, higher than a random copolymer reference based on the same monomers, **SP1-*r*-P2**, and displayed lower water uptake values compared to a similar polyphenylene homopolymer poly(*p*-phenoxybenzoyl-1,4-phenylene) (IEC = 2.86 meq. g^{-1}). Accordingly, block copolymerization may be viewed as an effective means of controlling polymer morphology and enhancing microphase separation in polyphenylene-based ionomers.

Kinked, sulfonated polyphenylenes

More recently, in 2017, K. Miyatake *et al.*[32] reported on a series of sulfonated polyphenylenes containing a mixture of *meta* and

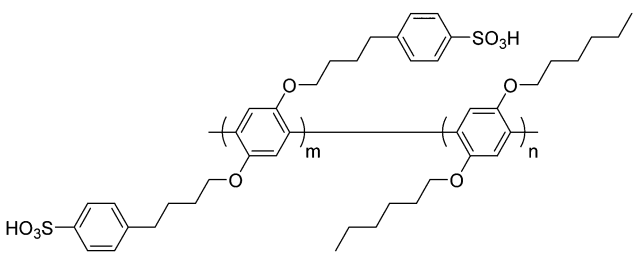

SP1-P2(*m*-*n*)

Fig. 9 Diblock copolymer **SP1-P2**.[177]

para-linkages throughout the polymer backbone. The sulfonated polymer **SPP-QP** (see Fig. 10) was prepared using a Ni-mediated cross-coupling reaction between monomer units **QP** and **SP**. In this report, the authors acknowledged limitations with poly(*para*-phenylene) ionomers, including low solvent solubility, poor-membrane forming capability, and low membrane flexibility.[32] It was proposed that incorporation of *meta*-phenylene groups would lead to small persistence lengths of the polymer chain, which would allow the polyphenylene backbone to behave as a flexible coil, promoting molecular entanglement and the formation of tough, flexible membranes.[32] Analysis of mechanical properties of **SPP-QP** membranes revealed an elongation at break of 68%, a value unparalleled among polyphenylene-based PEMs, that resulted in high *in situ* wet-dry cycle durability.[32] Moreover, **SPP-QP** is reported to possess oxidative stability, with nearly perfect retention of properties (~100%) including remaining weight, molecular weight, IEC, and membrane flexibility following 2 hours of treatment with Fenton's reagent (3% H_2O_2 and 2 ppm Fe^{2+}).[32] In contrast, a reference membrane containing ether, sulfone, and ketone linkages retained 7, 5, and 0% of its original weight, molecular weight, and IEC, respectively, following the same treatment.[32]

A follow up report by R. Shimizu *et al.*[178] in 2019 detailed an *in situ* accelerated stress durability assessment of the sulfonated polyphenylene **SPP-QP**.[178] The report presented similar oxidative stability, and **SPP-QP** outlived comparable heteroatomic linkage containing polyaromatics, and a Nafion® reference membrane. However, mechanical measurements suggested the **SPP-QP** membranes were brittle,[178] conflicting with the prior 2017 report.[32] To combat membrane brittleness, the authors modified MEA and fuel cell components such as gaskets and GDLs with softer variants to reduce physical stresses exerted upon the membrane during assembly and operation, which led to improved durability.[178] The effects of modifying **SPP-QP** with alkanediols with various chain lengths (C*n*: n = 4, 8, and 12) was also explored.[46] The results indicated only a minor change in properties (such as ionic domain size, water uptake, and proton conductivity) although elongation at break increased in the order of n = 12 (24%) < 8 (84%) < 4 (99%), providing possible avenues towards further improving on the flexibility of polyphenylenes.[46] In addition, J. Miyake *et al.* also applied **SPP-QP** as the polymer electrolyte membrane in state-of-the-art rechargeable PEMFCs comprised of a solid-state organic hydride hydrogen storage polymer.[179] When compared to reference cells containing Nafion 212 as the PEM, the **SPP-QP**-based cells exhibited ≥ 2× stable operation time, and were cyclable to at least 50 cycles.[179]

The **QP** monomer, which is used in synthesis of **SPP-QP** (see Fig. 10),[32] requires a two-step Suzuki–Miyaura coupling. In contrast, a next-generation sulfonated polyphenylene random copolymer **SPP-BP** containing a mixture of *meta*- and *para*-phenylene groups was prepared without the **QP** monomer, and hence without need for a multistep monomer synthesis.[45] Instead, a mixture of dichlorobenzenesulfonic acid as the sulfonated monomer, and two, differently substituted dichlorobiphenyls (*para–para* and *meta–meta*), was utilized.[45] This strategy reduced material cost by approx. 23% and simplified the overall polymer synthesis. In addition, a similar, but more tunable polymer backbone was achieved, wherein it was possible to modulate polymer properties by controlling the monomer feed ratio.[45]

In this work, the ratio of the *meta*-phenylene, *para*-phenylene, and sulfonated monomers, **BP*mm***, **BP*pp***, and **SP**, respectively, were varied to alter the IEC and overall *meta*-phenylene content of the resulting **SPP-BP** polymer.[45] As the *meta*-phenylene content was increased from 0 to 100%, the solubility in polar aprotic solvents, and molecular weights (up to M_w = 138 000 g mol^{-1}) of the polymers generally increased, compared to the strictly *para* sulfonated polyphenylene **SPP-BP-a**.[45] The composition, ion exchange capacity, molecular weight, yield, solubility, and membrane forming capability of this series of polymers is overviewed in Table 2. The polymers were prepared in high yield ranging from 85–98%. Of the polymers prepared, however, only **SPP-BP-d** formed thin, bendable membranes. The highest *meta* content polymers, **SPP-BP-e** and **f**, did not form self-standing membranes, potentially due to an inability to

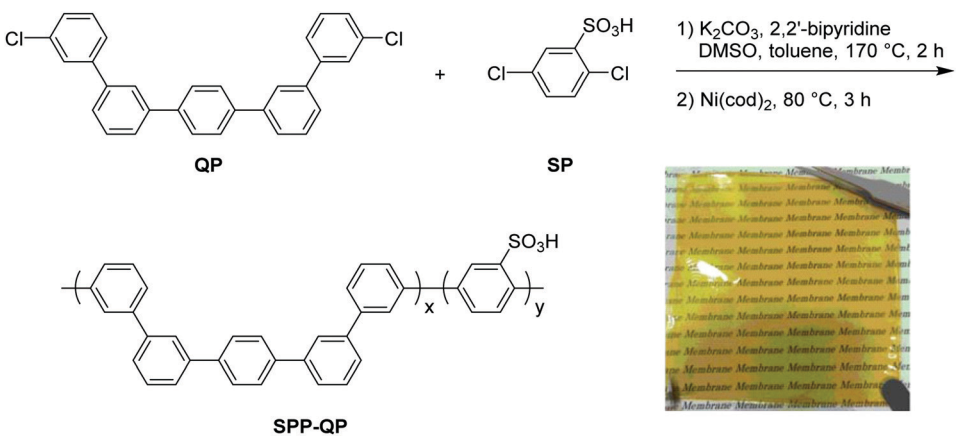

Fig. 10 Synthesis of SPP-QP. Adapted from previously published work. *Sci. Adv.*, 2017, **3** (10), Artiecle #eaao0476, J. Miyake *et al.*, "Design of Flexible Polyphenylene Proton-Conducting Membrane for next-Generation Fuel Cells".[32]

Table 2 Polymer properties of SPP-BP copolymers prepared *via* varied *meta–meta* (*m*), *para–para* (*p*), and sulfonated (s) phenylene monomer feed ratios[45]

		Monomer ratios				Molecular weight (M_n in kDa)				
		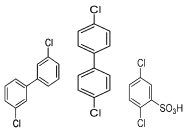								
	Polymer	*m*	*p*	*s*	IEC (meq. g^{-1})	M_n	$Đ$	DP$_n$	Solubility in DMSO or DMF	Membrane forming?
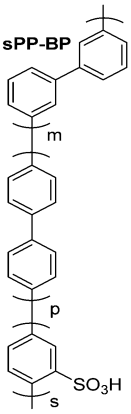	**SPP-BP-a**	0.00	1.09	1.00	3.8	16.8	7.1	36	✘	N/A
	SPP-BP-b	0.12	0.97	1.00	3.5	25.3	4.5	55	✘	N/A
	SPP-BP-c	0.55	0.55	1.00	2.8	35.2	3.9	75	✘	N/A
	SPP-BP-d	0.88	0.22	1.00	2.4	36.6	3.7	79	✔	✔
	SPP-BP-e	0.97	0.12	1.00	2.5	28.0	3.4	61	✔	✘
	SPP-BP-f	1.09	0.00	1.00	2.2	23.1	3.2	50	✔	✘
	SPP-QP	N/A	N/A	N/A	2.6	27.6	4.4	51	✔	✔

achieve sufficient chain entanglement; the authors did not comment on the *para*-dominant polymers **SPP-BP-a** through **c**.[45] However, it is worth noting that because **SPP-BP-a** is comprised purely of *para* phenyl-phenyl linkages, the challenges observed in its membrane forming and solubility are likely due to its rigid-rod nature, as per sulfonated poly(*p*-phenylenes).[29,40,42,43]

Numerical calculations revealed that the backbone of **SPP-BP-d**, containing an 88 : 22 *meta*-phenylene to *para*-phenylene ratio, was more likely to contain shorter sequenced lengths of the hydrophilic and hydrophobic components when compared to **SPP-QP**, which the authors rationalized may have contributed to the lower observed water uptake in the former. Small angle X-ray studies revealed a lack of periodic structure in the hydrophilic domains in **SPP-BP-d**, likely due to higher degree of randomness of the molecular sequences in its main chain. Proton conductivity of **SPP-BP-d** membranes at 80 °C was slightly lower than **SPP-QP**; however, when plotted as a function of hydration number (λ), the proton conductivities were nearly identical. This suggested that there were similar proton transport pathways through both polymer membranes. Oxidative stability, evaluated *via* Fenton's reagent test, revealed nearly complete retention of weight, molecular weight, and IEC for both **SPP-BP-d** and **SPP-QP**. A drastic difference in mechanical properties was however reported, with measured elongation at break (at 80 °C/60% RH) of 37 and 68% for **SPP-BP-d** and **SPP-QP**, respectively, possibly due to the smaller hydrophobic domain size in the former.[45]

Side-chain sulfonated polyphenylenes

The coupling of dichlorobenzophenones and derivatives to afford sterically-encumbered polyphenylene backbones has been reported by various research groups over recent decades.[49,51,180–183] These polyaromatics possess aryl ketone (benzoyl) side chains on a poly(*p*-phenylene) backbone. Post-sulfonated poly(benzophenone)s such as poly(benzoyl-1,4-phenylene) and its derivative poly(*p*-phenoxybenzoyl-1,4-phenylene), illustrated in Fig. 11, are thermally stable up to at least 215 °C. When evaluated as membranes in direct methanol fuel cells, the membranes possess considerably lower (approx. 10×) methanol permeability than Nafion®.[180] The polymers commonly exhibit good solubility in polar aprotic solvents and are able to form self-standing membranes, although at high degrees of sulfonation (*e.g.*, >65%) they are soluble in methanol and water.[49,51] Modifying poly(*p*-phenoxybenzoyl-1,4-phenylene) with alkyl grafts of varying lengths (*n*-propyl, *n*-dodecyl, or *n*-octadecyl) has negligible impact on proton conductivity and water uptake, however, gas permeability is significantly higher in the *n*-propyl grafted analogue.[183]

Post sulfonation of polymers affords ill-defined structures where individual rings may be mono or poly-sulfonated.[180] Pre-sulfonation of monomer units to afford sulfonated poly(benzophenone)s is a more robust method that allows precise control over the IEC through modification of monomer stoichiometric ratios.[181] Thus, a pre-sulfonated poly(benzophenone) with an IEC of 2.78 mmol g^{-1} displayed a proton conductivity of 174 mS cm^{-1} at 30 °C and 100% RH (approx. 2.5× higher than Nafion® reference) at a moderate 54 wt% water uptake.[181] In addition, a high tensile strength in the dry and hydrated state of 79 and 20 MPa, respectively, were noted.[181] Partially fluorinated poly(benzophenones) have also been investigated, with IECs more similar to that of Nafion® (1.3 *vs.* 0.9 meq. g^{-1}, respectively), although the electrochemical performance of such polymers as PEMs is rather poor in comparison.[182] In terms of morphology of alkyl grafted poly(benzophenone)s, longer side chains facilitate more phase segregation, however, the proton

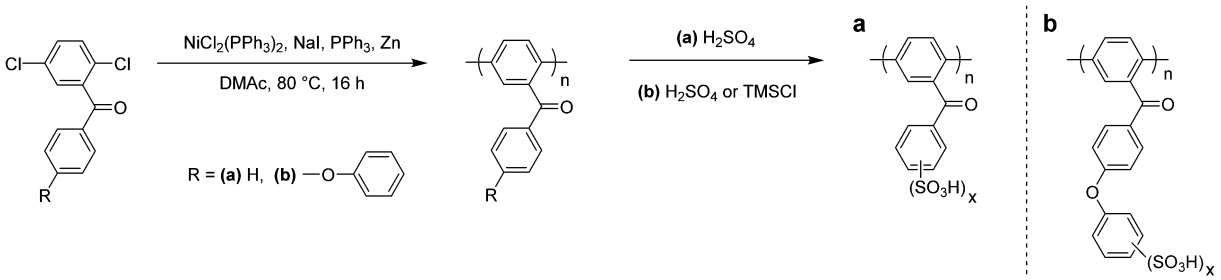

Fig. 11 Structure of two types of poly(benzophenone)s poly(benzoyl-1,4-phenylene) (a) and poly(*p*-phenoxybenzoyl-1,4-phenylene) (b).[180]

conduction is similar in both short and long alkyl grafted membranes.

Since 2014 W. Kim and co-workers,[53–63] reported on a number of side-chain sulfonated polyphenylene variants for PEMFC applications. These polyphenylenes, which were all prepared through Ni-catalyzed cross-coupling reactions of dichlorophenyl monomers, contained various combinations of tetraphenylethylene and/or benzoyl moieties, including branched and alkyl-chain-grafted derivatives. A summary listing the IEC, water uptake, hydration number (λ), proton conductivity (σ_{H^+}), and maximum power density (in a PEMFC), of the aforementioned polymer systems is collated in Table 3. The values listed correspond to the polymer within each system with the highest ion exchange capacity, as indicated. In all cases, polymer backbones are made up entirely of sp^2 linkages. Variants possessing ethers, ketones, sulfones, and imides in

Table 3 Comparison of ion exchange capacity (IEC), water uptake, hydration number (λ), *ex situ* proton conductivity (σ_{H^+}), and *in situ* fuel cell power density in PEMs prepared by W. Kim *et al.* Data in this table was accumulated from previously published work[53–63]

Polymer	IEC[a] (meq. g^{-1})	Water uptake[b] (wt%)	λ^b (nH_2O/SO_3H)	σ_{H^+} (mS cm^{-1})	Power density (W cm^{-2})	Ref.
a	3.02	114	21.0	109[c]	0.63[f]	53
b	2.51	105	23.3	108[c]	0.65[g]	54
c	2.14	72	18.6	103[c]	—	55
d	2.51	88	19.5	109[c]	0.65[g]	56
e	2.07	69	18.6	102[d]	0.56[g]	58
f	2.45	91	20.7	162[c]	—	59
g (linear)	1.85	42	12.6	92[c]	0.49[h]	60
g (branched)	1.65	35	11.8	95[c]	0.60[h]	60
h (post)	2.30	78	18.9	93[e]	0.61[h]	62
h (pre)	1.93	85	24.4	95[e]	0.61[h]	63
i	1.76	68	21.3[i]	143[e]	0.65[h]	61

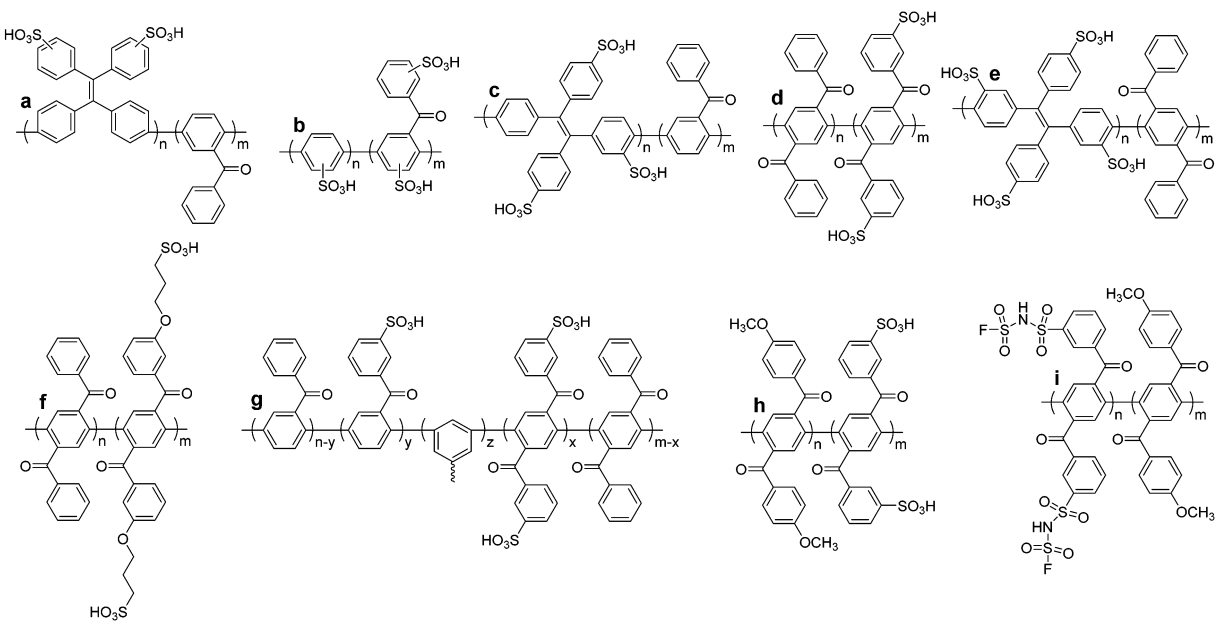

[a] Highest reported IEC value. [b] Measured at 80 °C. [c] Measured at 80 °C and 90% RH. [d] Measured at 80 °C and 100% RH. [e] Measured at 90 °C and 90% RH. [f] Measured under fully humidified inlet conditions at 80 °C under H_2/air. [g] Measured under fully humidified inlet conditions under H_2/air, temperature not reported. [h] Measured under fully humidified inlet conditions at 70 °C under H_2/air. [i] Hydration number defined as n H_2O per *n* sulfonimide.

the backbones were also reported,[57,184–188] however, these will not be discussed as this review focuses solely on wholly aromatic polyphenylene backbones.

Cumulatively, the work by W. Kim and co-workers introduced a number of promising polyphenylene-based candidates for electrochemical device applications. The PEMs generally exhibit proton conductivities comparable to that of Nafion®, with a few notable exceptions exceeding it (**f** and **i**). The flexible sulfonic acid alkyl side-chains in **f** may have promoted hydrophobic/hydrophilic phase separation creating well-connected ionic domains, leading to the enhanced proton conductivity observed. However, while polymer **f** possessed a significantly higher proton conductivity (162 mS cm^{-1}) than the other polymer systems, its *in situ* fuel cell performance was not evaluated. The high proton conductivity of **i** was likely due to the greater acidity of the sulfonyl imide group compared to sulfonic acid groups. The membranes also possessed appreciable chemical stability, owing to the polyphenylene backbone, as well as varying degrees of dimensional stability, where higher IEC values typically resulted in higher water uptake. Unfortunately, the studies lack an in-depth assessment of membrane mechanical properties, such as stress *vs.* strain relationships, as well as comprehensive *in situ* electrochemical characterization and stability evaluation (*e.g.*, accelerated stress tests at open circuit voltage and wet-dry cycling). Such aspects are critical to consider when designing materials for electrochemical device application and highlight an area in need of additional focus and improvement.

5 Sulfo-phenylated polyphenylenes

Phenylated polyphenylenes

In the early 1930's, W. Dilthey *et al.*[189] reported the first use of an alkyne-based dienophile (diphenylacetylene) with a cyclic cyclopentadienone diene (tetracyclopentadienone, or "tetracyclone") in a [4+2] Diels–Alder cycloaddition to give hexaphenylbenzene (Scheme 2a). Following formation of the expected Diels–Alder adduct, the bridging carbon monoxide moiety was spontaneously extruded to generate a new phenyl ring *in situ* which prevented reversibility of the reaction. This approach represented a new means of synthesizing oligophenylenes whereby the desired product was obtained simply from two reactants and heat, without use of catalysts or additives. W. Ried *et al.*[76,77] later performed this condensation reaction using di and tetra-functionalized dienophiles to generate more complex oligophenylenes. In addition, the reaction between a bi-functionalized diene (1,4-diethynylbenzene) and bi-functionalized dienophile (bistetracyclopentadienone, or "bistetracyclone") to generate a phenylated polyphenylene was described (Scheme 2b).[76,77] The resultant polymer exhibited a high melting point (T_m) of 420 °C.[78] The chemical linkages formed in these Diels–Alder polyphenylenes are drawn ambiguously because there are two possible orientations which the incoming diene may occupy with respect to the dienophile during reaction, resulting in formation of either a *meta* or *para* aryl bond, as per Scheme 3.[190]

In preliminary work reported by Z. B. Shifrina *et al.*[191] the ratio of *meta* to *para* linkages formed in the Diels–Alder polycondensation was probed using crystal structures of oligophenylene model compounds prepared using the same reaction.[191] The authors concluded that the primary isomer was *meta* (83% of isomers), however, no information regarding minor products or the respective polymer was reported.

In addition to the aforementioned reports, phenylated polyphenylenes were also comprehensively investigated by J. K. Stille and coworkers.[81,170,190,192–196] For example, H. Mukamal *et al.*[192] reported on a series of polymers prepared *via* Diels–Alder polycondensation using simple reagent grade toluene as solvent, *versus* the *cis*-β-dekalol previously employed by W. Ried *et al.*[76,77]

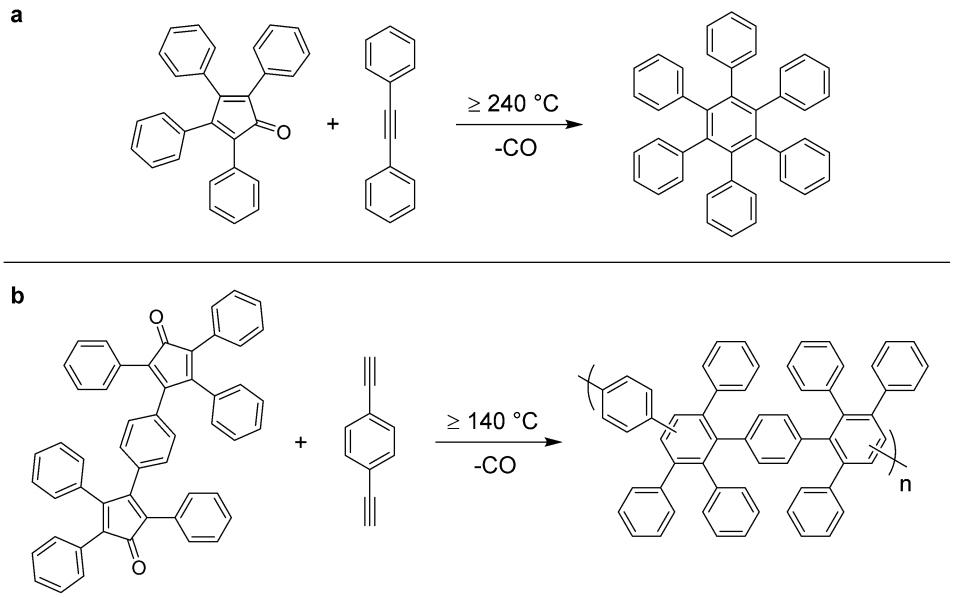

Scheme 2 Preparation of (a) hexaphenylbenzene, and (b) phenylated polyphenylene,[76,77] *via* Diels–Alder condensation.

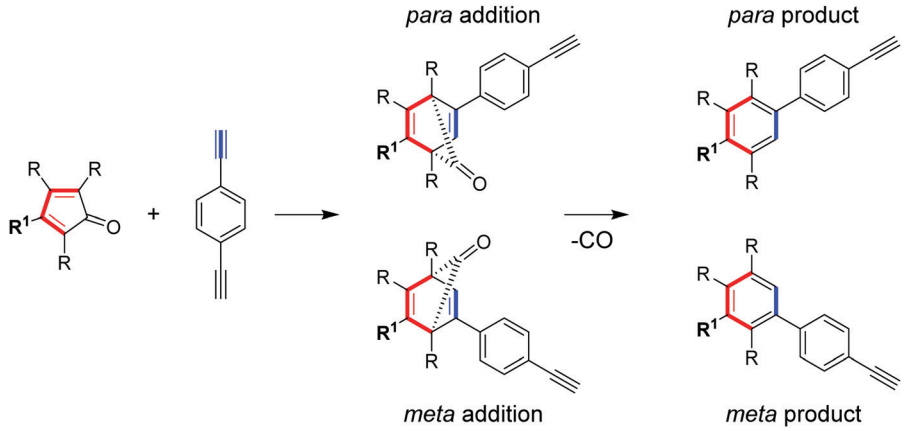

Scheme 3 A [4+2] Diels–Alder polycondensation with two possible regiomeric products per aryl linkage formed.

The white polymer powders, which were obtained following a pressurized reaction at 200 °C for 24 h in ~90% yield, showed excellent thermal stability *via* thermogravimetric analysis with a major decomposition onset point at 550 °C in air and 575 °C under nitrogen.[192] When pyrolyzed at 750 °C under nitrogen, volatile hydrocarbon products containing benzene, biphenyl, and larger oligophenylenes were obtained from the phenylated polyphenylenes totaling 30% of the initial sample mass.[192] The remaining black, insoluble residue contained markedly fewer monosubstituted phenyl units *via* IR analyses, indicating loss of phenyl groups from the highly phenylated polymer backbone and formation of poly(*p*-phenylene)-like structures.[192]

All the phenylated polyphenylene variants reported were readily soluble in common organic solvents (*e.g.*, toluene, chloroform) despite possessing a polyphenylene backbone.[190,192] The enhanced solubility *versus* poly(*p*-phenylene) was attributed to the large degree of phenyl substitution, which dramatically improved material processability.[81,170,195] For an overview on early work in cycloaddition polymerizations such as that described above, the reader is directed to the 1972 review published by J. K. Stille.[170] These early reports identified phenylated polyphenylenes as an interesting class of materials which were readily soluble and possessed a highly thermochemically stable backbone. In addition, the Diels–Alder polycondensation was established as a invaluable tool for synthesis of a diverse range of such polymers.[76,77,81,170,189,190,192–196] For additional reading on more recent developments in oligo and polyphenylenes, such as those prepared by Diels–Alder polycondensation,[197] as well as higher order polyphenylene nanosctructures derived therefrom,[169] the reader is directed to reviews by A. J. Berresheim *et al.*,[169] and I. Hou *et al.*[197]

Post-sulfonated phenylated polyphenylenes

In 2005, a series of sulfonic acid-functionalized polyphenylenes for electrochemical applications was reported by C. H. Fujimoto and coworkers.[30] These materials are referred to as sulfonated phenylated polyphenylenes (sPPPs), or sulfonated Diels–Alder polyphenylenes (SDAPP). Because two different nomenclatures exist in the literature, this review will use both acronyms as per the original work being reviewed. The reader is reminded that both acronyms – sPPP and SDAPP – refer to the same class of materials, which are obtained *via* Diels–Alder polycondensation, are comprised *entirely* of aryl–aryl linkages free of heteroatoms and contain side-chain sulfonation in the form of benzenesulfonic acid moieties. The synthetic approach reported for these polyelectrolyte materials differed greatly from other PEMs in literature, such as transition metal-catalyzed cross-coupling reactions, in that no additives (*e.g.*, acids, bases, or catalysts and ligands) were required to generate the parent non-functionalized phenylated polyphenylene (PPP) backbone. While post-functionalization of a similar phenylated polyphenylene (PPP) backbone was successfully achieved decades prior by VanKerckhoven *et al.*,[82] who used sulfuric acid to impart water solubility onto the hydrophobic polymer, no information regarding acid content or position of the attached sulfonic acid groups, or any further work, was reported for the materials.

C. H. Fujimoto *et al.*[30] reported the synthesis and controlled post-functionalization of PPP using chlorosulfonic acid to give SDAPP (see Scheme 4), which was for the first time examined as a proton exchange membrane. The post-functionalization technique imparted solubility in polar aprotic solvents such as DMSO, but the polymer remained insoluble in water. Sulfonation was thought to occur predominantly at the *para* position of the pendant phenyl rings due to steric limitations of the highly encumbered structure, although structural characterization was insufficient to support this hypothesis unambiguously. Four statistically-sulfonated polymers with varied acid contents were examined, containing from 0.8 to 2.1 sulfonic acid moieties per repeat unit (Scheme 4) with molecular weights (M_n) up to 83 kDa, corresponding to a degree of polymerization of ~89 repeat units.

The initial investigation of sPPPs provided sufficient motivation of their viability as a class of polymers for PEM applications.[30] Furthermore, the simple D–A synthesis, free of potentially sensitive additives or complicated synthetic procedures, was notably attractive. B. R. Cherry *et al.*[198] probed the hydrated morphologies and ionic domain sizes within dehydrated membranes of the aforementioned sPPPs using solid-state ^{1}H magic angle spinning NMR.[198] In the dehydrated state, the activation energy of membranes was found to be ~18 kJ mol^{-1}, which was much lower than

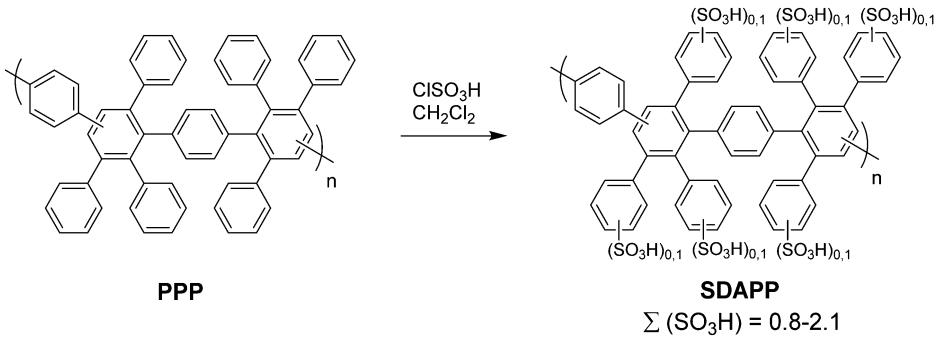

Scheme 4 Post-sulfonation of PPP to sPPP (SDAPP).[30]

that of imidazole-based PEMs (128 kJ mol^{-1}) and suggested that proton conduction arose from a combination of vehicular and Grötthuss transport mechanisms. The domain size of the hydrophilic sulfonic acid moieties (clusters) depended on the dimensionality (ε) of the hydrophilic domains present, and calculated to be ~4.4, 8.8, or 13.2 nm for ε = 1, 2, or 3, respectively, which is slightly less than that reported for a sulfonated poly(arylene ether sulfone) reference material (10–25 nm).[199] While the latter measurement was obtained using different characterization techniques,[199] the authors hypothesized that the reduced domain size observed in SDAPP membranes was a result of reduced rotational freedom associated with the highly rigid polyphenylene backbone.[198] These findings provide important information regarding the morphology of sPPPs in membrane form, and their potential implications to proton conductivity.

An alternative method to post-functionalization of phenylated polyphenylene uses Friedel–Crafts chemistry, as reported by S. M. Budy and D. A. Loy.[64] Here, PPP in dilute solution was reacted with 1,3,5-benzenetrisulfonyl chloride and $FeCl_3$ Lewis acid, which yielded its quantitative conversion to a sulfonylated-branch phenylated polyphenylene possessing either 1 or 2 pendant aryl sulfones. When hydrolyzed, polymers possessing 2 or 4 sulfonic acid moieties per repeat unit, respectively, were obtained, which exhibited IEC values of 1.87 and 2.90 meq. g^{-1}, respectively.[64] High IEC membranes were insoluble in water,[64] which was an improvement over previously reported post-sulfonated sPPPs which formed hydrogels at high degrees of sulfonation (>2.1 acid groups per repeat unit).[30] The reduced solubility in water was attributed to a high extent of segregation of the hydrophilic acid groups from the hydrophobic polymer backbone.[64]

Hydration and proton conductivity of SDAPP membranes. The water uptake and proton conductivity of post-sulfonated phenylated polyphenylenes were probed by M. Hickner *et al.*,[200] who evaluated sPPPs (**SDAPP**) with varying degrees of acid functionalization, ranging from 0.8 to 2.1 sulfonic acid groups per repeat unit (IEC = 1.04 to 2.20 meq. g^{-1}) prepared by controlling the degree of sulfonation, and compared them to a Nafion 117 reference (IEC = 0.91 meq. g^{-1}). A clear relationship between polymer IEC and membrane water uptake, hydration number (λ), and proton conductivity (σ_{H^+}) was observed (see Table 4).[200] The membranes exhibited appreciable proton conductivity (123 mS cm^{-1}), higher than the Nafion 117 reference (100 mS cm^{-1}), at the highest IEC evaluated, but simultaneously displayed much larger water uptake and hydration number values.[200] The lower IEC membranes contained primarily bound water, whereas the higher IEC membranes possessed a larger volume of unbound water, enabling more favorable proton conduction.

E. G. Sorte *et al.*[65] examined an expanded series of post-sulfonated phenylated polyphenylenes with differing degrees of functionalization, wherein the number of sulfonic acid groups, *S*, per polymeric repeat unit was synthetically varied from *S* = 1.3 to 3.6. The corresponding membranes exhibited experimental ion exchange capacities of 1.5 to 3.4 meq. g^{-1}, respectively.[65] The mass of membrane samples and their corresponding water content increased as a function of both relative humidity and degree of sulfonation. Each sample exhibited non-linear water adsorption similar to that of Nafion, with increased water uptake occurring at >50% relative humidity. These changes were attributed to morphological changes occurring within the gradually hydrating samples, such as formation of a percolated network of ionic domains.[65] At 98% RH, the number of water molecules per sulfonic acid moiety, λ, decreased with increasing IEC, from λ = 20.3 to 11.6 for membranes with IECs of 1.5 to 3.4 meq. g^{-1}, respectively.[65] The maximum proton conductivity (90 °C, 90% RH) measured for each sample was strongly dependent on degree of sulfonation (and hence IEC), increasing from 30 mS cm^{-1} at 1.5 meq. g^{-1} to 169 mS cm^{-1} at 3.4 meq. g^{-1}.[65] Proton conductivity activation energies, calculated from NMR and impedance data, generally decreased from 31.3 kJ mol^{-1} (highest) to 9.2 kJ mol^{-1} (lowest) with increasing degree of sulfonation (*S* = 1.3 to 3.6, respectively) and relative humidity (RH = 33 to 98%). A decrease in activation energy at higher degrees of sulfonation was linked to an increased contribution from the Grötthuss ion conduction mechanism. These values compared favorably to those of sulfonated poly(ether ketone)-based membranes (30 to 90 kJ mol^{-1}), as well as Nafion (10–29 kJ mol^{-1}).[65] These findings further affirmed that transport occurs most readily in high IEC post-sulfonated phenylated polyphenylenes.

The role of water on ultrathin post-sulfonated phenylated polyphenylenes membranes was probed by L. He *et al.*[201] *via* neutron reflectometry using films less than 60 nm thick with differing IECs (0.98, 1.60, and 2.20 meq. g^{-1}). Non-uniform distributions of water were observed within the films due to interfacial forces stemming from polymer interactions with both the solid support (oxidized silicon wafers), as well as the

Table 4 Membrane properties of post-sulfonated phenylated polyphenylenes (SDAPP) with varied degrees of acid functionalization, and Nafion 117, measured at 30 °C. Reprinted from *Polymer*, **47** (11), 4238–4244, M. Hickner *et al.*, "Transport in Sulfonated Poly(Phenylene)s: Proton Conductivity, Permeability, and the State of Water", Copyright (2006), with permission from Elsevier[200]

Polymer	IEC (meq. g^{-1})	Water uptake (wt%)	λ (nH_2O/SO_3H)	σ_{H^+} (mS cm^{-1})
SDAPP	2.20	137	34	123
	1.80	75	23	87
	1.40	36	14	49
	1.04	21	11	13
Nafion 117	0.91	36	22.0	100

air interface. Excess water was found to accumulate at both interfaces, akin to surface (interfacial) wetting. These effects appeared to have an appreciable impact on the water diffusivity of sPPP films, which was significantly lower in the early stages of exposure to water vapor than during bulk transport. The authors ascribed this phenomenon to the highly rigid PPP backbone, which is too inflexible to allow for considerable phase segregation and folding to bury its ionic functional groups away from the surface of membranes or thin films.[201] The membranes were hence hypothesized to possess a dual nature surface with coexisting hydrophilic and hydrophobic components, generating interfaces which exhibit defined wetting layers.[201] These findings are particularly important with respect to hydrogen fuel cells, where thin ionomer films in the catalyst layer exist in complex microstructures in a three-phase environment interacting with solid catalyst and support materials, water, and the reactant O_2 and H_2 gases.[13,202]

Water transport dynamics in SDAPP membranes. Water transport dynamics in post-sulfonated PPP membranes were investigated by L. He *et al.* using ^{1}H NMR and Fourier transform infrared (FTIR) spectroscopies.[203] The degree of sulfonation (IEC, 0.98, 1.60, and 2.20 meq. g^{-1}) was found to strongly dictate water content, as expected. The absorbed water was significantly more "liquid-like" in the high IEC polymer (2.20 meq. g^{-1}) than in the low IEC polymer (0.98 meq. g^{-1}), and also exhibited enhanced exchange between hydrophilic sites.[203] The low IEC polymer did not exhibit a measurable water diffusion, from which it is inferred that water transport is extremely slow. Conversely, water diffusion in the high IEC membrane was 3.5× faster than in a Nafion reference. This is attributed to formation of larger ionic domains when adequately hydrated, due to the rigid backbone occupying bundled structures.[203,204] Time-dependent FTIR spectroscopy data supports the presence of free, loosely, and bound water, and suggests that confined water evaporates more slowly from the membranes than bulk water.

The dynamics of water within post-sulfonated PPP membranes were further probed by N. C. Osti *et al.*[205] using quasi-elastic neutron scattering (QENS) as a function of temperature and water content. Heavy emphasis was placed on the rigidity of the polyphenylene backbone, which yielded formation of unique network macrostructures that remained rigid and displayed a glassy behavior even when membranes were in the hydrated state.[205] These findings were related to the unique bundled structures previously found in sPPPs, which persist in polymer solution, through membrane casting and during hydration.[204] On the timescale of the QENS measurements performed, the polymer molecules were effectively immobile, and impenetrable to water molecules.[205] Water is found to reside in a loosely bound state, and exhibits notable mobility throughout the polymer network and exchange between multiple sites, even under reduced relative humidity (ambient) conditions.[205] Slow and fast water dynamics were identified, which were attributed to free water which exists between polymer bundles in hydrated channels, and water molecules associated to polar SO_3H groups, respectively.[205] Water-jump diffusion coefficients were calculated to quantify the observed water dynamics. In both populations, water molecule mobility was dependent on and increased with water content and temperature and was greater in sPPPs than in Nafion. At elevated temperature (T = 60 °C), there was evidence of structural changes occurring within the hydrated polymer whereby water molecules begin to penetrate into polymer bundles.[205] This was a particularly important finding which may address why the *ex situ* conductivity,[200,206] and *in situ* MEA performance of post-functionalized sPPP membranes,[206] is higher at elevated temperatures and RH.

Morphology of SDAPP membranes. Related to transport properties is the morphology of post-sulfonated PPP membranes. An in-depth investigation on nanoscale structures of sPPPs in both dilute solutions and hydrated thin films as a function of acid content was reported by L. He *et al.* in 2009.[204] Using membranes with IECs ranging from 0.98 to 3.22 meq. g^{-1}, the surface morphology was found to consist of relatively uniform domains with approximate dimensions 300 × 150 Å (length × width) which lined up along an axis as result of polymer self-assembly during membrane casting.[204] Small angle X-ray scattering (SAXS) reveals the absence of crystalline domains, nor any evidence of tight π–π interactions between aromatic rings. Hydrophobic domains impenetrable to water are, however, evident.[204] Large domains of radius between 350 and 540 Å consistent with the presence of clusters are also evident by SANS.[204] In solution, SANS reveals cylindrical structures with radii of 60 Å and lengths of 500 Å.[204] Note, the radius of a single rod-like molecule is calculated to be 20 Å, which supports the conjecture that the structures are aggregates, or bundles, of polymer strands. Polymer bundles are hypothesized to persist through solvent evaporation during membrane casting, whereby they associate to form large polymer aggregates in membranes.[204] The rigidity of the parent polyphenylene backbone is identified as a determining characteristic of the structure–morphology relationship in sPPPs, and has broad implications on membrane properties, compared to flexible ionomers such as those containing heteroatomic linkages or backbones comprised of sp^3-hybridized atoms.[30,198,200,201,207]

The effects of hydration and degree of sulfonation on the nanostructure of hydrophilic domains within post-sulfonated phenylated polyphenylenes have been evaluated by A. J. Abbott and A. L. Frischknecht using atomistic simulations.[208] Explicit

hydrophilic/hydrophobic phase segregation into respective nanoscale domains was observed, which was driven by aggregation of ionic groups and water molecules (clusters) within the systems. The local structure of hydrophilic domains was notably affected by hydration, in that an increase in the number of water molecules resulted in sulfonate groups becoming more hydrated and pushed farther apart (increased spacing). Low degrees of hydration (λ = 3 and 5) yielded formation of hydronium ions which displayed strong electrostatic interactions with neighboring sulfonate moieties, which would likely result in hindered ion mobility. The effects weakened at higher hydration levels (λ = 10 and 20) due to increased solvation of the sulfonate groups and resulted in more mobile hydronium ions.[208] The atomistic simulations complemented previously reported experimental data on proton conductivity of post-sulfonated sPPPs well, which showed rapid increases in proton conductivity as a function of membrane water content (λ),[30] as well as relative humidity.[206] Moreover, the degree of sulfonation (S) is found to impact the nanoscale morphology of hydrophilic domains.[208] A low degree of sulfonation particularly under low hydration conditions revealed distinct clusters of ionic groups and water molecules which varied in shape and are *not* appreciably interconnected. Increasing the degree of sulfonation (S = 2 and 4) and hydration (λ = 10 and 20) parameters caused the hydrophilic clusters to increase in size, become more spherical, and become more interconnected. This ultimately resulted in formation of a fully percolated and connected ionic domain (Fig. 12).[208] The take home message is that high connectivity of ionic domains in these SPPs, and hence high conductivity, requires relatively high degrees of sulfonation (high IEC), compared to incumbent PFSAs such as Nafion.

A comprehensive computational study of the hydration and morphological characteristics of post-sulfonated PPP membranes using *ab initio* and density functional theory (DFT) calculations was reported by T. M. Alam.[126] A series of *para*-diphenyl sulfonic acid [*p*-DIP-SA·n(H_2O)] clusters were used as preliminary models for calculating the proton dissociation behavior. A gradual lengthening of the SO–H bond was observed from n = 0 (0.985 Å) to n = 2 (1.05 Å) water molecules, after which spontaneous proton dissociation and formation of a distorted H_3O^+ cation occurred (at n = 3, SO–H bond length = 1.55 Å). At intermediate hydration levels of $n > 3$ water molecules, the formed H_3O^+ cation existed in different configurations that were generally in a contact ion pair with the sulfonate anion, and at higher hydration levels of $n \geq 6$ the acid was fully solvated and dissociated from the sulfonate anion. This behavior is remarkably similar to what is observed in PFSAs (dissociation at n = 3), but not sulfonated poly(arylene ether ether ketone) model systems, and suggests that benzenesulfonic acid moieties are capable of proton dissociation at lower levels of hydration than expected for hydrocarbon systems which did not possess perfluorinated superacidic moieties.[126] These findings offer an explanation as to why proton conductivities of post-sulfonated PPP membranes are reportedly similar to that of PFSAs,[200,206,209] and higher than that of other hydrocarbon-based systems such as sulfonated poly(arylene ether sulfone)s and polyimides.[30]

Fuel cells incorporating SDAPP membranes. An investigation into hydrogen and methanol fuel cell performances of post-sulfonated phenylated polyphenylenes membranes was first reported in 2010 by R. J. Stanis *et al.*,[206] who used membranes which possessing IECs of 0.72, 1.2, 1.7, and 2.30 meq. g^{-1}. Methanol solubility experiments revealed that the two highest IEC polymers dissolved, whereas the low IEC polymers remained largely intact. The hydrocarbon-based membranes were found to be less permeable than Nafion 212. Membrane permeability related to the extent of membrane swelling.[206] When evaluated as membranes in direct methanol fuel cell MEAs, the more conductive (higher IEC) membranes exhibit greater maximum power density in 1 M methanol.[206] In the presence of 3 M methanol, however, those with lower methanol permeability performed better due to a lower fuel crossover. Hydrogen fuel cells constructed with post-sulfonated phenylated polyphenylenes membranes were evaluated under H_2/O_2 and H_2/air at 80 °C.[206] Fuel cells containing low IEC

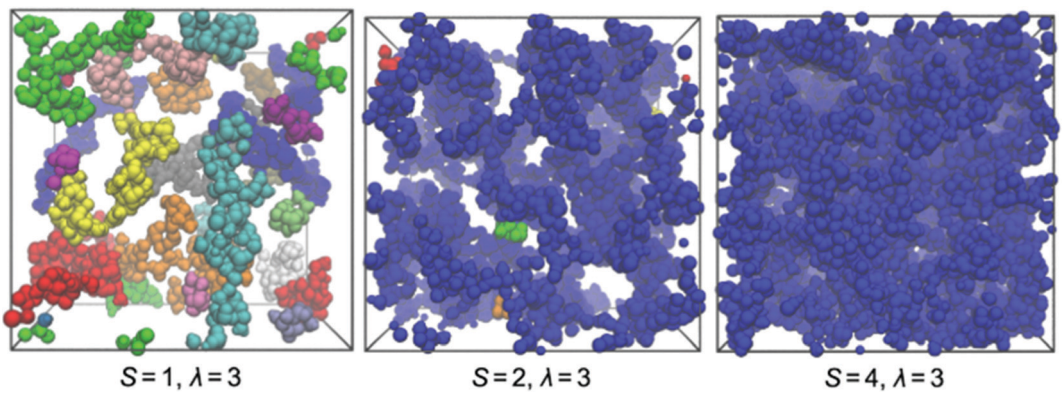

Fig. 12 Snapshots from MD simulations of post-sulfonated phenylated polyphenylenes possessing degrees of sulfonation S = 1, 2, or 4 at hydration of λ = 3. Only hydrophilic domains are shown, with distinct clusters given in individual colors. Reprinted (adapted) with permission from *Macromolecules* 2017, 50 (3), 1184–1192, L. Abbott, A. Frischknecht, "Nanoscale Structure and Morphology of Sulfonated Polyphenylenes *via* Atomistic Simulations". Copyright (2017) American Chemical Society.[208]

membranes performed poorly, but high IEC membranes exhibited polarization curves approaching Nafion 212 MEA under H_2/O_2.[206] *E.g.*, at 0.65 V, a maximum current density of 1020 mA cm^{-2} was found (compared to 1204 mA cm^{-2} for a Nafion 212 MEA). Under H_2/air supply, the performance of all membranes was generally much poorer, with post-sulfonated phenylated polyphenylenes membranes comparing less favorably to the Nafion 212 reference, attributed to mass transport limitations.[206] Nonetheless, these studies represented the first *in situ* evaluation of sulfonated phenylated polyphenylenes, and identified this class of PEMs as prospective materials for use in fuel cells.[26,206]

Overall, the work reviewed in the above section highlights progress in establishing post-sulfonated, phenylated polyphenylenes as materials for study for electrochemical energy conversion applications. Nonetheless, post-sulfonation of polymers comes with the penalty that the polymers, while tunable, are not synthesized in a definitively reproducible manner due to uncertainty of placement (location) of the sulfonate groups both on the repeat unit, and along the polymer backbone. This is highlighted by the typically reported non-integer degrees of sulfonation (*e.g.*, 1.3–3.6 sulfonic acid moieties per polymeric repeat unit).[65] As the field of hydrocarbon-based PEMs continues to advance, it is becoming increasingly evident that efforts to increase the molecular precision and reproducibility of sPPP must be achieved in order to improve the versatility and inherent properties of this class of polymer.[8,102,210,211]

Pre-sulfonated monomer approach to sulfo-phenylated polyphenylenes

Over the past 6 years, significant progress has been made developing structurally-defined sulfo-phenylated polyphenylenes. In 2015, T. Skalski *et al.*[31] demonstrated a novel, pre-functionalization approach to the preparation of sPPPs. This was achieved through modification of the cyclopentadienone diene monomer (bistetracyclone), to afford a precisely functionalized analogue TEAsBTC (Scheme 5) which possesses 4 sulfonate moieties affixed *para* on its exterior pendant phenyl rings.[31] A series of model compounds with structural motifs analogous to the respective polymer were prepared to evaluate monomer reactivity and stability, and it was determined that all four acid moieties were retained after the Diels–Alder reaction.[31] Subsequently, a proof-of-concept pre-functionalized polymer **sPPP-H+** was prepared (Scheme 5). The triethylammonium-sulfonate salts served as internal NMR probes, and their integration ratios relative to the polymer backbone supported presence of 4 sulfonate functional groups per polymer repeat unit. The *meta* to *para* ratio of backbone phenyl linkages formed during polymerization was also elucidated for the first time (1 : 1).[31] The experimental IEC (3.47 meq. g^{-1}) determined by titration was close to the theoretical and ^{1}H NMR-measured IEC (both 3.70 meq. g^{-1}), which was the highest value reported for sPPPs to date.[30,31,64,204] Despite this, these pre-sulfonated **sPPP-H+** membranes were insoluble in water at 30 °C, although excessive swelling was observed at 80 °C. A preliminary oxidative stability test conducted by soaking membranes in Fenton's reagent (3% H_2O_2, 3 ppm Fe^{3+}, 80 °C, 1 h) showed no observable changes to the polymeric structure *via* ^{1}H NMR characterizations.[31] This was an important step to evaluating the previously experimentally unprobed thermochemical stability of sulfonated phenylated polyphenylenes.

The *ex situ* proton conductivity of pre-sulfonated **sPPP-H+** membranes (8.65 to 106 mS cm^{-1}) was comparable to or exceeded that of a Nafion 211 reference across the entire humidity range evaluated (40 to 95% RH at 30 °C), but decreased by ~27% in liquid water (77 mS cm^{-1}).[31] The latter is attributed to high water uptake and hence membrane swelling of **sPPP-H+**, which resulted in a notably lower analytical acid concentration ([–SO_3H] = 0.92 M) *versus* that of Nafion 211 (1.55 M).[31] Preliminary *in situ* investigations of **sPPP-H+** as ionomer in the catalyst layer of a fuel cell MEA *vs.* Nafion D520, both on a Nafion 211 membrane, showed that performance of the sulfonated phenylated polyphenylene-based catalyst layer approached that of Nafion D520 at 90% RH, but performed approx. 4× better than that of Nafion D520 at 0% RH (cathode). In both cases the anode RH was maintained at 100%. A complete *in situ* investigation was however limited due to

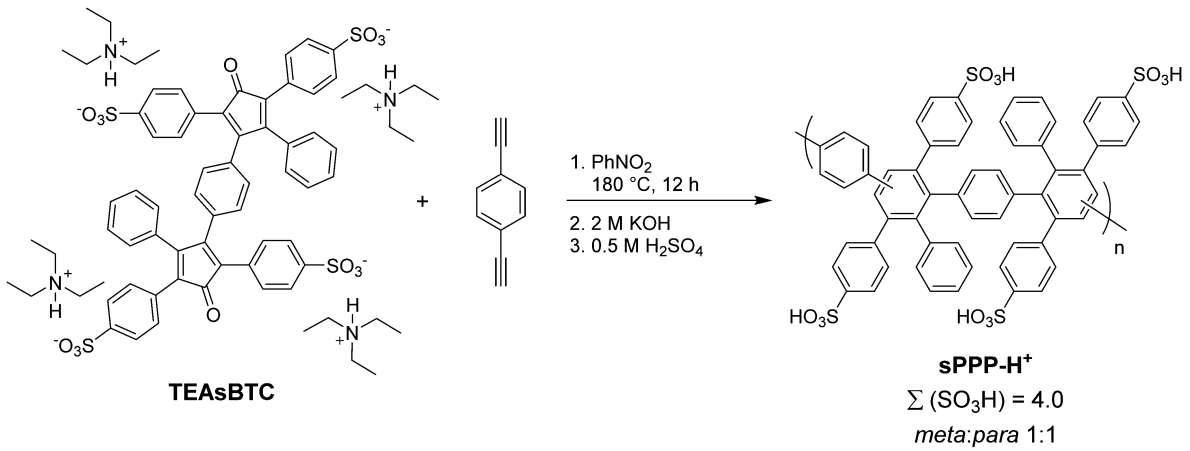

Scheme 5 Synthesis of a pre-functionalized sulfonated phenylated polyphenylene **sPPP-H+** *via* pre-functionalized diene monomer TEAsBTC.

challenges with membrane swelling at elevated temperatures and RH, and mechanical integrity.[31]

To circumvent the challenges related to excessive water uptake by **sPPP-H+** membranes, M. Adamski *et al.*[66,212] synthesized a series of larger naphthyl, biphenyl, and terphenyl-based dienophile monomers, from which polymers with reduced hydrophilicity **sPPN-H+**, **sPPB-H+**, and **sPPT-H+**, respectively, were prepared (Table 5).[66,212] Each of the polymers possessed 4 sulfonate moieties per repeat unit and experimental IECs decreased incrementally with increasing polymer repeat unit size. The membranes of **sPPN-H+** and **sPPB-H+** were reportedly robust and flexible during handling, whereas membranes of the terphenyl-containing

Table 5 Comparison of ion exchange capacity (IEC), water uptake, hydration number (λ), *ex situ* proton conductivity (σ_{H^+}), and *in situ* fuel cell power density in PEMs prepared by S. Holdcroft *et al.*[31,66,67,69,72,73,212,213] Data in this table were accumulated from previously published work

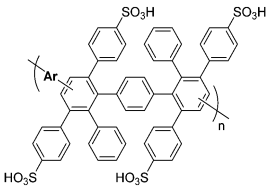

Ar =	Polymer	IEC[a] (meq. g^{-1})	Water uptake[b] (wt%)	λ^b ($n H_2O$ $n SO_3H^{-1}$)	$\sigma_{H^+}{}^c$ (mS cm^{-1})	Maximum power density (W cm^{-2})	Ref.
	**sPPP-H+**	3.47	319	50.7	338	0.42[d]	31 and 67
	**sPPN-H+**	3.28	183	31.0	268	0.93[e]	66 and 212
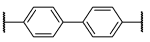	**sPPB-H+**	3.19	119	20.7	172	1.24[e]	66 and 212
	**sPPT-H+**	2.98	55	10.3	—	—	66 and 212
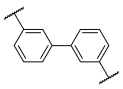	**sPPBm-H+**	2.87	257	49.7	273	—	72 and 73
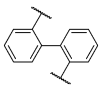	**sPPB*o*-H$^+$**	—[f]	—[f]	—[f]	—[f]	—[f]	72 and 73
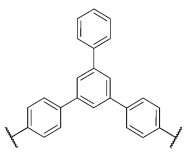	**sPPP N-free**	2.90	80	15.3	155	1.08[e]	69 and 213
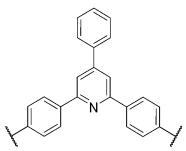	**sPPP (1 + 0)N**	1.98	54	15.2	119	0.93[e]	69 and 213
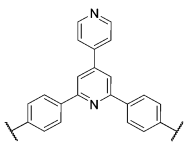	**sPPP (1 + 1)N**	1.80	52	16.0	13	—	213
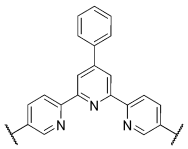	**sPPP (3 + 0)N**	1.58	—[g]	—[g]	—[g]	—[g]	213
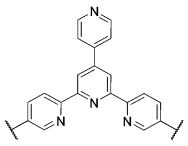	**sPPP (3 + 1)N**	1.38	49	20.0	12	—	213

[a] Highest reported experimental IEC value. [b] Measured at 22 °C in liquid water. [c] Measured at 80 °C, 95% RH. [d] Measured at 80 °C, 95% RH, 0.5/1.0 slpm H_2/O_2, with **sPPP-H+** in the anode and cathode catalyst layers. [e] Measured at 80 °C, 95% RH, 0.5/1.0 slpm H_2/O_2, zero backpressure with Nafion D520 ionomer in the anode and cathode catalyst layers. [f] Polymer membranes were water soluble. [g] Polymer membranes were extremely brittle and could not be characterized.

polymer **sPPT-H+** were not.[212] It is postulated that the linear terphenyl induces poorer solubility during polymerization, resulting in polymers with poor molecular weights which formed fragile membranes.[212] The tensile strength and Young's modulus values reported for **sPPN-H+** and **sPPB-H+** were up to 3.5× greater than that of Nafion 211, but elongation at break values were up to 8.5× lower.[66] The water uptake (wt%) and volumetric expansion (vol%) of membranes following immersion in liquid water decreased appreciably with increasing polymer hydrophobic character, despite the high polymer IECs measured in all membranes. Both were in the order **sPPP-H+** > **sPPN-H+** > **sPPB-H+** > **sPPT-H+**, and decreased from 319 to 55 wt%, and 364 to 80 vol%, respectively.[66,212]

After exposure to Fenton's reagent (3% H_2O_2, 3 ppm Fe^{2+}, 1 h, 80 °C), **sPPN-H+** and **sPPB-H+** membranes displayed no observable mass loss, and no changes in mechanical integrity, or chemical structure per ^{1}H NMR analyses.[66] The *ex situ* proton conductivities of **sPPN-H+** and **sPPB-H+** membranes were comparable to that of a Nafion 211 reference membrane at low humidity, and exceeded it significantly at high humidity, up to 268 and 172 mS cm^{-1}, *vs.* 113 mS cm^{-1}, respectively, at 95% RH and 80 °C.[66] The *ex situ* findings were corroborated by appreciable *in situ* fuel cell performance, wherein **sPPB-H+** membrane (33 μm) peak power densities were within 5% of that of Nafion 211 (25 μm), and **sPPN-H+** membranes (80 μm) outperformed a Nafion 212 (51 μm) reference by up to 17%. At 80 °C and 95% RH, the *in situ* membrane proton conductivies of **sPPN-H+** (261 mS cm^{-1}) and **sPPB-H+** (172 mS cm^{-1}) also reflected *ex situ* data.[66] Collectively, these findings suggest that pre-sulfonated sPPPs possessed a markedly high chemical and mechanical resilience, and demonstrated their efficacy and tunability as PEMs for electrochemical energy conversion devices, such as fuel cells.

Sterically-hindered, sulfo-phenylated polyphenylenes. A detailed investigation into structure–property relationships in sulfonated phenylated polyphenylenes was recently reported by N. Peressin *et al.*,[72] who prepared a series of sPPPs and analogous model compounds possessing either *ortho*, *meta*, or *para*-substituted biphenyl moieties (Table 5, **sPPB*o*-H$^+$**, **sPPBm-H+**, and **sPPB-H+**, respectively).[72] Each polymer possessed the same number of acidic functional groups per repeat (4) unit *via* ^{1}H NMR characterizations, but the *meta* biphenyl-containing polymer **sPPBm-H+** (2.87 meq. g^{-1}) exhibited a lower experimental IEC than that of the *para* biphenyl-containing polymer **sPPB-H+** (3.03 meq. g^{-1}). The IEC of the *ortho* biphenyl-containing polymer **sPPB*o*-H$^+$** was not reported because the polymer was surprisingly water soluble, despite possessing similar molecular weights to the former two polymers. Membranes prepared from **sPPBm-H+** exhibited lower mechanical strength and elongation at break, and higher water sorption parameters, than membranes prepared from **sPPB-H+**. This held true even when **sPPBm-H+** membranes were prepared from much higher molecular weight polymer than that of **sPPB-H+** (M_n = 656 *vs.* 83 kDa, respectively). Proton conductivity values for **sPPBm-H+** also measured lower than, or similar to that of **sPPB-H+**, due to reduced analytical acid concentration values in **sPPBm-H+** membranes.

Similar negative trends in physical and electrochemical properties were reported in copolymers possessing mixtures of *ortho* and *para*, or *meta* and *para*-substituted biphenyl moieties, when compared to **sPPB-H+**.[73] The dramatic differences in membrane characteristics with changes in polymer regiomeric connectivity from *ortho* (water soluble membranes) to *meta* (fragile) to *para* (robust) were attributed to a lack of macroscopic chain entanglement caused by sterically encumbered, rotationally-restricted polymer backbones, reinforcing the importance of chain flexibility and entanglement in PEM materials.[72,73] That is, the *para*-substituted biphenyls within the **sPPB-H+** polymer backbone afford the greatest degrees of rotational freedom, which results in enhanced chain entanglement and formation of robust, flexible membranes.

Pyridyl-containing sulfo-phenylated polyphenylenes. To further reduce membrane water uptake, swelling, and increase chemical durability, S. Xu *et al.*[69] prepared sPPPs using larger hydrophobic dienophile monomers, with or without a sterically-hindered pyridine moiety (Table 5, **sPPP(1 + 0N)** *vs.* **sPPP N-free**). In both cases water uptake and swelling values were reduced, reaching values as low as 54.4 wt% and 62.4 vol%, respectively, in the case of **sPPP(1 + 0N)**.[69] In addition, elongation at break was increased by nearly 1.5×, up to 55.5%. The experimental IEC of the pyridine-containing polymer was 1.98 meq. g^{-1}, which is much lower than the nitrogen-free reference polymer (**sPPP N-free**, 2.90 meq. g^{-1}). These findings were attributed to an acid–base interaction between the pyridine lone-pair electrons and a sulfonic acid proton, which resulted in neutralization of one of the 4 available protons per repeat unit.[69] The proposed mechanism was supported by e*x situ* proton conductivity and *in situ* fuel cell polarization data, where pyridine-containing membranes (up to 119 mS cm^{-1} and 931 mW cm^{-2}) measured 23 and 14% lower, respectively, than those of the nitrogen-free polymer (up to 155 mS cm^{-1} and 1080 mW cm^{-2}).[69] Effective proton mobility values were also ∼17% lower in **sPPP(1 + 0N)**. These differences were however less significant than expected, because the pyridine moiety incorporated was sufficiently sterically hindered such that its hydrogen bonding capabilities were limited, and the pK_a of the corresponding pyridinium conjugate acid was reduced.[69]

In terms of chemical stability, **sPPP(1 + 0N)** exhibited reduced degradation in Fenton's reagent (up to 20% less sample mass loss) and elongated lifetimes *in situ* under OCV conditions in an accelerated stress test.[69] For example, during 1000 h of operation under OCV, membranes of the pyridine-containing polymer exhibited a decline in OCV of 0.11 mV h^{-1}, which was ∼6× less than previously reported values for **sPPB-H+** (0.64 mV h^{-1}),[66,212] and ∼20× less than a Nafion 211 reference cell (2.14 mW h^{-1}).[69] Following the degradation protocol, a peak power density of 728 mW cm^{-2} is reported, which is only 21% lower than beginning-of-life performance.[69] Incorporation of a sterically-hindered pyridine hence provides exceptional chemical and mechanical reinforcement to sPPP-based membranes due to intramolecular acid–base interactions, at the cost of minor reductions to electrochemical performance.[69]

Sterically-hindered pyridine-containing sPPPs were expanded on by S. Xu *et al.*[213] through preparation of a series of polymers

containing an increasing number of pyridine rings in the dienophile monomer, and hence polymer, from 0 to 4 (Table 5, **sPPP N-free** through **sPPP(3 + 1)N**).[213] As the number of pyridine rings was increased, important polymer membrane properties including IEC, water sorption, dimensional swelling, and proton conductivity decreased.[213] These changes were ascribed to increasing degrees of intra- and inter-molecular acid–base interactions between acidic sulfonic acid protons and basic pyridine lone pair electrons within the membranes, as was previously described with **sPPP(1 + 0)N**.[69] Notably, presence of the external, non sterically-hindered pyridine ring in **sPPP(1 + 1N)** and **sPPP(3 + 1N)** resulted in a dramatic reduction in electrochemical properties such as proton conductivity.[213] For example, the proton conductivity (80 °C, 95% RH) of **sPPP(1 + 0N)** was 119 mS cm^{-1}, *versus* just 13 and 12 mS cm^{-1} in the case of **sPPP(1 + 1N)** and **sPPP(3 + 1)N**, respectively. Given the marginal difference in experimental IEC values of the membranes, 1.98 *vs.* 1.80 *vs.* 1.38 meq. g^{-1} for **sPPP(1 + 0N)**, **sPPP(1 + 1N)**, and **sPPP(3 + 1N)**, respectively, it is evident that the external pyridine ring exhibited markedly enhanced proton neutralization capabilities compared to that of the sterically-hindered pyridine rings.[213] These findings agreed with the hypotheses previously proposed regarding the limited drawbacks, in the form of strong acid–base neutralization of proton exchange membranes, in sPPPs containing sterically-hindered pyridine moieties.[69]

Copolymers of sulfo-phenylated polyphenylenes. A series of random copolymers based on the **sPPP-H+** architecture, **sPPP(*m*)-H$^+$** (Fig. 13) demonstrating synthetic tunability of physical and electrochemical properties was reported by T. Skalski *et al.*[67] The authors combined specified ratios of pre-sulfonated (*m*, TEAsBTC) and non-functionalized (*x*, bistetracyclone) diene monomers with the 1,4-diethynylbenzene dienophile comonomer to generate 6 copolymers with decreasing degrees of sulfonation, and hence increasing hydrophobicity.[67] The values measured for membrane IEC decreased from 3.50 to 1.86 meq. g^{-1} for polymers containing from 0 to 50 mol% of the non-functionalized monomer (x = 0 to 0.5) respectively. The water sorption and electrochemical properties of **sPPP(*m*)-H$^+$** membranes are strongly dependent on x. For example, as x increases from 0 to 0.5, water uptake, volumetric expansion, and *ex situ* proton conductivity decreases stepwise from 319 to 65 wt%, 364 to 68 vol%, and 120 to 5 mS cm^{-1} (at 30 °C and 95% RH), respectively.[67] However, all membranes of the **sPPP(*m*)-H$^+$** copolymers possess similar mechanical properties, which were comparable to other pre-,[66] and post-sulfonated phenylated polyphenylenes.[30] This is attributed to dominant contributions from the rigid PPP backbone.[67] No measurable changes to membrane mass or polymer chemical structure (*via* ^{1}H NMR spectroscopy) following immersion in Fenton's reagent (3% H_2O_2, 3 ppm Fe^{2+}, 80 °C, 1 h) were reported, however eventual membrane fragmentation and dissolution was noted. Membranes with reduced IEC generally exhibited a longer lifetime in Fenton's reagent, up to 6 h for those containing 50 mol% of the non-functionalized monomer (x = 0.5).[67]

The *in situ* proton conductivity of **sPPP(*m*)-H$^+$** membranes increases expectedly as a function of IEC, from 74 mS cm^{-1} (2.49 meq. g^{-1}, x = 0.4) to 256 mS cm^{-1} (3.50 meq. g^{-1}, x = 0), which compares well to a Nafion 212 membrane reference (81 mS cm^{-1}).[67] Wholly hydrocarbon fuel cells were prepared using **sPPP(*m*)-H$^+$**, which exhibited H_2 crossover currents that were only 4–15% that of a Nafion reference cell.[67] In addition, peak power densities up to 770 mW cm^{-2} were measured for **sPPP(*m*)-H$^+$** containing 20% non-sulfonated monomer (x = 0.2), which was unprecedented performance for a wholly-hydrocarbon fuel cell and compared very well to a Nafion 212 reference (792 mW cm^{-2}).[67] A lower performance was noted in polymers possessing both more (x = 0), or less (x = 0.4) of the non-functionalized monomer. The former was attributed to significant kinetic-region losses in cell performance due to swelling of the highly hydrophilic polymer as ionomer in the catalyst later, while the latter to the decrease in IEC and *ex situ* proton conductivity observed in polymers possessing larger amounts of hydrophobic monomer.[67] Hence, an important balance, or need for tunability, between high acid content and *ex situ* electrochemical properties, and reduced membrane hydrophilicity (swelling) was identified for sPPP-based PEMs.

Branched, sulfo-phenylated polyphenylenes. An alternative means of improving on sPPP membrane dimensional stability and mechanical integrity using branched polymer architectures was reported by M. Adamski *et al.*[70] A series of polymers were prepared by adding between 0.25 and 2.00 mol% of trifunctional monomer into the Diels–Alder polycondensation, which yielded polymers **sPPB(*x*% DB)-H$^+$** where x = 0, 0.25, 0.50, 1.00, or 2.00 percent degree of branching (%DB, see Fig. 14).

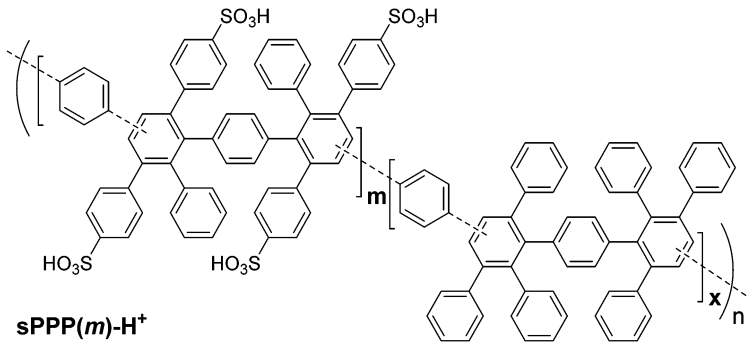

sPPP(*m*)-H$^+$

Fig. 13 Chemical structure of the **sPPP(*m*)-H$^+$** random copolymers.

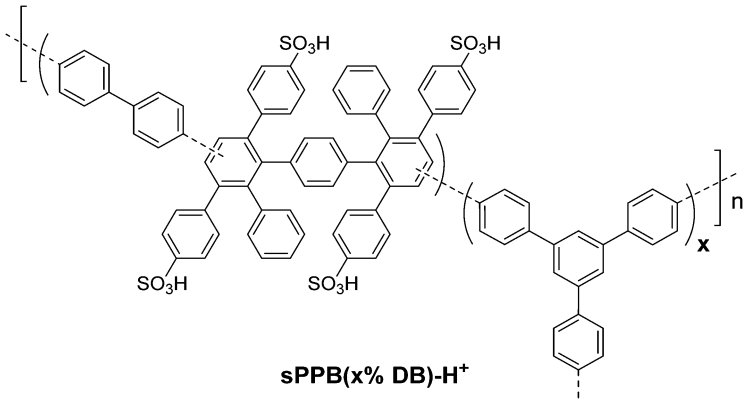

Fig. 14 Chemical structure of branched polymers **sPPB(*x*% DB)-H$^+$**.[70]

Molecular weights of polymers possessing 0 to 1.00% DB were very similar, but solution (1.25% w/w in DMSO) shear viscosities increase linearly from 16 to 93 mPa s, indicating significant changes to the overall polymeric structure. At 2.00% DB, reductions in both molecular weight and viscosity were observed, which is attributed to poor solubility of the polymer at high branching content (insoluble fractions were filtered prior to characterization).[70] Membranes prepared from **sPPB(*x*% DB)-H$^+$** showed increases in mechanical strength, and decreases in elongation at break, as a function of increasing DB in the dry state. Fully hydrated membranes, however, exhibit increases in both of these parameters, up to 14 MPa and 48%, respectively. Branching generally improves the mechanical properties of the sPPP-based polymers over the non-branched reference polymer **sPPB-H+**,[70] as well as previously reported materials possessing the same phenylated polyphenylene backbone.[30,66,67]

The ion exchange capacities of **sPPB(*x*% DB)-H$^+$** decreases stepwise with increasing DB, from 3.23 to 2.93 meq. g^{-1} for 0 to 2.00% DB, respectively, despite possessing the same theoretical and ^{1}H NMR-derived experimental IEC of 3.46 meq. g^{-1}.[70] This is attributed to the branched polymers possessing morphologies which limited the number of acid groups available for ion exchange during titration experiments. The water uptake (wt%) and volumetric swelling (vol%) of membranes upon hydration at rt decreased stepwise with increasing degree of branching, from 119 wt% and 145 vol% at 0% DB (unbranched), to 45 wt% and 61 vol% at 2.00% DB.[70] X-ray scattering experiments found that branching causes restrictions to morphological rearrangement within membranes, such as in the clustering of –SO_3H pendant groups. In addition, presence of extended polymer structures was noted. It is postulated that such structures may interfere with larger-scale entropic chain rearrangements, which would alter membrane mechanical properties.[70] Thermograms of **sPPB(*x*% DB)-H$^+$** showed an increase in backbone decomposition temperature of approx. 100 °C when any amount of branching was present, from 543 °C (unbranched, $x = 0\%$) to >640 °C (branched, $x \geq 0.25$). The oxidative stability of membranes possessing branched polymers increased stepwise with increasing DB, exhibiting lifetimes from 5.3 to 6.6 h in Fenton's reagent (3% H_2O_2, 3 ppm Fe^{2+}, 80 °C) prior to membrane fragmentation, for polymers possessing 0 to 1.00% DB, respectively.[70] The *ex situ* proton conductivity and *in situ* fuel cell performance of **sPPB(*x*% DB)-H$^+$** membranes increases as a function of DB. For example, at 95% RH and 80 °C, the unbranched polymer (0% DB, 172 mS cm^{-1}) performed 19% poorer than sPPB(1.00% DB)-H$^+$ (212 mS cm^{-1}) *ex situ*, and 14% poorer *in situ* under H_2/air (546 *vs.* 635 mW cm^{-2}, respectively). The findings reported by M. Adamski *et al.*[70] collectively show that the positive attributes of sPPPs can be synthetically improved *via* installation of branching sites within the phenylated polyphenylene architecture.

Microwave-assisted synthesis of sulfo-phenylated polyphenylenes. The synthesis of both post and pre-functionalized sulfonated phenylated polyphenylenes involves a mutual Diels–Alder polycondensation step to generate the polyphenylene backbone.[30,31,66] To obtain appreciable molecular weights, the reaction has commonly been performed in high boiling point solvents, at high temperatures (*e.g.*, 180 to 220 °C), and for prolonged durations (*e.g.*, 24 to 72 h).[30,31,66,190,192] By conducting the polycondensation using microwave (MW)-assisted synthetic techniques, an alternative method in which reaction times were reduced 24-fold was reported by M. Adamski *et al.* in 2019.[71] The inputted microwave energy was temperature-regulated using a fiber optic, such that reaction temperatures were kept constant and comparable to that of thermal experiments (180 °C). Higher temperatures (up to 220 °C) and longer reactions times (up to 5 h) generally yielded insoluble matter, which was attributed to microwave-induced thermal decomposition of the polymer.[71] Both methods gave high molecular weight polymers, however the maximum obtained using thermal techniques (M_w = 501 400 Da; $Đ$ = 2.34) was higher than that of microwave-assisted techniques (M_w = 340 900 Da; $Đ$ = 2.74).[71]

Membranes of pre-sulfonated polymers obtained *via* MW-assisted synthesis exhibit very similar properties to that of thermally-prepared reference materials.[71] The IECs (3.23 meq. g^{-1}) of each were identical, but the water uptake and swelling values of the microwave-prepared polymer were 2 and 10% higher, respectively. In addition, the microwave-prepared polymer exhibited a 6% greater tensile strength and 11% greater Young's modulus than the thermally-prepared polymer, but

also a 39% lower elongation at break.[71] Using ^{1}H NMR spectroscopy, the authors found that polymers prepared *via* MW-assisted techniques contained more *para–para* Diels–Alder linkages than those prepared thermally, which was ascribed to the observed stiffer nature of the membranes.[71] This was corroborated by X-ray scattering experiments which found that while both polymers exhibited similar spacing between ion clusters, the polymer prepared *via* MW-assisted synthesis exhibited greater ordering, potentially due to a more rigid or aligned *para* linkage-containing backbone.[71] An *ex situ* oxidative (Fenton's reagent test) and thermal (thermogravimetric analysis) stabilities, as well as *ex situ* proton conductivities and *in situ* fuel cell performance of both polymers were nearly identical.[71] Collectively, both synthetic techniques produced polymers with comparable membrane physical and electrochemical properties, which established microwave-assisted synthesis as a powerful tool for reducing the time required to sufficiently polymerize pre-sulfonated phenylated polyphenylenes 24-fold, from 3 days to 3 hours reaction time.[71] Similar findings have been reported using non-sulfonated Diels–Alder polyphenylenes, where the molecular weight of a phenylated polyphenylene obtained from a 35 h MW-assisted polymerization was higher than that of the same polymer obtained from a 480 h conventional (thermal) polymerization.[214]

Water transport through sulfo-phenylated polyphenylenes. The water transport within pre-functionalized sPPPs was investigated by Y. Wu *et al.*,[125] who used **sPPB-H+** as the model sPPP-based membrane, and compared it to membranes prepared from a highly phenylated sulfonated poly(arylene ether), **SPAE**. The experimental IEC of both polymers was 3.2 meq. g^{-1}. Vapor sorption isotherms at 70 °C showed that membrane water uptake was higher in **sPPB-H+** than in **SPAE**, which agreed with liquid water uptake measurements. These parameters were measurably higher than a Nafion 211 reference membrane, attributed to the higher IEC exhibited by the hydrocarbon polymers. The sorption isotherms were deconvoluted using the Park model to quantify specific membrane-water interactions occurring during water sorption. While **SPAE** exhibited a higher concentration, or density, of surficial hydrophilic moieties (a greater specific site capacity, a_L), **sPPB-H+** possessed an approx. 2× greater affinity constant (K_L), which indicated that the strength by which water molecules are anchored (H-bonded) to its surficial hydrophilic moieties,[215] was higher in the sulfonated phenylated polyphenylene. In contrast, Nafion 211 membranes possessed the lowest relative value for a_L, and highest K_L, because it contains fewer, but more acidic hydrophilic functional groups.[125]

The process of water penetration into, and subsequent extent of interaction with acidic groups within bulk membranes is described by Henry's law coefficient, K_H, which is dependent on IEC,[215] and was in the order Nafion 211 < **SPAE** ≈ **sPPB-H+**.[125] The extent of water cluster formation in clustering-type sorption at high relatively humidity, quantified by the aggregation equilibrium constant, K_A, was higher in **sPPB-H+** than in **SPAE**. This parameter is typically accompanied by a measure of the relative size of the water clusters within each cluster, n, which was *lower* in **sPPB-H+** than in **SPAE**. Both parameters are linked to polymer backbone structure, which dictates polymer chain mobility and morphological adaptions necessary to accommodate incoming water molecules.[215] Hence, at high relatively humidity, **sPPB-H+** exhibited greater affinity for water molecules and formed water clusters to a greater extent than the sulfonated poly(arylene ether) reference, but due to its less flexible backbone, each water cluster was smaller in size. By comparison, the values for K_A and n were highest in Nafion 211, which was attributed to its highly flexible backbone and superacidic hydrophilic functional groups.[125]

Steady-state water permeation measurements showed that **sPPB-H+** was more permeable to water than **SPAE** and Nafion 211 in both liquid–vapor and liquid–liquid permeation experiments.[125] Of the 3-types, at thicknesses > 30 μm, **sPPB-H+** membranes were most permeable to water transport due to a lower internal water transport resistance. The differences were attributed to a structure–morphology relationship, wherein **sPPB-H+** membranes possessed a more hydrophobic membrane surface than **SPAE**, but simultaneously an internal morphology more favorable for water transport. The findings coincided well with previously reported work by L. He *et al.*[201] on ultrathin post-functionalized sPPP membranes, who reported that water diffusivity was low in the early stages of exposure to water vapor (higher interfacial resistance), but increased measurably during bulk transport (low internal resistance).[201]

Morphology of sulfo-phenylated polyphenylenes. Morphological analyses of pre-sulfonated **sPPP(*m*)-H$^+$** random copolymers using small angle X-ray and neutron scattering techniques showed a specific feature, denoted ξ_1, with correlation lengths ranging from 1.53 to 1.36 nm which did not change in vacuum or under ambient conditions, but increased with the amount of non-sulfonated hydrophobic monomer present.[67] This feature was attributed to individual polymeric repeat units (Fig. 15a),[67] because the sulfonated and non-sulfonated monomers possessed different estimated X-ray scattering length densities.[216,217] In contrast, such a feature has not been reported in morphological analyses of post-functionalized sPPPs,[204] likely because the monomers are not distinct.[67] The characteristic spacing, d_2 (Fig. 15b), between a second feature in the scattering data was found to vary in length with membrane hydration and degree of sulfonation (mol% content of sulfonated monomer). At <50% RH, d_2 was approx. 2 nm in all samples, but increased to maximum of 4.30 nm for polymers with no hydrophobic segments at 100% RH. This characteristic spacing was ascribed to the size and distance between small clusters of ionic functional groups and water molecules within the polymer, and is the region which facilitates ion conductivity.[67]

M. Adamski *et al.*[71] examined morphological differences in **sPPB-H+** membranes prepared from polymers synthesized either *via* traditional thermally-mediated heating (oil baths) or microwave reactor, using X-ray scattering techniques. The scattering profiles obtained for the two materials were very similar, with three distinct features: two wide-angle peaks corresponding to interatomic length scales (<6 Å), and a small peak at 0.4 Å^{-1} corresponding to features of approximately 16 Å, which was assigned to spacing between ion-rich clusters.[67,71]

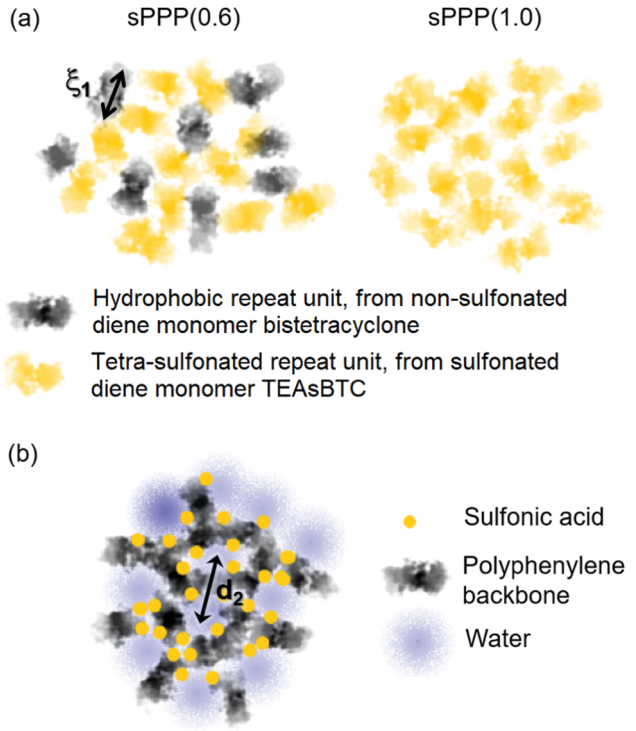

Fig. 15 Schematics representing the authors' interpretations of the origins of Features 1 and 2 from small angle X-ray and neutron scattering data. (a) Feature 1, denoted "ξ_1", was attributed to the size of a polymeric repeat unit. (b) Feature 2 was attributed to the size and spacing of the water-rich regions within the membrane samples. Reprinted from *ChemSusChem*, **11** (23), 4033–4043, T. Skalski *et al.*, "Sulfophenylated Terphenylene Copolymer Membranes and Ionomers", Copyright (2018), with permission from Wiley.[67]

The latter peak was apparently more intense in polymers prepared *via* microwave reactor. The authors attributed this observed difference to a greater number of *para–para* linkages in the microwave-prepared polymer backbones. This purportedly lead to greater ordering of the polymer once formed into membranes, resulting in greater ordering of the ion-rich regions at the 16 Å length scale.[71]

Additionally, morphological differences in **sPPB(*x*% DB)-H$^+$** with varying degrees of branching (DB) between 0 and 2 mol% were examined using X-ray scattering experiments.[70] A mid-*q* peak observed at all RH values at approximately 0.4 Å^{-1} in the unbranched polymer, previously assigned to spacing between ion-rich clusters,[67,71] was only visible at RH values $\geq$90% in the 1% DB analogue. When measured under vacuum, this mid-*q* peak was found to broaden and decrease in intensity with increased degrees of branching, becoming difficult to discern in the higher 1–2 mol% DB samples. When fully-hydrated, all samples from 0 to 2 mol% DB exhibited very similar scattering profiles with a broad feature at approximately 0.15 Å^{-1}, suggesting that surprisingly, the spacing between water and ion-rich domains in fully-hydrated samples were not affected by degree of branching. Introducing branching moieties into sulfonated phenylated polyphenylene biphenyls appears to limit the reorganizational ability of polymer chains within membranes, which was likely the main contributor to the observed reductions in their water sorption characteristics as a function of increasing degree of branching. The limited degree of chain reorganization also likely interferes with larger-scale entropic chain rearrangements, which would alter the mechanical properties of membranes, as was experimentally observed.[70]

Degradation of sulfo-phenylated polyphenylenes. The hydroxyl radical degradation pathways of sulfonated phenylated polyphenylenes were reported by T. Holmes *et al.*,[68] using a structurally-analogous oligophenylene model compound **sPP**. In the presence of hydroxyl radicals, the authors found that **sPP** degraded approx. 5× slower than a model compound based on sulfonated poly(arylene ether ketone)s, which demonstrated the chemical sensitivity of the heteroatomic linkages in the latter.[68] The reported primary degradation route of **sPP** began with oxidation of a pendant, non-sulfonated phenyl ring, which led to ring-opening and formation of a carboxylic acid substituent. This intermediate, in turn, underwent an acid-catalyzed intramolecular Friedel–Crafts acylation with a neighboring aromatic ring, yielding a fluorenone, which subsequently formed short-lived lactones *via* Baeyer–Villiger oxidation. Further oxidation resulted in opening of a second aromatic ring and formation of dicarboxylic acids, after which a core phenyl ring was destroyed to give benzoic acid, sulfobenzoic acid, and a carboxylic acid-containing degradation product.[68] The final step was equated to chain scission within the corresponding **sPPP-H+** polymer, which was demonstrated *via* both measurable reductions in polymer molecular weight, and detection of sulfobenzoic acid in the samples, following the degradation protocol. The proposed mechanism for hydroxyl radical-induced degradation of sPPPs is provided in Scheme 6.[68]

Fuel cells incorporating sulfo-phenylated polyphenylenes. Pre-functionalized sPPPs have been evaluated in hydrogen fuel cells, either as ionomer binder in the catalyst layer, or as a polymer electrolyte membrane. Preliminary examination of **sPPP-H+** (Table 5, first entry) as ionomer in the catalyst layer showed its performance was notably higher than a Nafion D520 reference ionomer at 0% RH (cathode), although the trend was reversed under humidified conditions (90% RH).[31] A series of **sPPP-H+** membranes were also evaluated, and the calculated *in situ* membrane conductivity of **sPPP-H+** was between 3× to 6× as conductive as Nafion 212 under varied RH, up to a maximum of 290 mS cm^{-1} at 90% RH. However, the membrane thickness (150 μm) employed was not preferred for long-term cell operation or complete *in situ* characterization due to excessive swelling and poor mechanical integrity.[31]

M. Adamski *et al.*[66,212] investigated the *in situ* performance of sPPPs containing elongated hydrophobic spacer units, sulfonated phenylated polyphenylene biphenyl and naphthyl (**sPPB-H+** and **sPPN-H+**, respectively, see Table 5), which exhibited improved *ex situ* membrane mechanical strength and reduced water uptake and swelling characteristics. When evaluated as membranes with Nafion D520 ionomer in the catalyst layer, **sPPB-H+** (33 μm, 1237 mW cm^{-1}) and **sPPN-H+** (80 μm, 927 mW cm^{-1}) exhibited performance curves and maximum power densities which

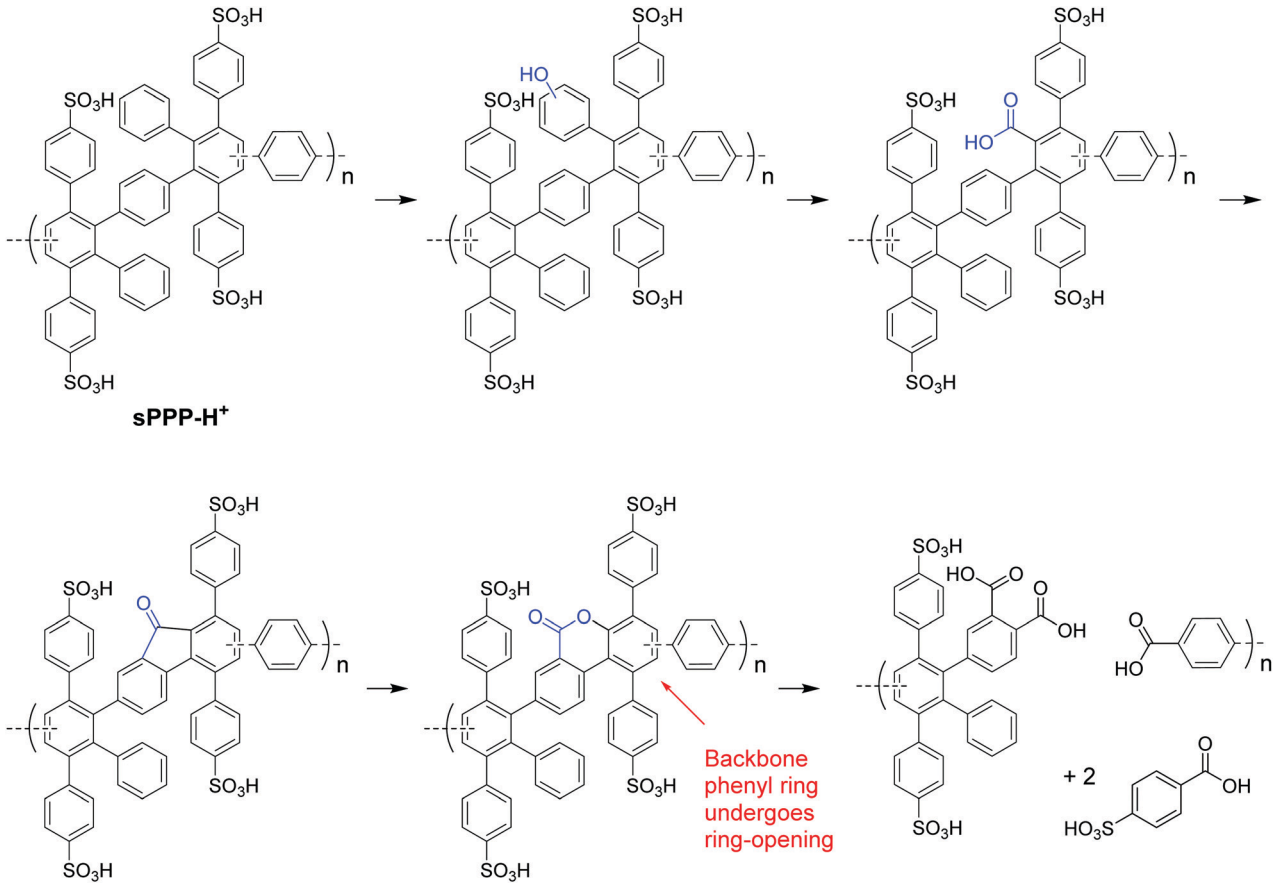

Scheme 6 The proposed mechanism for hydroxyl radical-induced degradation of sPPPs, as previously described.[68]

compared favorably to similar thickness PFSA reference membranes, Nafion 211 (25 μm, 1301 mW cm^{-1}) and Nafion 212 (51 μm, 792 mW cm^{-1}), respectively, under H_2/O_2 at 80 °C and 100% RH (Fig. 16). Similar comparisons in performance were reported for cells evaluated under H_2/air. These data represented a benchmark performance for hydrocarbon-based membranes.

In situ accelerated stress tests (AST) at open circuit voltage (OCV) for MEAs containing **sPPB-H+** membranes showed that **sPPB-H+** exhibited ~4× the lifetime of a Nafion 211 PFSA reference. After 100 h of testing, the MEA containing Nafion 211 exhibited H_2 crossover currents approaching 100 mA cm^2, and failed at 153 h. In contrast, the **sPPB-H+** MEA exhibited cell crossover currents of 12 mA cm^2 after 100 h, and continued to function and provide polarization data after the 400 h AST was complete.[66] While the *in situ* **sPPB-H+** membrane proton conductivity (117 mS cm^{-1}) decreased by 31% from beginning of life (170 mS cm^{-1}), the final value was still 21% greater than that of Nafion 211 at beginning of life (97 mS cm^{-1}). In addition, the OCV of the **sPPB-H+** cell decreased from 0.965 to 0.710 V following the AST,[66] yielding a noteworthy decay rate of 0.638 mV h^{-1}.

Random copolymers based on the **sPPP-H+** architecture, **sPPP(*m*)-H$^+$** (Fig. 13), were evaluated in fuel cells as both membrane and ionomer in the catalyst layer by T. Skalski *et al.*,[67] affording the first report of wholly-hydrocarbon fuel cells containing sulfonated phenylated polyphenylenes. MEAs from three polymers with differing hydrophilic–hydrophobic monomer ratios, and hence IECs, were evaluated: 2.49 meq. g^{-1} – sPPP(0.6)-H^+; 2.88 meq. g^{-1} – sPPP(0.8)-H^+; and 3.50 meq. g^{-1} – sPPP(1.0)-H^+. *In situ* membrane conductivities measured 74, 244, and 256 mS cm^{-1}, respectively, which reflected *ex situ* membrane conductivity, and compared favorably to that of a Nafion 212 PFSA reference which measured 81 mS cm^{-1}. Hydrogen crossover currents measured 4.3 to 15.3% of the PFSA reference cell (Table 6). In addition, *in situ* peak power densities under both H_2/O_2 and H_2/air of **sPPP(0.8)-H+** were comparable to that of Nafion 212. The performance measured for **sPPP(0.8)-H+** represented the highest reported for wholly-hydrocarbon fuel cells to date.[67]

The efficacy of sPPPs as standalone solid-state ion-conducting media in hydrogen fuel cells was further evaluated by E. Balogun *et al.*[218] The authors applied **sPPB-H+** as both a membrane, and ionomer binder in the catalyst layer, in membrane electrode assemblies which were electrochemically evaluated and compared to PFSA-based references comprised of Nafion 211 membrane and Nafion D520 ionomer.[218] The preferred loading of the hydrocarbon-based **sPPB-H+** ionomer in the catalyst layer, which yielded the highest performing MEAs, was 15 wt%.[218] This was in contrast to previously reported work on sulfonated poly(arylene ether)s which had

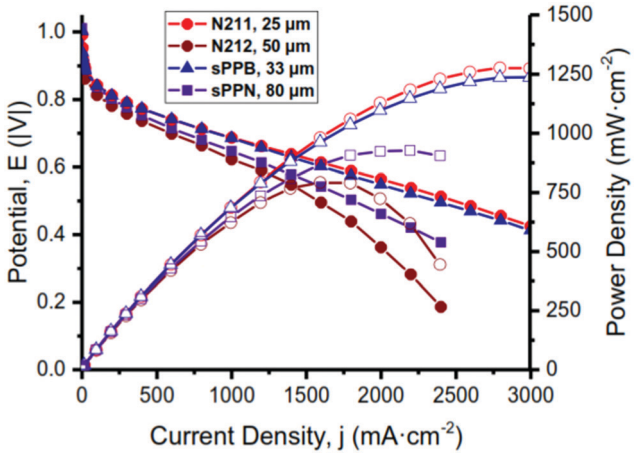

Fig. 16 Polarization (left axis, solid markers) and power density (right axis, hollow markers) curves for *in situ* fuel cell evaluation of sPPB-H$^+$, sPPN-H$^+$, Nafion 211, and Nafion 211 membranes. Catalyst layers contained Nafion D520 ionomer as binder, with 0.4 mg cm^{-2} Pt in the cathode and 0.2 mg cm^{-2} Pt in the anode. Measurement conditions were 80 °C, 100% RH, 0.5/1.0 slpm anode (H_2)/cathode (O_2) gas flows, zero backpressure. Adapted from *Angew. Chem., Int. Ed.*, **56** (31), 9058–9061, M. Adamski *et al.*, "Highly Stable, Low Gas Crossover, Proton-Conducting Phenylated Polyphenylenes", Copyright (2017), with permission from Wiley.

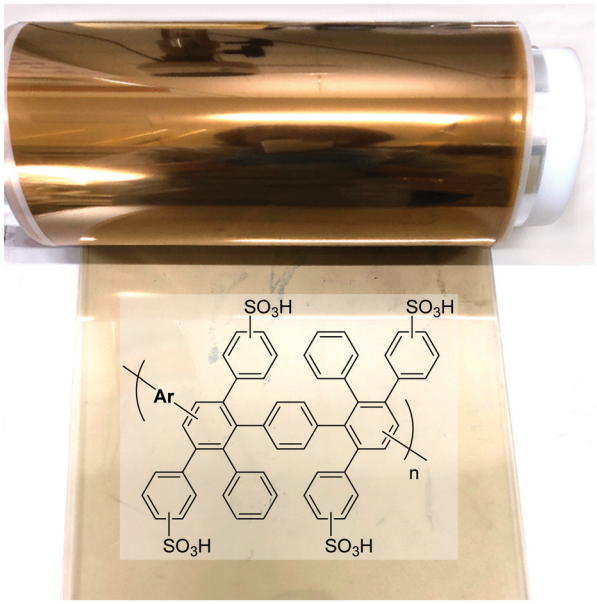

Fig. 17 Representative chemical structure and roll of PEMION®. Courtesy of Ionomr Innovations, Inc.

used 20 wt%,[219] as well as what is typically set for PFSA-based materials (30 wt%).[66,219,220] With lower, or higher **sPPB-H+** ionomer loading (*e.g.*, 10, 20, 25, 30 wt%), the authors described poorer performing cells.[218] Under both H_2/O_2 and H_2/air conditions, lower (<15 wt%) ionomer contents resulted in increased protonic resistance of the cell associated with too little proton-conducting media. Higher (>15 wt%) ionomer contents progressively increased charge transfer resistance of the cell because too much ionomer hindered reactant transfer processes in the catalyst layer. The maximum cell power densities obtained for the wholly-hydrocarbon **sPPB-H+** cells were 1100 and 677 mW cm^{-2} under H_2/O_2 and H_2/air, respectively,[218] which were the highest reported for hydrocarbon-based fuel cells to date. The cells compared well to those incorporating Nafion-based MEAs, which exhibited peak power densities of 1480 and 673 mW cm^{-2} under H_2/O_2 and H_2/air, respectively.[218]

Commercialisation of sulfo-phenylated polyphenylenes. The findings above demonstrate the viability of sulfonated phenylated polyphenylenes as strong candidates of interest for alternatives to PFSA-based materials for fuel cell applications. Indeed, Ionomr Innovations Inc., a Canadian company specializing in ion-exchange membrane and polymer solutions, has taken this a step further by upscaling synthesis of sPP-based materials and fabricating large-scale, advanced hydrocarbon membranes using roll-to-roll manufacturing (Fig. 17). According to Ionomr Innovations, Inc.,[83] hydrocarbon-based polymer membranes offer advantages over perfluorinated analogs, such as reduced cost, lower gas crossover, and fewer environmental concerns. Reduced gas crossover is a particular standout because it reduces the prevalence of hydrogen peroxide formed as a result of reactant gas crossover, and leads to a reduction in parasitic current density losses *in situ*. The properties of Ionomr's 15 μm thick reinforced hydrocarbon membrane, Pemion® PF1-HLE9-15-X,[84] are provided in Table 8 in the following section.

Table 6 Ion exchange capacity of **sPPP(*m*)-H$^+$** random copolymers and Nafion 212, as well as *in situ* fuel cell hydrogen crossover and peak power density data for MEAs fabricated therefrom[67]

Polymer	IEC (meq. g^{-1})	Film thickness (μm)	H_2 crossover (mA cm^{-2})	Peak power density (mW cm^{-2})	
				H_2/O_2	H_2/air
sPPP(0.6)-H+	2.49	56	0.41	500	244
sPPP(0.8)-H+	2.88	37	0.57	770	456
sPPP(1.0)-H+	3.50	49	0.16	418	256
Nafion 212	0.92	51	3.73	792	455

6 Summary and outlook

While care must be taken in comparing different polymers prepared by different research groups using different polymerization and functionalization approaches, cast under different conditions, and integrated into devices using different components and operated under different conditions, it is worthwhile making generalized comparisons of the various classes of sulfonated polyphenylenes to glean attributes and search for similarities, and dissimilarities. A non-exhaustive summary of synthesis methods and materials obtained therefrom for each class of sPPs is given below in Table 7. For post-sulfonated materials, the polymerization and post-sulfonation steps are split into two entries. Thereafter, we provide tabulated representative values of various membrane

Table 7 Summary of synthesis methods and polymers obtained for linear, kinked, side-chain, and phenylated sulfonated polyphenylenes (SPPs)

Category	# of monomers[a]	Other reagents	Solvent[b]	Reaction temp. (°C)	Reaction time (h)	Average yield (%)	M_n (kDa)	DP$_n$ (# of repeat units)[c]	Ref.
Linear SPPs	1–2	Cu	NMP	120–140	10–36	84	11–28	35–120	29, 38, 41 and 44
Kinked SPPs[d]	2–3	Ni(COD)$_2$[e] or NiBr$_2$/Zn with BPY[f]	DMSO or DMAc	60–80	3	94–97	8–37	14–113[g]	32, 45, 47 and 48
Side-chain SPPs[h]	1–2	NiBr$_2$/Zn[e] with PPh$_3$	DMAc	80–110	12–24	—	—	—	55, 56, 63 and 221
Sulfonation	—	ClSO$_3$H	CHCl$_3$	0 → rt	3	—	25–31[i]	96–141	
		Concentrated H$_2$SO$_4$		40–45	24	—			
Post-sulfonated phenylated PPs	2	—	Diphenyl ether	180	36	96	—	—	30, 65 and 206
Sulfonation	—	ClSO$_3$H	DCM	−50 → rt	0.5	—	55–83	65–89	
Pre-sulfonated phenylated PPs	2–3	—	Nitro-benzene	160–200	72–120	90–95	90–235	69–204	31, 66 and 69–71

[a] Does not include branched copolymers, which typically required one additional monomer (branching reagent). [b] Solvent is anhydrous (dry) unless otherwise reported. [c] Calculated from reported number-average molecular weights and the molecular weight of a single polymeric repeat unit. [d] Only membrane-forming, fluorine-free polyphenylenes are considered. [e] Catalyst(s). [f] 2,2′-Bipyridine ligand. [g] Monomer feed ratios used to approximate the molecular weight of a single polymer repeat unit. [h] Also referred to as sulfonated poly(benzophenone)s. [i] M_n is only reported in one publication,[55] with corresponding M_w values of 58–68 kDa (D = 2.10–2.34). M_w values of other polymers prepared using this methodology range from 58 to 189 kDa.[53,54,56–63]

Table 8 Overview of membrane tensile strength, elongation at break, ion exchange capacity (IEC), water uptake and swelling, *ex situ* proton conductivity (σ_{H^+}), and *in situ* fuel cell power density in linear, kinked, side-chain, and phenylated sulfonated polyphenylenes (SPPs), as well as commercially available hydrocarbon (Pemion®) and PFSA (Nafion 211) materials

Category	Tensile strength[a] (MPa)	Elongation at break[a] (%)	Experimental IEC (meq. g^{-1})	Water uptake[b] (wt%)	Swelling (vol%)	*Ex situ* σ_{H^+}[c] (mS cm^{-1})	*In situ* power density[d] (W cm^{-2}) H$_2$/O$_2$	H$_2$/air	Ref.
Linear SPPs[e]	23–54	4–9	4.3–8.3	66–213[f]	59–112[f]	400–900	—	0.43	29, 37 and 40–44
Kinked SPPs[g]	40–43[h]	11–68[h]	2.3–2.7	39–79[i]	20–27[i]	166–220	0.95	—	32 and 45–48
Side-chain SPPs	18–47[j]	5–15[j]	1.0–3.0	29–114	—	36–162	—	0.65	49–63
Post-sulfonated phenylated PPs	∼75	12	1.5–3.4	36–137	—	41–169[k]	0.90	—	30, 65 and 206
Pre-sulfonated phenylated PPs[l]	40–60	15–37	2.9–3.5	80–319	81–364	155–338	1.24	0.68[m]	31 and 66–73
Pemion®	90–100	60–90	∼3.0	110–160	<161	140	—	—	84
Nafion 211	17–28	148–311	0.95–1.01	16.6	33.3	95–110	1.48	0.67	66, 109, 218 and 222

[a] Tested at room temperature and relative humidity (19–29% RH) unless otherwise indicated. [b] Measured at room temperature in liquid water unless otherwise indicated. [c] Measured at 80 °C and 95% RH unless otherwise indicated. [d] Highest reported value utilizing a membrane comprised of the indicated polymer with PFSA ionomer (catalyst layer binder), unless otherwise indicated. [e] Includes cross-linked and alkylbenzene-grafted copolymers. [f] Measured in vapor-humidified membranes at 98% RH and room temperature. [g] Includes only membrane-forming polymers. [h] Measured at 80 °C and 60% RH. [i] Measured at 40 °C. [j] Measured at rt and 50% RH; parameters only reported in two publications.[60,61] [k] Measured at 90 °C and 90% RH. [l] Does not include nitrogen-containing variants. [m] Wholly-hydrocarbon MEA (no PFSA as ionomer/catalyst layer binder); H$_2$/O$_2$ peak power density of this system was 1.10 W cm^{-2}.[218]

physicochemical and electrochemical properties of interest, of each class of sPP described in the previous sections, in Table 8. Data represent median and maximum values reported for each class of polymer. For fine details and exhaustive data, the reader is directed to the respective original publications.

Linear sulfonated poly(*p*-phenylene)s prepared by M. Litt and coworkers,[29,40,42,43] represent one of the first comprehensively investigated derivatives of sulfonated polyphenylene-based polymer electrolytes. The reported work collectively demonstrated that this class of materials held promise in the realms of electrochemical energy applications, namely in hydrogen fuel cells. However, the rigid rod-like nature of the poly(*p*-phenylene) backbone resulted in challenges with membrane integrity, mechanical properties, and *in situ* evaluation. Poor mechanical properties may also have been due to the heterogeneous Ullman-type polymerization, whereby premature precipitation of the growing polymer chain from the reaction medium leads to low molecular weight polymers. Subsequently, M. Rikukawa *et al.*[177] demonstrated that some of the challenges associated with sulfonated poly(*p*-phenylene)s may be addressed by employing a block copolymerization approach, which helped tune polymer morphology and enhance microphase separation.[177] K. Miyatake *et al.*[32,178] further demonstrated that interrupting the linearity of sulfonated polyphenylenes can overcome poor mechanical properties by employing mixtures of *meta* and *para*-linkages in the backbone to form kinked sulfonated polyphenylenes. Subtle changes in linkages lead to materials with excellent solubility capable of forming highly flexible and tough membranes. These findings, which are in stark contrast to sulfonated poly(*p*-phenylene)s, are due to enhanced chain entanglement of the bent polymer backbone, which adopts flexible coil-like morphologies.

Side-chain sulfonated polyphenylenes prepared by M. Rikukawa *et al.*,[49,50] J. McGrath *et al.*,[51,52] and W. Kim *et al.*[53,54,56–63] based on sulfonated poly(benzophenone)s, yield materials with IEC values ranging from 1 to 3 meq. g^{-1} and varying water sorption and electrochemical characteristics for a given IEC, which demonstrates structure–property tunability in sulfonated polyphenylenes. These materials yield high *ex situ* proton conductivities which match or exceeded Nafion® references, and provide consistent beginning of life performance when assessed in hydrogen fuel cells. However, additional investigation into membrane mechanical properties, nanoscale morphology, and broader *in situ* evaluations are necessary to establish sulfonated polyphenylenes as a ubiquitous option for PEM applications. In our opinion, membranes prepared from these polymers require in-depth studies of mechanical properties, comprehensive *in situ* electrochemical characterization, and appropriate accelerated stress tests at open circuit voltage and wet-dry cycling in order to critically consider their validity in fuel cells.

Since the initial report on post-sulfonated phenylated polyphenylenes by C. Fujimoto *et al.* in 2005,[30] there has been a steadily expanding body of work on this class of polymer membrane. Collectively, post-functionalized sPPPs have been demonstrated as a unique and highly promising class of PEMs, with facile polymer synthesis and membrane preparation processes which are likely scalable and low-cost.[30,65,206] The highly rigid, rod-like polyphenylene backbone gives rise to macromolecules with limited degrees of molecular freedom resulting in formation of interesting microstructures.[126,198,203] The hydrophilic–hydrophobic phase segregated morphology integral to polymer electrolyte membranes, found in other sulfonated polyphenylene derivatives, is maintained, while important membrane characteristics such as ionic conductivity and gas barrier properties are improved.[65] Nevertheless, high connectivity of ionic domains requires relatively high degrees of sulfonation compared to incumbent PFSAs, despite studies which indicate that sulfonic acid moieties dissociate at lower levels of hydration than expected for hydrocarbon systems. The lack of specificity and control of post-sulfonation reactions hinders synthetic reproducibility, and the randomness of the sulfonation process renders polymers that swell excessively or simply dissolve at IECs typically required for desirable proton conductivity.

Introduction of the pre-sulfonated monomers into the preparation of phenylated polyphenylenes yields a marked improvement in control and properties, as evidenced by enhanced proton conductivity, both *ex situ*, and *in situ* in hydrogen fuel cells.[31] Subsequent modification of sPPPs with larger systems of non-sulfonated blocks – biphenyls,[66,72] terphenyls,[69,212] and phenyl-substituted pyridines[69] – yields materials with unprecedented *ex situ* and *in situ* membrane performance and chemical stability. The synthetic versatility of pre-sulfonated phenylated polyphenylenes opens doors to macromolecular sequence control and the introduction of macroscopic chain entanglement caused by sterically encumbered, rotationally restricted polymer backbones, molecular branching, acid–base interactions, and other controlled cross-linking strategies.[70,72,73,213] Synthetic versatility also facilitates up-scaled syntheses using traditional thermal methods, as well as microwave-assisted techniques.[71]

Of note, the synthetic versatility of pre-sulfonated phenylated polyphenylenes is being adopted by Ionomr Innovations, Inc., who have taken a step to commercialize hydrocarbon membranes based on reinforcements and roll-to-roll manufacturing. Mechanical reinforcement of ultra-thin membranes improves its resistance to tearing and stretching, which is especially important in MEA manufacturing processes. The need to reinforce is clearly understood, as demonstrated by commercially available reinforced PFSA materials such as Nafion™ and Aquivion®. In hydrocarbon PEMs, which are prone to excessive swelling, reinforcement appears essential,[223] and has been shown to dramatically improve *in situ* mechanical durability, particularly in response to wet/dry cycling, which increases *in situ* fuel cell lifetimes.[224] MEAs prepared from such reinforced hydrocarbon membranes can be operated at larger reactant gas backpressures, yielding higher fuel cell performance as well.[225] Several approaches to reinforced sulfonated hydrocarbon polymers have been reported, including the incorporation of PET composite fibers and glass fibre,[224] polysulfone fibres,[223] and mats.[225] The mechanical reinforcement of sulfonated polyphenylenes, therefore, is expected to be similarly beneficial, and a key objective in the evolution of hydrocarbon-based PEMs.

Related to mechanical durability that may be enhanced by reinforcement, is chemical durability, which is put to the test in the presence of H_2/O_2 fuel cells because the electrocatalyst promotes the formation of $H^{\bullet}$, $HO^{\bullet}$, and $HOO^{\bullet}$ radicals,[211,226–228] which are the primary sources of oxidative degradation.[20,228] In commercial fuel cells, degradation of PFSA PEMs is slowed by incorporation of Ce^{3+} ions as an antioxidant which neutralizes reactive oxidative radical species.[211,229–231] The Ce^{4+} product is re-reduced through a secondary reaction with a hydroperoxyl radical ($HOO^{\bullet}$) or with H_2O_2, regenerating Ce^{3+} ions.[229] Despite the recognized utility in PFSA-based PEMs, similar investigations with hydrocarbon-based PEMs are limited,[228,232,233] and absent with polyphenylene-based PEMs. This is particularly surprising, as the *Achille's heel* of hydrocarbon-based PEMs has traditionally been perceived to be their poor resistance to radical-induced degradation. A concern here is that, cerium cations, to remain in the membranes and be effective, must interact with sulfonate moieties tethered to the polymer backbone.[233–235] This typically leads to a reduction in proton conductivity and water sorption, due to a reduction in IEC caused by displacement of three protons per Ce^{3+} ion.[228,232,233] It also represents a site of cross-linking because Ce^{3+} can bind up to three sulfonate groups. As the ions reside in the aqueous domains and are subject to large fluxes of water, cerium cations are susceptible to migration within the membrane, and leaching.[211,229,231,232,235] Thus, future studies on the integration of antioxidants into sulfonated polyphenylenes and their initial impact on electrochemical device performance must be complemented by end-of-life studies, and the search for anti-oxidants

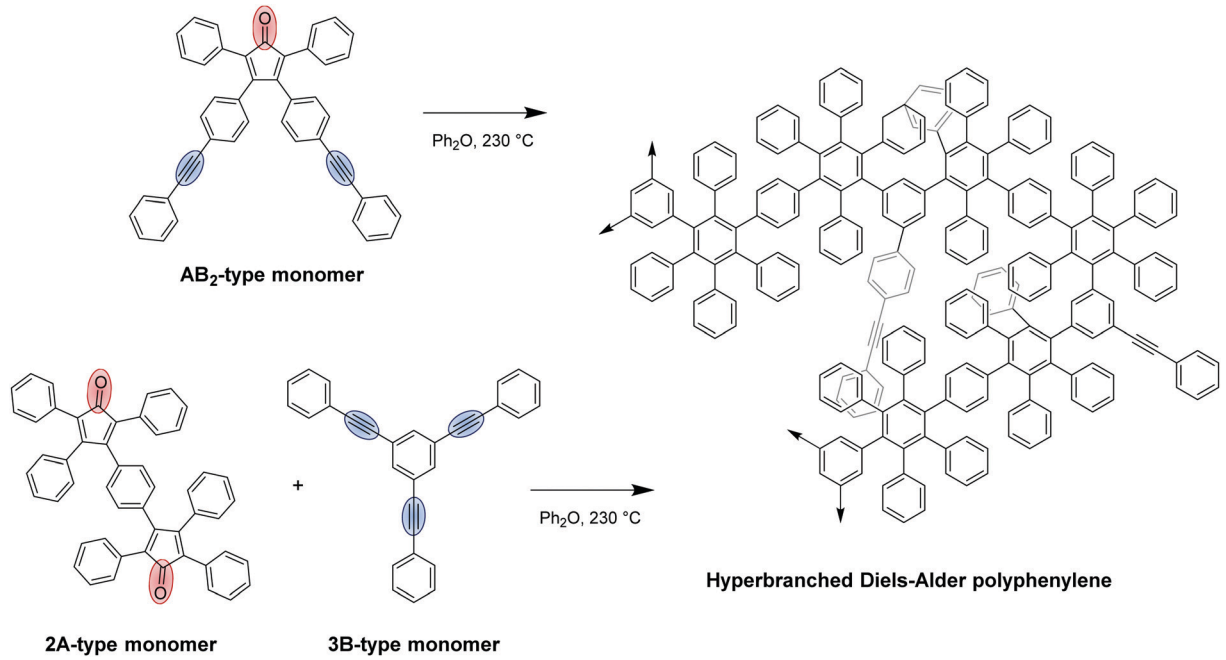

Scheme 7 Hyperbranched Diels–Alder polyphenylenes prepared from multifunctional AB_2-type, or combination of 2A and 3B-type monomers. The A and B reactive groups are highlighted in red and blue, respectively.[236,237]

with more complex architectures to mitigate their leaching over time.

Continued development of advanced molecular architectures with emphasis on polymer chain entanglement and morphologies which are advantageous to membrane water sorption parameters, such as reduced swelling, and retention of water content at in low humidity environments, is also crucial. For instance, utilization of predominantly or wholly multifunctional monomers which possess ≥ 3 reactive sites to generate more complex, highly branched or "hyperbranched" polymer architectures that begin to resemble dendrimers,[169,236] ladder-type, and nanoribbon polymers,[169,197] is a direction of interest. Recent reviews on polyphenylene nanostructures,[169] hyperbranched and highly branched polymers,[236] and the Diels–Alder polymerization for synthesis of functional and complex polymeric architectures,[197] provide valuable insight for what can be achieved from a simple phenylene or oligophenylene building block. For example, the homopolymerization of an AB_2-type oligophenylene, or the copolymerization of a 2A-type monomer with a 3B-type monomer, have generated hyperbranched Diels–Alder polyphenylenes with weight-average molecular weights exceeding 600 kDa whilst remaining soluble in common organic solvents (see Scheme 7).[236,237] T. Suda *et al.*[238] employed a similar methodology to synthesize a series of sulfonated star-hyperbranched polyimide copolymers which possessed a degree of branching of 64%. Whereas a linear analogue polymer used as reference did not form durable membranes and was not further examined, the hyperbranched material formed tough membranes due to enhanced polymer chain entanglement, which exhibited markedly low swelling (29–32 vol%, 80 °C in liquid water) and high proton conductivity (340–510 mS cm^{-1} 80 °C, 98% RH). It is only a matter of time before such strategies are employed in the development of next-generation sulfonated polyphenylenes.

Progress of sulfonated polyphenylenes to date represents a momentous step forward in development of all-encompassing alternatives to incumbent PFSAs. Exceptional chemical stability, and physical and electrochemical properties have been demonstrated in membranes cast at the academic research scale. This work exemplifies promise for hand-cast membranes in numerous electrochemical devices, from proof-of-concept to sub-commercial. However, equally important to achieving benchmark material properties, built upon synthetic scalability and reproducibility, is stable and high-throughput preparation of end-user products. Such high throughput processes turn polymer electrolyte resins into value-added products; in this case, widely applicable rolls of polymer electrolyte membrane rolls. Successful coating operations require sufficient polymer feedstock of materials with consistent properties of interest, such as molecular weight and corresponding solution viscosity. In addition, the materials must be soluble or form stable dispersions in common, low-risk solvents, such that coating solutions with high polymer content may be prepared.

7 Conclusion

The key findings presented in this work collectively demonstrate that sulfonated polyphenylenes are strong candidates for integration into PEMFCs. Important developments in the understanding of the structure–morphology–property relationships have led to better insight into the implications of building around a highly rigid, rod-like backbone such as polyphenylene. Pre-sulfonation, and generally higher acid contents on higher molecular weight polymers have been identified as important features owing to improved membrane performance. Strategies to further improve membrane properties through introduction of

elongated and more hydrophobic oligophenylene moieties, sterically hindered heterocycles, as well as branching sites, into the polymeric structure represent future steps forward to enhance membrane stability (through chain entanglement and inter-chain interactions) and electrochemical performance. Additional research is necessary to continue the advancement of sPPPs to a state comparable, or exceeding, that of state-of-the-art PFSA-based materials, with emphasis on advanced polymer architectures and morphologies, continued reduction of membrane water uptake and swelling, mechanical reinforcement, and the inclusion of anti-oxidants to improve their chemical and physical durability *in situ*.

Lastly, in the current research climate, any synthetic strategy truly considered for large scale PEM manufacture should be highly repeatable and produce polymers with predictable properties. If replacement of incumbent PFSA technologies is to be truly considered then synthetic procedures should evaluate the consequences of producing material on the 000's kg scale, where inexpensive and benign preparation and purification strategies for monomer, reagent, solvent, and catalyst are essential; and where synthetic and membrane casting processes must comply with local environmental regulations. In essence, a synthetic protocol must be competitively scalable and appropriately green.

Conflicts of interest

Steven Holdcroft is a scientific advisor to Ionomr Innovations Inc.

Acknowledgements

The authors thank: Drs Thomas Skalski, Thomas Weissbach, and Shaoyi Xu (Simon Fraser University, Chemistry), Drs Barbara Frisken and Eric Schibli (Simon Fraser University, Physics), Drs Tim Peckham, Benjamin Britton, Hsu-Feng Lee, and Mr Bill Haberlin (Ionomr Innovations, Inc.), and Drs Severin Vierrath and Matthias Breitwieser (University of Freiburg, Department of Microsystems Engineering – IMTEK) for valued discussions; Dr Simon Cassegrain for illustration of Fig. 8; and the Natural Sciences and Engineering Research Council of Canada (NSERC) and Simon Fraser University (SFU) for financial support.

References

1 M. Eikerling and A. Kulikovsky, *Polymer Electrolyte Fuel Cells: Physical Principles of Materials and Operation*, CRC Press, Inc, 2014.
2 M. Carmo, D. L. Fritz, J. Mergel and D. Stolten, A Comprehensive Review on PEM Water Electrolysis, *Int. J. Hydrogen Energy*, 2013, **38**(12), 4901–4934, DOI: 10.1016/j.ijhydene.2013.01.151.
3 K.-D. Kreuer, Ion Conducting Membranes for Fuel Cells and Other Electrochemical Devices, *Chem. Mater.*, 2013, **26**(1), 361–380, DOI: 10.1021/cm402742u.
4 T. Luo, S. Abdu and M. Wessling, Selectivity of Ion Exchange Membranes: A Review, *J. Membr. Sci.*, 2018, **555**, 429–454, DOI: 10.1016/j.memsci.2018.03.051.
5 A. Kusoglu and A. Z. Weber, New Insights into Perfluorinated Sulfonic-Acid Ionomers, *Chem. Rev.*, 2017, **117**(3), 987–1104, DOI: 10.1021/acs.chemrev.6b00159.
6 M. Zatoń, J. Rozière and D. J. Jones, Current Understanding of Chemical Degradation Mechanisms of Perfluorosulfonic Acid Membranes and Their Mitigation Strategies: A Review, *Sustainable Energy Fuels*, 2017, 409–438, DOI: 10.1039/C7SE00038C.
7 M. A. Yandrasits, M. J. Lindell and S. J. Hamrock, New Directions in Perfluoroalkyl Sulfonic Acid–Based Proton-Exchange Membranes, *Curr. Opin. Electrochem.*, 2019, **18**, 90–98, DOI: 10.1016/j.coelec.2019.10.012.
8 J. A. Kerres, Design Concepts for Aromatic Ionomers and Ionomer Membranes to Be Applied to Fuel Cells and Electrolysis, *Polym. Rev.*, 2015, **55**(2), 273–306, DOI: 10.1080/15583724.2015.1011754.
9 C. Heitner-Wirguin, Recent Advances in Perfluorinated Ionomer Membranes: Structure, Properties and Applications, *J. Membr. Sci.*, 1996, **120**(1), 1–33, DOI: 10.1109/ChiCC.2016.7553957.
10 S. J. Hamrock, A. M. Herring and T. A. Zawodzinski, in *Fuel Cell Chemistry and Operation*, ed. S. J. Hamrock, A. M. Herring and T. A. Zawodzinski, American Chemical Society, Washington, DC, 2010, DOI: 10.1016/j.jpowsour.2007.05.082.
11 A. Kraytsberg and Y. Ein-Eli, Review of Advanced Materials for Proton Exchange Membrane Fuel Cells, *Energy Fuels*, 2014, **28**(12), 7303–7330, DOI: 10.1021/ef501977k.
12 M. Yandrasits, *V.C.1. New Fuel Cell Membranes with Improved Durability and Performance*, Washington, DC., 2017.
13 S. Holdcroft, Fuel Cell Catalyst Layers: A Polymer Science Perspective, *Chem. Mater.*, 2014, **26**(1), 381–393, DOI: 10.1021/cm401445h.
14 J. Miyake and K. Miyatake, Fluorine-Free Sulfonated Aromatic Polymers as Proton Exchange Membranes, *Polym. J.*, 2017, **49**, 487–495, DOI: 10.1038/pj.2017.11.
15 D. W. Shin, M. D. Guiver and Y. M. Lee, Hydrocarbon-Based Polymer Electrolyte Membranes: Importance of Morphology on Ion Transport and Membrane Stability, *Chem. Rev.*, 2017, **117**(6), 4759–4805, DOI: 10.1021/acs.chemrev.6b00586.
16 The Chemours Company, *Nafion Ion Exchange Materials*, Fayetteville, NC, 2016.
17 O. Z. Sharaf and M. F. Orhan, An Overview of Fuel Cell Technology: Fundamentals and Applications, *Renewable Sustainable Energy Rev.*, 2014, **32**, 810–853, DOI: 10.1016/j.rser.2014.01.012.
18 S. J. Peighambardoust, S. Rowshanzamir and M. Amjadi, *Review of the Proton Exchange Membranes for Fuel Cell Applications*, Elsevier Ltd, 2010, vol. 35, DOI: 10.1016/j.ijhydene.2010.05.017.
19 H. Zhang and P. K. Shen, Recent Development of Polymer Electrolyte Membranes for Fuel Cells, *Chem. Rev.*, 2012, **112**(5), 2780–2832, DOI: 10.1021/cr200035s.

20 M. Mench, E. C. Kumbur and T. N. Veziroglu, *Polymer Electrolyte Fuel Cell Degradation*, Elsevier Inc., Amsterdam, NLD, 1st edn, 2011, DOI: 10.1016/B978-0-12-386936-4.10001-6.

21 A. B. LaConti, H. Liu, C. Mittelsteadt and R. C. McDonald, Polymer Electrolyte Membrane Degradation Mechanisms in Fuel Cells – Findings over the Past 30 Years and Comparison with Electrolyzers, *ECS Trans.*, 2006, **1**(8), 199–219, DOI: 10.1149/1.2214554.

22 J. Fang, J. Qiao, D. P. Wilkinson and J. Zhang, *Electrochemical Polymer Electrolyte Membranes*, CRC Press, Inc., Boca Raton, FL., 2015.

23 T. J. Peckham and S. Holdcroft, Structure-Morphology-Property Relationships of Non-Perfluorinated Proton-Conducting Membranes, *Adv. Mater.*, 2010, **22**(42), 4667–4690, DOI: 10.1002/adma.201001164.

24 C. H. Park, S. Y. Lee, D. S. Hwang, D. W. Shin, D. H. Cho, K. H. Lee, T. W. Kim, T. W. Kim, M. Lee, D. S. Kim, C. M. Doherty, A. W. Thornton, A. J. Hill, M. D. Guiver and Y. M. Lee, Nanocrack-Regulated Self-Humidifying Membranes, *Nature*, 2016, **532**(7600), 480–483, DOI: 10.1038/nature17634.

25 H. Hou, M. L. Di Vona and P. Knauth, Durability of Sulfonated Aromatic Polymers for Proton-Exchange-Membrane Fuel Cells, *ChemSusChem*, 2011, **4**(11), 1526–1536, DOI: 10.1002/cssc.201000415.

26 H. Pu, *Polymers for PEM Fuel Cells*, John Wiley & Sons, Hoboken, NJ, 2014, DOI: 10.1002/9781118869345.

27 S. Takamuku and P. Jannasch, Multiblock Copolymers Containing Highly Sulfonated Poly(Arylene Sulfone) Blocks for Proton Conducting Electrolyte Membranes, *Macromolecules*, 2012, **45**(16), 6538–6546, DOI: 10.1021/ma301245u.

28 E. A. Weiber, S. Takamuku and P. Jannasch, Highly Proton Conducting Electrolyte Membranes Based on Poly(Arylene Sulfone)s with Tetrasulfonated Segments, *Macromolecules*, 2013, **46**(9), 3476–3485, DOI: 10.1021/ma4002929.

29 S. Granados-focil and M. Litt, A New Class of Polyelectrolytes, Poly (Phenylene Sulfonic Acids) and Its Copolymers As Proton Exchange Membranes for PEMFC'S, *Prepr. Pap.-Am. Chem. Soc., Div. Fuel Chem.*, 2004, **49**(2), 528–529.

30 C. Fujimoto, M. Hickner, C. Cornelius and D. Loy, Ionomeric Poly (Phenylene) Prepared by Diels-Alder Polymerization: Synthesis and Physical Properties of a Novel Polyelectrolyte, *Macromolecules*, 2005, **38**(12), 5010–5016, DOI: 10.1021/ma0482720.

31 T. J. G. Skalski, B. Britton, T. J. Peckham and S. Holdcroft, Structurally-Defined, Sulfo-Phenylated, Oligophenylenes and Polyphenylenes, *J. Am. Chem. Soc.*, 2015, **137**(38), 12223–12226, DOI: 10.1021/jacs.5b07865.

32 J. Miyake, R. Taki, T. Mochizuki, R. Shimizu, R. Akiyama, M. Uchida and K. Miyatake, Design of Flexible Polyphenylene Proton-Conducting Membrane for next-Generation Fuel Cells, *Sci. Adv.*, 2017, **3**(10), eaao0476, DOI: 10.1126/sciadv.aao0476.

33 R. S. Raja Rafidah, W. Rashmi, M. Khalid, W. Y. Wong and J. Priyanka, Recent Progress in the Development of Aromatic Polymer-Based Proton Exchange Membranes for Fuel Cell Applications, *Polymers*, 2020, **12**(5), 1061–1087, DOI: 10.3390/POLYM12051061.

34 D. R. Dekel, Review of Cell Performance in Anion Exchange Membrane Fuel Cells, *J. Power Sources*, 2018, **375**, 158–169, DOI: 10.1016/j.jpowsour.2017.07.117.

35 W. You, K. J. T. Noonan and G. W. Coates, Alkaline-Stable Anion Exchange Membranes: A Review of Synthetic Approaches, *Prog. Polym. Sci.*, 2020, **100**, 101177, DOI: 10.1016/j.progpolymsci.2019.101177.

36 F. Xu, Y. Su and B. Lin, Progress of Alkaline Anion Exchange Membranes for Fuel Cells: The Effects of Micro-Phase Separation, *Front. Mater.*, 2020, **7**, 1–7, DOI: 10.3389/fmats.2020.00004.

37 S. Granados-Focil and M. H. Litt, Novel Highly Conductive Poly(Phenylene Sulfonic Acid)s and Its Evaluation as Proton Exchange Membranes for Fuel Cells, *Abstracts of Papers of the American Chemical Society*, 2003, vol. 226, p. U502.

38 S. Granados-focil, *A New Class of Polyelectrolytes, Poly (Phenylene Sulfonic Acids) and Its Copolymers As Proton Exchange Membranes for PEMFC'S*, Case Western Reserve University, 2006.

39 M. Litt, S. Granados-Focil and J. Kang, Rigid Rod Polyelectrolytes with Frozen-In Free Volume: High Conductivity at Low RH, *ACS Symp. Ser.*, 2010, **1040**, 49–63, DOI: 10.1016/B978-0-323-60984-5.00062-7.

40 M. Litt, S. Granados-Focil, J. Kang, K. Si and R. Wycisk, Rigid Rod Poly(*p*-Phenylene Sulfonic Acid) PEMs: High Conductivity At Low Relative Humidity Due To "Frozen-In-Free Volume, *ECS Trans.*, 2010, **33**(1), 695–710, DOI: 10.1149/1.3484565.

41 K. Si and M. H. Litt, Rigid Rod Poly(Phenylene Sulfonic Acid) PEMs and MEAs with Grafted and Crosslinked Biphenyl Groups: Mechanical and Electrical Properties, *ECS Trans.*, 2011, **41**(1), 1645–1656, DOI: 10.1149/1.3635696.

42 K. Si, D. Dong, R. Wycisk and M. Litt, Synthesis and Characterization of Poly(Para-Phenylene Disulfonic Acid), Its Copolymers and Their n-Alkylbenzene Grafts as Proton Exchange Membranes: High Conductivity at Low Relative Humidity, *J. Mater. Chem.*, 2012, **22**(39), 20907–20917, DOI: 10.1039/c2jm33066k.

43 K. Si, R. Wycisk, D. Dong, K. Cooper, M. Rodgers, P. Brooker, D. Slattery and M. Litt, Rigid-Rod Poly (Phenylenesulfonic Acid) Proton Exchange Membranes with Cross-Linkable Biphenyl Groups for Fuel Cell Applications, *Macromolecules*, 2013, **46**, 422–433, DOI: 10.1021/ma301875n.

44 M. Litt and R. Wycisk, Poly(Arylenesulfonic Acids) with Frozen-in Free Volume as Hydrogen Fuel Cell Membrane Materials, *Polym. Rev.*, 2015, **55**(2), 307–329, DOI: 10.1080/15583724.2015.1023955.

45 K. Shiino, J. Miyake and K. Miyatake, Highly Stable Polyphenylene Ionomer Membranes from Dichlorobiphenyls, *Chem. Commun.*, 2019, **55**, 7073–7076, DOI: 10.1039/c9cc02475a.

46 Z. Long, Y. Zhang, J. Miyake and K. Miyatake, Effect of Alkanediol Additives on the Properties of Polyphenylene-Based Proton Exchange Membranes, *Ind. Eng. Chem. Res.*, 2019, **58**(23), 9915–9920, DOI: 10.1021/acs.iecr.9b01564.

47 I. Hosaka, T. Sawano, T. Kimura, A. Matsumoto, J. Miyake and K. Miyatake, Differences in the Synthetic Method Affected Copolymer Sequence and Membrane Properties of Sulfonated Polymers, *Bull. Chem. Soc. Jpn.*, 2020, **93**, 393–398, DOI: 10.1246/bcsj.20190309.

48 K. Shiino, T. Otomo, T. Yamada, H. Arima, K. Hiroi, S. Takata, J. Miyake and K. Miyatake, Structural Investigation of Sulfonated Polyphenylene Ionomers for the Design of Better Performing Proton-Conductive Membranes, *ACS Appl. Polym. Mater.*, 2020, **2**(12), 5558–5565, DOI: 10.1021/acsapm.0c00895.

49 T. Kobayashi, M. Rikukawa, K. Sanui and N. Ogata, Proton-Conducting Polymers Derived from Poly(Ether-Etherketone) and Poly (4-Phenoxybenzoyl-1,4-Phenylene), *Solid State Ionics*, 1998, **106**, 219–225, DOI: 10.1016/S0167-2738(97)00512-2.

50 M. Rikukawa and K. Sanui, Proton-Conducting Polymer Electrolyte Membranes Based on Hydrocarbon Polymers, *Prog. Polym. Sci.*, 2000, **25**(10), 1463–1502, DOI: 10.1016/S0079-6700(00)00032-0.

51 H. Ghassemi and J. E. McGrath, Synthesis and Properties of New Sulfonated Poly(*p*-Phenylene) Derivatives for Proton Exchange Membranes. I, *Polymer*, 2004, **45**(17), 5847–5854, DOI: 10.1016/j.polymer.2004.06.021.

52 H. Ghassemi, G. Ndip and J. E. McGrath, New Multiblock Copolymers of Sulfonated Poly(4′-Phenyl-2,5- Benzophenone) and Poly(Arylene Ether Sulfone) for Proton Exchange Membranes. II, *Polymer*, 2004, 5855–5862, DOI: 10.1016/j.polymer.2004.06.009.

53 Y. Lim, D. Lee, S. Choi, S. Lee, H. Jang, S. Lee, T. Hong and W. Kim, Synthesis and Characterization of Sulfonated Polyphenylene Containing DCTPE for PEMFC Potential Application, *Int. J. Hydrogen Energy*, 2014, **39**(36), 21531–21537, DOI: 10.1016/j.ijhydene.2014.07.074.

54 Y. Lim, S. Lee, H. Jang, M. A. Hossain, T. Hong, H. Ju, T. Hong and W. Kim, Studies of Sulfonated Polyphenylene Membranes Containing Benzophenone Moiety for PEMFC, *Int. J. Hydrogen Energy*, 2014, **39**(36), 21595–21600, DOI: 10.1016/j.ijhydene.2014.06.160.

55 H. Jang, T. Hong, J. Yoo, S. Lee, J. Pyo, S. C. Sutradhar, H. Ju and W. Kim, Preparation and Characterization of Sulfonated Poly(Phenylene)s Membranes Containing Conjugated Moiety via Nickel Catalyzed Carbonecarbon Coupling Polymerization, *Int. J. Hydrogen Energy*, 2015, **40**(41), 14364–14370, DOI: 10.1016/j.ijhydene.2015.05.015.

56 H. Jang, T. Hong, J. Yoo, S. Lee, J. Ha, K. Choi, C. Lee and W. Kim, Synthesis and Characterization of Sulfonated Polyphenylene Containing Benzophenone Moiety via Nickel Catalyzed Polymerization, *Electrochim. Acta*, 2015, **177**, 161–167, DOI: 10.1016/j.electacta.2015.02.047.

57 H. Jang, T. Hong, J. Yoo, J. Pyo, J. Ha, C. Lee, K. Choi, T. Ryu, W. Kim and H. S. Jeon, The Sulfonated Poly(Phenylene) Membranes Containing Multi-Phenylrings Prepared by Nickel Catalyst, *J. Ind. Eng. Chem.*, 2016, **37**, 131–136, DOI: 10.1016/j.jiec.2016.03.016.

58 H. Jang, S. C. Sutradhar, J. Yoo, J. Ha, J. Pyo, C. Lee, T. Ryu and W. Kim, Synthesis and Characterization of Sulfonated Poly(Phenylene) Containing a Non-Planar Structure and Dibenzoyl Groups, *Energies*, 2016, **9**(2), 1–11, DOI: 10.3390/en9020115.

59 S. C. Sutradhar, H. Jang, N. Banik, J. Yoo, T. Ryu, H. Yang, S. Yoon and W. Kim, Synthesis and Characterization of Proton Exchange Poly (Phenylenebenzophenone)s Membranes Grafted with Propane Sulfonic Acid on Pendant Phenyl Groups, *Int. J. Hydrogen Energy*, 2017, **42**(17), 12749–12758, DOI: 10.1016/j.ijhydene.2016.11.054.

60 F. Ahmed, S. C. Sutradhar, T. Ryu, H. Jang, K. Choi, H. Yang, S. Yoon, M. M. Rahman and W. Kim, Comparative Study of Sulfonated Branched and Linear Poly(Phenylene)s Polymer Electrolyte Membranes for Fuel Cells, *Int. J. Hydrogen Energy*, 2018, **43**(10), 5374–5385, DOI: 10.1016/j.ijhydene.2017.08.175.

61 S. C. Sutradhar, M. Rahman, F. Ahmed, T. Ryu, J. Lei, S. Yoon, S. Lee, Y. Jin and W. Kim, Improved Proton Conductive Membranes from Poly(Phenylenebenzophenone)s with Pendant Sulfonyl Imide Acid Groups for Fuel Cells, *J. Power Sources*, 2019, **442**, 227233, DOI: 10.1016/j.jpowsour.2019.227233.

62 S. C. Sutradhar, M. M. Rahman, F. Ahmed, T. Ryu, S. Yoon, S. Lee, J. Kim, Y. Lee, Y. Jin and W. Kim, Thermally and Chemically Stable Poly(Phenylenebenzophenone) Membranes for Proton Exchange Membrane Fuel Cells by Ni (0) Catalyst, *J. Ind. Eng. Chem.*, 2019, **76**, 233–239, DOI: 10.1016/j.jiec.2019.03.045.

63 S. C. Sutradhar, M. Rahman, F. Ahmed, T. Ryu, S. Yoon, S. Lee, J. Kim, Y. Lee, Y. Jin and W. Kim, Synthesis of Nickel Catalyzed Sulfonated Poly (Phenylenebenzophenone)s from Primarily Sulfonated Monomer for Proton Exchange Membranes, *Int. J. Hydrogen Energy*, 2019, **44**(22), 11311–11320, DOI: 10.1016/j.ijhydene.2019.02.107.

64 S. M. Budy and D. A. Loy, Highly Sulfonated Polyelectrolytes through Friedel-Crafts Sulfonylation of Polyarylenes, *J. Polym. Sci., Part A: Polym. Chem.*, 2014, **52**(10), 1381–1384, DOI: 10.1002/pola.27139.

65 E. G. Sorte, B. A. Paren, C. G. Rodriguez, C. Fujimoto, C. Poirier, L. J. Abbott, N. A. Lynd, K. I. Winey, A. L. Frischknecht and T. M. Alam, Impact of Hydration and Sulfonation on the Morphology and Ionic Conductivity of Sulfonated Poly(Phenylene) Proton Exchange Membranes, *Macromolecules*, 2019, **52**(3), 857–876, DOI: 10.1021/acs.macromol.8b02013.

66 M. Adamski, T. Skalski, B. Britton, T. Peckham, L. Metzler and S. Holdcroft, Highly Stable, Low Gas Crossover, Proton-Conducting Phenylated Polyphenylenes, *Angew. Chem., Int. Ed.*, 2017, **56**(31), 9058–9061, DOI: 10.1002/anie.201703916.

67 T. Skalski, M. Adamski, B. Britton, E. Schibli, T. Peckham, T. Weissbach, T. Moshisuki, S. Lyonnard, B. J. Frisken and S. Holdcroft, Sulfo-Phenylated Terphenylene Copolymer

Membranes and Ionomers, *ChemSusChem*, 2018, **11**(23), 4033–4043, DOI: 10.1002/cssc.201801965.

68 T. Holmes, T. Skalski, M. Adamski and S. Holdcroft, On the Stability of Hydrocarbon Fuel Cell Membranes: Reaction of Hydroxyl Radicals with Sulfonated Phenylated Polyphenylenes, *Chem. Mater.*, 2019, **31**(4), 1441–1449, DOI: 10.1021/acs.chemmater.8b05302.

69 S. Xu, M. Adamski, M. Killer, E. M. Schibli, B. J. Frisken and S. Holdcroft, Sulfo-Phenylated Polyphenylenes Containing Sterically-Hindered Pyridines, *Macromolecules*, 2019, **52**(6), 2548–2559, DOI: 10.1021/acs.macromol.8b02289.

70 M. Adamski, T. Skalski, E. M. Schibli, M. Killer, Y. Wu, N. Peressin, B. J. Frisken and S. Holdcroft, Molecular Branching as a Simple Approach to Improving Polymer Electrolyte Membranes, *J. Membr. Sci.*, 2020, **595**, #117539, DOI: 10.1016/j.memsci.2019.117539.

71 M. Adamski, T. Skalski, S. Xu, M. Killer, E. M. Schibli, B. J. Frisken and S. Holdcroft, Microwave-Assisted Diels-Alder Polycondensation of Proton Conducting Poly(Phenylene)S, *Polym. Chem.*, 2019, **10**(13), 1668–1685, DOI: 10.1039/c8py01804a.

72 N. Peressin, M. Adamski, E. M. Schibli, E. Ye, B. J. Frisken and S. Holdcroft, Structure-Property Relationships in Sterically-Congested Proton-Conducting Poly(Phenylene)s: The Impact of Biphenyl Linearity, *Macromolecules*, 2020, **53**(8), 3119–3138, DOI: 10.1021/acs.macromol.0c00310.

73 N. Peressin, M. Adamski and S. Holdcroft, Effect of Steric Constraints on the Physico-Electrochemical Properties of Sulfonated Polyaromatic Copolymers, *Polym. Int.*, 2021, **70**(1), 96–106, DOI: 10.1002/pi.6097.

74 G. Goldfinger, Polyphenyl, *J. Polym. Sci.*, 1949, **4**(1), 93–96, DOI: 10.1002/pol.1949.120040110.

75 G. A. Edwards and G. Goldfinger, Polyphenyl, *J. Polym. Sci., Part A: Gen. Pap.*, 1955, **16**(82), 589–597, DOI: 10.1002/pol.1955.120168241.

76 W. Ried and K. H. Bonnighausen, Diene Syntheses with Diynes, *Chem. Ber.*, 1960, **93**, 1769–1773.

77 W. Ried and D. Freitag, Synthesis of Polyphenyl Polyphenylenes, *Naturwissenschaften*, 1966, **53**(12), 306.

78 W. Ried and D. Freitag, Oligophenyls, Oligophenylenes, and Polyphenyls, a Class of Thermally Very Stable Compounds, *Angew. Chem., Int. Ed. Engl.*, 1968, **7**(11), 835–844, DOI: 10.1002/anie.196808351.

79 J. K. Stille, Diels-Alder Polymerization, *Fortschritte Hochpolym.*, 1961, **3**(1), 48–58, DOI: 10.1007/BF02189383.

80 J. K. Stille, A Novel Diels-Alder Polymerization, *J. Polym. Sci., Part A: Gen. Pap.*, 1964, **2**(3), 1487–1491, DOI: 10.1002/pol.1964.100020342.

81 G. Noren and J. Stille, Polyphenylenes, *J. Polym. Sci. Macromol. Rev.*, 1971, **5**(1), 385–430, DOI: 10.1002/pol.1971.230050105.

82 H. F. VanKerckhoven, Y. K. Gilliams and J. K. Stille, Poly(*p*-Phenylene). The Reaction of 5,5′-*p*-Phenylenebis-2-Pyrone with *p*-Diethynylbenzene, *Macromolecules*, 1972, **5**(5), 541–546, DOI: 10.1021/ma60029a002.

83 Ionomr Innovations Inc. Our Technology: Pemion® https://ionomr.com/solutions/pemion/.

84 Ionomr Innovations Inc. Properties of Pemion® Hydrocarbon Proton Exchange Membranes. Product Information Sheet: FM-6027-A.

85 G. Gebel, Structural Evolution of Water Swollen Perfluorosulfonated Ionomers from Dry Membrane to Solution, *Polymer*, 2000, **41**(15), 5829–5838, DOI: 10.1016/S0032-3861(99)00770-3.

86 K. A. Mauritz and R. B. Moore, State of Understanding of Nafion, *Chem. Rev.*, 2004, **104**(10), 4535–4586, DOI: 10.1021/cr0207123.

87 K. D. Kreuer and G. Portale, A Critical Revision of the Nano-Morphology of Proton Conducting Ionomers and Polyelectrolytes for Fuel Cell Applications, *Adv. Funct. Mater.*, 2013, **23**(43), 5390–5397, DOI: 10.1002/adfm.201300376.

88 Q. Zhao, P. Majsztrik and J. Benziger, Diffusion and Interfacial Transport of Water in Nafion, *J. Phys. Chem. B*, 2011, **115**(12), 2717–2727, DOI: 10.1021/jp1112125.

89 G. Gebel, S. Lyonnard, H. Mendil-Jakani and A. Morin, The Kinetics of Water Sorption in Nafion Membranes: A Small-Angle Neutron Scattering Study, *J. Phys.: Condens. Matter*, 2011, 23, DOI: 10.1088/0953-8984/23/23/234107.

90 A. Kusoglu, M. A. Modestino, A. Hexemer, R. A. Segalman and A. Z. Weber, Subsecond Morphological Changes in Nafion during Water Uptake Detected by Small-Angle X-Ray Scattering, *ACS Macro Lett.*, 2012, **1**, 33–36, DOI: 10.1021/mz200015c.

91 A. Z. Weber, Gas-Crossover and Membrane-Pinhole Effects in Polymer-Electrolyte Fuel Cells, *J. Electrochem. Soc.*, 2008, **155**(6), B521, DOI: 10.1149/1.2898130.

92 A. Kusoglu, A. M. Karlsson, M. H. Santare, S. Cleghorn and W. B. Johnson, Mechanical Behavior of Fuel Cell Membranes under Humidity Cycles and Effect of Swelling Anisotropy on the Fatigue Stresses, *J. Power Sources*, 2007, **170**(2), 345–358, DOI: 10.1016/j.jpowsour.2007.03.063.

93 A. Kusoglu, S. Savagatrup, K. T. Clark and A. Z. Weber, Role of Mechanical Factors in Controlling the Structure-Function Relationship of PFSA Ionomers, *Macromolecules*, 2012, 7467–7476, DOI: 10.1021/ma301419s.

94 K. A. Page, J. W. Shin, S. A. Eastman, B. W. Rowe, S. Kim, A. Kusoglu, K. G. Yager and G. R. Stafford, *In Situ* Method for Measuring the Mechanical Properties of Nafion Thin Films during Hydration Cycles, *ACS Appl. Mater. Interfaces*, 2015, **7**(32), 17874–17883, DOI: 10.1021/acsami.5b04080.

95 J. Zhao and X. Li, A Review of Polymer Electrolyte Membrane Fuel Cell Durability for Vehicular Applications: Degradation Modes and Experimental Techniques, *Energy Convers. Manage.*, 2019, **199**, 112022, DOI: 10.1016/j.enconman.2019.112022.

96 K. D. Kreuer, On the Development of Proton Conducting Polymer Membranes for Hydrogen and Methanol Fuel Cells, *J. Membr. Sci.*, 2001, **185**(1), 29–39, DOI: 10.1016/S0376-7388(00)00632-3.

97 T. J. Peckham, J. Schmeisser, M. Rodgers and S. Holdcroft, Main-Chain, Statistically Sulfonated Proton Exchange

Membranes: The Relationships of Acid Concentration and Proton Mobility to Water Content and Their Effect upon Proton Conductivity, *J. Mater. Chem.*, 2007, **17**(30), 3255, DOI: 10.1039/b702339a.

98 T. Weissbach, E. M. W. Tsang, A. C. C. Yang, R. Narimani, B. J. Frisken and S. Holdcroft, Structural Effects on the Nano-Scale Morphology and Conductivity of Ionomer Blends, *J. Mater. Chem.*, 2012, **22**(46), 24348–24355, DOI: 10.1039/c2jm31287e.

99 Y. Yang, A. Siu, T. J. Peckham and S. Holdcroft, Structural and Morphological Features of Acid-Bearing Polymers for PEM Fuel Cells, *Fuel Cells I*, 2008, **215**, 55–126, DOI: 10.1007/12_2008_134.

100 X. Yuan and H. Wang, in *PEM Fuel Cell Electrocatalysts and Catalyst Layers: Fundamentals and Applications*, ed. Zhang, J., Springer-Verlag, London, UK, 2008.

101 Y. Tanaka, *Ion Exchange Membranes: Fundamentals and Applications*, Elsevier, Amsterdam, 2nd edn, 2015.

102 L. Gubler and G. G. Scherer, Trends for Fuel Cell Membrane Development, *Desalination*, 2010, **250**(3), 1034–1037, DOI: 10.1016/j.desal.2009.09.101.

103 K. D. Kreuer, S. J. Paddison, E. Spohr and M. Schuster, Transport in Proton Conductors for Fuel Cell Applications: Simulation, Elementary Reactions and Phenomenology, *Chem. Rev.*, 2004, **104**(10), 4637–4678, DOI: 10.1021/cr020715f.

104 N. Li and M. D. Guiver, Ion Transport by Nanochannels in Ion-Containing Aromatic Copolymers, *Macromolecules*, 2014, **47**(7), 2175–2198, DOI: 10.1021/ma402254h.

105 S. P. Fernandez Bordín, H. E. Andrada, A. C. Carreras, G. E. Castellano, R. G. Oliveira and V. M. Galván Josa, Nafion Membrane Channel Structure Studied by Small-Angle X-Ray Scattering and Monte Carlo Simulations, *Polymer*, 2018, **155**, 58–63, DOI: 10.1016/j.polymer.2018.09.014.

106 S. Shi, A. Z. Weber and A. Kusoglu, Structure/Property Relationship of Nafion XL Composite Membranes, *J. Membr. Sci.*, 2016, **516**, 123–134, DOI: 10.1016/j.memsci.2016.06.004.

107 J. S. da Silva, S. G. M. Carvalho, R. P. da Silva, A. C. Tavares, U. Schade, L. Puskar, F. C. Fonseca and B. R. Matos, SAXS Signature of the Lamellar Ordering of Ionic Domains of Perfluorinated Sulfonic-Acid Ionomers by Electric and Magnetic Field-Assisted Casting, *Phys. Chem. Chem. Phys.*, 2020, **22**(24), 13764–13779, DOI: 10.1039/d0cp01864c.

108 X. Liu, Y. Zhang, S. Deng, C. Li, J. Dong, J. Wang, Z. Yang, D. Wang and H. Cheng, Semi-Interpenetrating Polymer Networks toward Sulfonated Poly(Ether Ether Ketone) Membranes for High Concentration Direct Methanol Fuel Cell. *Chinese*, *Chem. Lett.*, 2019, **30**(2), 299–304, DOI: 10.1016/j.cclet.2018.09.021.

109 J. Peron, A. Mani, X. Zhao, D. Edwards, M. Adachi, T. Soboleva, Z. Shi, Z. Xie, T. Navessin and S. Holdcroft, Properties of Nafion NR-211 Membranes for PEMFCs, *J. Membr. Sci.*, 2010, **356**(1–2), 44–51, DOI: 10.1016/j.memsci.2010.03.025.

110 Y. Chang, G. F. Brunello, M. Hawley, Y. S. Kim, M. Disabb-miller, M. A. Hickner, S. S. Jang and C. Bae, Aromatic Ionomers with Highly Acidic Sulfonate Groups: Acidity, Hydration, and Proton Conductivity, *Macromolecules*, 2011, **44**(21), 8458–8469, DOI: 10.1021/ma201759z.

111 Y. Chang, G. F. Brunello, J. Fuller, M. Disabb-Miller, M. Hawley, Y. Kim, M. Hickner, S. Jang and C. Bae, Polymer Electrolyte Membranes Based on Poly(Arylene Ether Sulfone) with Pendant Perfluorosulfonic Acid, *Polym. Chem.*, 2013, **4**, 272–281, DOI: 10.1039/C2PY20666H.

112 S. B. Smedley, Y. Chang, C. Bae and M. A. Hickner, Measuring Water Hydrogen Bonding Distributions in Proton Exchange Membranes Using Linear Fourier Transform Infrared Spectroscopy, *Solid State Ionics*, 2015, **275**, 66–70, DOI: 10.1016/j.ssi.2015.03.020.

113 E. M. Garanin, M. S. Towers, P. W. Toothaker, K. Laali and Y. V. Tolmachev, Conductivity of Highly Sulfonated Polyphenylene Sulfide in the Powder Form as a Function of Temperature and Humidity, *Polym. Bull.*, 2010, **64**(6), 595–605, DOI: 10.1007/s00289-009-0206-0.

114 H. F. Lee, Y. C. Huang, P. H. Wang, C. C. Lee, Y. S. Hung, R. Gopal, S. Holdcroft and W. Y. Huang, Synthesis of Highly Sulfonated Polyarylene Ethers Containing Alternating Aromatic Units, *Mater. Today Commun.*, 2015, **3**, 114–121, DOI: 10.1016/j.mtcomm.2015.01.006.

115 S. Matsushita and J. D. Kim, Organic Solvent-Free Preparation of Electrolyte Membranes with High Proton Conductivity Using Aromatic Hydrocarbon Polymers and Small Cross-Linker Molecules, *Solid State Ionics*, 2018, **316**, 102–109, DOI: 10.1016/j.ssi.2017.12.033.

116 Y. A. Elabd and M. Hickner, Block Copolymers for Fuel Cells, *Macromolecules*, 2011, **44**(1), 1–11, DOI: 10.1021/ma101247c.

117 J. Y. Lee, D. M. Yu, T. H. Kim, S. J. Yoon and Y. T. Hong, Multi-Block Copolymers Based on Poly(*p*-Phenylene)s with Excellent Durability and Fuel Cell Performance, *J. Membr. Sci.*, 2015, **492**, 209–219, DOI: 10.1016/j.memsci.2015.04.013.

118 K. Oh, K. Ketpang, H. Kim and S. Shanmugam, Synthesis of Sulfonated Poly(Arylene Ether Ketone) Block Copolymers for Proton Exchange Membrane Fuel Cells, *J. Membr. Sci.*, 2016, **507**, 135–142, DOI: 10.1016/j.memsci.2016.02.027.

119 T. E. Springer, T. A. Zawodzinski and S. Gottesfeld, Polymer Electrolyte Fuel Cell Model, *J. Electrochem. Soc.*, 1991, **138**(8), 2334–2341, DOI: 10.1149/1.2085971.

120 P. von Schroeder, Über Erstarrungs- Und Qnellnngserscheinnngen von Gelatine, *J. Phys. Chem.*, 1903, **45U**(1), 75–117.

121 G. Alberti, R. Narducci and M. Sganappa, Effects of Hydrothermal/Thermal Treatments on the Water-Uptake of Nafion Membranes and Relations with Changes of Conformation, Counter-Elastic Force and Tensile Modulus of the Matrix, *J. Power Sources*, 2008, **178**(2), 575–583, DOI: 10.1016/j.jpowsour.2007.09.034.

122 V. Freger, Hydration of Ionomers and Schroeder's Paradox in Nafion, *J. Phys. Chem. B*, 2009, **113**(1), 24–36, DOI: 10.1021/jp806326a.

123 K. J. Park, A. Bin, F. Pedro and R. Brod, Sorption Isotherms Data and Mathematical Models for Pear Bartlett (Pyrus Sp.)

with and without Osmotic Dehydration, *Ciênc. Tecnol. Aliment.*, 2001, **21**(1), 73–77, DOI: 10.1590/S0101-20612001000100016.

124 V. Detallante, D. Langevin, C. Chappey, M. Métayer, R. Mercier and M. Pinéri, Water Vapor Sorption in Naphthalenic Sulfonated Polyimide Membranes, *J. Membr. Sci.*, 2001, **190**(2), 227–241, DOI: 10.1016/S0376-7388(01)00437-9.

125 Y. Wu, M. Adamski, H.-F. Lee and S. Holdcroft, Water Transport through Hydrocarbon-Based Proton Exchange Membranes, *J. Membr. Sci.*, 2020, **610**, 118276, DOI: 10.1016/j.memsci.2020.118276.

126 T. M. Alam, Computational Study of Microhydration in Sulfonated Diels-Alder Poly(Phenylene) Polymers, *J. Phys. Chem. A*, 2018, **122**(15), 3927–3938, DOI: 10.1021/acs.jpca.8b01354.

127 J. A. Clark, E. E. Santiso and A. L. Frischknecht, Morphology and Proton Diffusion in a Coarse-Grained Model of Sulfonated Poly(Phenylenes), *J. Chem. Phys.*, 2019, **151**(10), 104901, DOI: 10.1063/1.5116684.

128 C. Park, S. Lee and C. Lee, Investigation of Water Channel Formation in Sufonated Polyimides Via Mesoscale Simulation, *Membr. J.*, 2017, **27**(5), 389–398, DOI: 10.14579/membrane_journal.2017.27.5.389.

129 E. M. Schibli, J. C. Stewart, A. A. Wright, B. Chen, S. Holdcroft and B. J. Frisken, The Nanostructure of HMT-PMBI, a Sterically Hindered Ionene, *Macromolecules*, 2020, **53**(12), 4908–4916, DOI: 10.1021/acs.macromol.0c00978.

130 F. Akinori, S. Hironori and T. Takashi, Theoretical Study of High Performance Hydrocarbon-Based Ion-Exchange Membranes, *Comput. Theor. Chem.*, 2017, **1121**, 44–48, DOI: 10.1016/j.comptc.2017.10.008.

131 C. K. Mittelsteadt and J. Staser, Simultaneous Water Uptake, Diffusivity and Permeability Measurement of Perfluorinated Sulfonic Acid Polymer Electrolyte Membranes, *ECS Trans.*, 2019, **41**(1), 101–121, DOI: 10.1149/1.3635547.

132 P. M. Mangiagli, C. S. Ewing, K. Xu, Q. Wang and M. A. Hickner, Dynamic Water Uptake of Flexible Polymer Networks Ion-Containing Polymer Networks, *Fuel Cells*, 2009, **9**(4), 432–438, DOI: 10.1002/fuce.200800157.

133 A. M. Pivovar and B. S. Pivovar, Dynamic Behavior of Water within a Polymer Electrolyte Fuel Cell Membrane at Low Hydration Levels, *J. Phys. Chem. B*, 2005, **109**(2), 785–793, DOI: 10.1021/jp046029x.

134 J.-C. Perrin, S. Lyonnard and F. Volino, Quasielastic Neutron Scattering Study of Water Dynamics in Hydrated Nafion Membranes, *J. Phys. Chem. C*, 2007, **111**(8), 3393–3404, DOI: 10.1021/jp065039q.

135 D. T. Hallinan, M. G. De Angelis, M. Giacinti Baschetti, G. C. Sarti and Y. A. Elabd, Non-Fickian Diffusion of Water in Nafion, *Macromolecules*, 2010, **43**(10), 4667–4678, DOI: 10.1021/ma100047z.

136 C. He, F. Mighri, M. D. Guiver and S. Kaliaguine, Tuning Surface Hydrophilicity/Hydrophobicity of Hydrocarbon Proton Exchange Membranes (PEMs), *J. Colloid Interface Sci.*, 2016, **466**, 168–177, DOI: 10.1016/j.jcis.2015.12.023.

137 M. Adachi, *Proton Exchange Membrane Fuel Cells: Water Permeation Through Nafion Membranes*, Simon Fraser University, 2010.

138 X. Luo, *Water Permeation through Polymer Electrolyte Membranes*, Simon Fraser University, 2017.

139 L. Gubler, S. M. Dockheer and W. H. Koppenol, Radical ($HO^{\bullet}$, $H^{\bullet}$ and $HOO^{\bullet}$) Formation and Ionomer Degradation in Polymer Electrolyte Fuel Cells, *J. Electrochem. Soc.*, 2011, B755, DOI: 10.1149/1.3581040.

140 M. Inaba, T. Kinumoto, M. Kiriake, R. Umebayashi, A. Tasaka and Z. Ogumi, Gas Crossover and Membrane Degradation in Polymer Electrolyte Fuel Cells, *Electrochim. Acta*, 2006, **51**, 5746–5753, DOI: 10.1016/j.electacta.2006.03.008.

141 L. Wen and D. Zuckerbrod, *In situ* Detection of Hydrogen Peroxide in PEM Fuel Cells, *ECS Proc.*, 2004, **21**(492), A1165–A1170, DOI: 10.1149/200421.0492pv.

142 J. P. Hoare, The Electrochemistry of Oxygen, *J. Electrochem. Soc.*, 1969, **116**(8), 1168, DOI: 10.1149/1.2412261.

143 A. B. LaConti, M. Hamdan and R. C. McDonald, Mechanisms of Membrane Degradation, in *Handbook of Fuel Cells: Fundamentals, Technology and Applications*, Wiley-VCH, Weinheim, 2003, pp. 1–16.

144 R. Borup, J. Meyers, B. Pivovar, Y. S. Kim, R. Mukundan, N. Garland, D. Myers, M. Wilson, F. Garzon, D. Wood, P. Zelenay, K. More, K. Stroh, T. Zawodzinski, J. Boncella, J. E. McGrath, M. Inaba, K. Miyatake, M. Hori, K. Ota, Z. Ogumi, S. Miyata, A. Nishikata, Z. Siroma, Y. Uchimoto, K. Yasuda, K. Kimijima and N. Iwashita, Scientific Aspects of Polymer Electrolyte Fuel Cell Durability and Degradation, *Chem. Rev.*, 2007, **107**(10), 3904–3951, DOI: 10.1021/cr050182l.

145 S. M. Dockheer, L. Gubler, P. L. Bounds, A. S. Domazou, G. G. Scherer, A. Wokaun and W. H. Koppenol, Damage to Fuel Cell Membranes. Reaction of HO. With an Oligomer of Poly(Sodium Styrene Sulfonate) and Subsequent Reaction with O2, *Phys. Chem. Chem. Phys.*, 2010, **12**(37), 11609–11616, DOI: 10.1039/c0cp00082e.

146 V. O. Mittal, H. R. Kunz and J. M. Fenton, Membrane Degradation Mechanisms in PEMFCs, *J. Electrochem. Soc.*, 2007, **154**(7), B652, DOI: 10.1149/1.2734869.

147 S. Xiao, H. Zhang, X. Li and Z. Mai, Investigation of the Differences between the *in Situ* Open Circuit Voltage Test and Ex Situ Fenton Test for PEM Oxidation Characterization, *Int. J. Hydrogen Energy*, 2011, **36**(17), 10934–10939, DOI: 10.1016/j.ijhydene.2011.05.182.

148 F. Arena, J. Mitzel and R. Hempelmann, Permeability and Diffusivity Measurements on Polymer Electrolyte Membranes, *Fuel Cells*, 2013, **13**(1), 58–64, DOI: 10.1002/fuce.201200116.

149 T. Sakai, H. Takenaka and E. Torikai, Gas Diffusion in the Dried and Hydrated Nafions, *J. Electrochem. Soc.*, 1986, **133**(1), 88–92, DOI: 10.1149/1.2108551.

150 A. Parthasarathy, S. Srinivasan, A. J. Appleby and C. R. Martin, Temperature Dependence of the Electrode Kinetics of Oxygen Reduction at the Platinum/Nafion®

Interface—A Microelectrode Investigation, *J. Electrochem. Soc.*, 1992, **139**(9), 2530–2537, DOI: 10.1149/1.2221258.

151 P. D. Beattie, V. I. Basura and S. Holdcroft, Temperature and Pressure Dependence of O2 Reduction at Pt|Nafion 117 and Pt|BAM 407 Interfaces, *J. Electroanal. Chem.*, 1999, **468**(2), 180–192, DOI: 10.1016/S0022-0728(99)00164-3.

152 J. Zhang, H. A. Gasteiger and W. Gu, Electrochemical Measurement of the Oxygen Permeation Rate through Polymer Electrolyte Membranes, *J. Electrochem. Soc.*, 2013, **160**(6), F616–F622, DOI: 10.1149/2.081306jes.

153 M. Giacinti Baschetti, M. Minelli, J. Catalano and G. C. Sarti, Gas Permeation in Perflurosulfonated Membranes: Influence of Temperature and Relative Humidity, *Int. J. Hydrogen Energy*, 2013, **38**(27), 11973–11982, DOI: 10.1016/j.ijhydene.2013.06.104.

154 D. Novitski, Z. Xie and S. Holdcroft, Time-Dependent Mass Transport for O2 Reduction at the Pt | Perfluorosulfonic Acid Ionomer Interface, *ECS Electrochem. Lett.*, 2015, **4**(1), F9–F12, DOI: 10.1149/2.0051501eel.

155 U.S. Department of Energy. Fuel Cell Technologies Program Multi-Year Research, Development, and Demonstration Plan, Section 3.4. U.S. Department of Energy's (DOE's) Office of Energy Efficiency and Renewable Energy (EERE), 2017.

156 J. Wu, X. Z. Yuan, J. J. Martin, H. Wang, J. Zhang, J. Shen, S. Wu and W. Merida, A Review of PEM Fuel Cell Durability: Degradation Mechanisms and Mitigation Strategies, *J. Power Sources*, 2008, **184**(1), 104–119, DOI: 10.1016/j.jpowsour.2008.06.006.

157 B. Wahdame, D. Candusso, X. François, F. Harel, M. C. Péra, D. Hissel and J. M. Kauffmann, Comparison between Two PEM Fuel Cell Durability Tests Performed at Constant Current and under Solicitations Linked to Transport Mission Profile, *Int. J. Hydrogen Energy*, 2007, **32**(17), 4523–4536, DOI: 10.1016/j.ijhydene.2007.03.013.

158 Y. Singh, R. T. White, M. Najm, T. Haddow, V. Pan, F. P. Orfino, M. Dutta and E. Kjeang, Tracking the Evolution of Mechanical Degradation in Fuel Cell Membranes Using 4D *in Situ* Visualization, *J. Power Sources*, 2019, **412**, 224–237, DOI: 10.1016/j.jpowsour.2018.11.049.

159 C. Lim, L. Ghassemzadeh, F. Van Hove, M. Lauritzen, J. Kolodziej, G. G. Wang, S. Holdcroft and E. Kjeang, Membrane Degradation during Combined Chemical and Mechanical Accelerated Stress Testing of Polymer Electrolyte Fuel Cells, *J. Power Sources*, 2014, **257**, 102–110, DOI: 10.1016/j.jpowsour.2014.01.106.

160 A. Z. Weber and J. Newman, A Theoretical Study of Membrane Constraint in Polymer-Electrolyte Fuel Cells, *AIChE J.*, 2004, **50**(12), 3215–3226, DOI: 10.1002/aic.10230.

161 M. B. Satterfield, P. Majsztrik, H. Ota, J. B. Benziger and A. B. Bocarsly, Mechanical Properties of Nafion and Titania/Nafion Composite Membranes for Polymer Electrolyte Membrane Fuel Cells, *J. Polym. Sci., Part B: Polym. Phys.*, 2006, **44**(16), 2327–2345, DOI: 10.1002/polb.20857.

162 K. A. Page, A. Kusoglu, C. M. Stafford, S. Kim, R. J. Kline and A. Z. Weber, Confinement-Driven Increase in Ionomer Thin-Film Modulus, *Nano Lett.*, 2014, **14**(5), 2299–2304, DOI: 10.1021/nl501233g.

163 S. Banerjee and D. E. Curtin, Nafion® Perfluorinated Membranes in Fuel Cells, *J. Fluorine Chem.*, 2004, **125**(8), 1211–1216, DOI: 10.1016/j.jfluchem.2004.05.018.

164 M. Yandrasits and S. Hamrock, *Poly(Perfluorosulfonic Acid) Membranes*, Elsevier B.V., 2012, vol. 10, DOI: 10.1016/B978-0-444-53349-4.00283-1.

165 J. Rozière and D. J. Jones, Non-Fluorinated Polymer Materials for Proton Exchange Membrane Fuel Cells, *Annu. Rev. Mater. Res.*, 2003, **33**, 503–555, DOI: 10.1146/annurev.matsci.33.022702.154657.

166 T. Higashihara, K. Matsumoto and M. Ueda, Sulfonated Aromatic Hydrocarbon Polymers as Proton Exchange Membranes for Fuel Cells, *Polymer*, 2009, **50**(23), 5341–5357, DOI: 10.1016/j.polymer.2009.09.001.

167 Y. R. Luo, *Handbook of Bond Dissociation Energies in Organic Compounds*, CRC Press, Inc., Boca Raton, FL., 2002, DOI: 10.1201/9781420039863.

168 J. Walkowiak-Kulikowska, J. Wolska and H. Koroniak, Polymers Application in Proton Exchange Membranes for Fuel Cells (PEMFCs), *Phys. Sci. Rev.*, 2017, **2**(8), 1–34, DOI: 10.1515/psr-2017-0018.

169 A. J. Berresheim, M. Müller and K. Müllen, Polyphenylene Nanostructures, *Chem. Rev.*, 1999, **99**(7), 1747–1785, DOI: 10.1021/cr970073.

170 J. K. Stille, Cycloaddition Polymerization, *Makromol. Chem.*, 1972, **154**(1), 49–61, DOI: 10.1002/macp.1972.021540104.

171 M. Remmers, B. Müller, K. Martin, H.-J. Räder and W. Köhler, Poly(p-Phenylene)s. Synthesis, Optical Properties, and Quantitative Analysis with HPLC and MALDI−TOF Mass Spectrometry, *Macromolecules*, 1999, **32**(4), 1073–1079, DOI: 10.1021/ma981260s.

172 A. Abdulkarim, F. Hinkel, D. Jänsch, J. Freudenberg, F. E. Golling and K. Müllen, A New Solution to an Old Problem: Synthesis of Unsubstituted Poly(Para-Phenylene), *J. Am. Chem. Soc.*, 2016, **138**(50), 16208–16211, DOI: 10.1021/jacs.6b10254.

173 J. K. Kallitsis, M. Rehahn and G. Wegner, Synthesis of Telechelic Poly(p-Phenylene) Derivatives, *Makromol. Chem.*, 1992, **193**(4), 1021–1029, DOI: 10.1002/macp.1992.021930418.

174 J. K. Kallitsis and H. Naarmann, Synthesis of Some Disubstituted Poly(p-Terphenylenes), *Synth. Met*, 1991, **44**(3), 247–257, DOI: 10.1016/0379-6779(91)91813-P.

175 X. Zhang, T. Higashihara, M. Ueda and L.-J. Wang, Polyphenylenes and the Related Copolymer Membranes for Electrochemical Device Applications, *Polym. Chem.*, 2014, **5**, 6121–6141, DOI: 10.1039/C4PY00898G.

176 K. Umezawa, T. Oshima, M. Yoshizawa-Fujita, Y. Takeoka and M. Rikukawa, Synthesis of Hydrophilic-Hydrophobic Block Copolymer Ionomers Based on Polyphenylenes, *ACS Macro Lett.*, 2012, **1**(8), 969–972, DOI: 10.1021/mz300290x.

177 Y. Takeoka, K. Umezawa, T. Oshima, M. Yoshida, M. Yoshizawa-Fujita and M. Rikukawa, Synthesis and Properties of Hydrophilic-Hydrophobic Diblock

Copolymer Ionomers Based on Poly(p-Phenylene)S, *Polym. Chem.*, 2014, **5**(13), 4132–4140, DOI: 10.1039/c4py00082j.

178 R. Shimizu, K. Otsuji, A. Masuda, N. Sato, M. Kusakabe, A. Iiyama, K. Miyatake and M. Uchida, Durability of Newly Developed Polyphenylene-Based Ionomer Membranes in Polymer Electrolyte Fuel Cells: Accelerated Stress Evaluation, *J. Electrochem. Soc.*, 2019, **166**(7), F3105–F3110, DOI: 10.1149/2.0131907jes.

179 J. Miyake, Y. Ogawa, T. Tanaka, J. Ahn, K. Oka and K. Miyatake, Rechargeable Proton Exchange Membrane Fuel Cell Containing an Intrinsic Hydrogen Storage Polymer, *Commun. Chem.*, 2020, **3**(138), DOI: 10.1038/s42004-020-00384-z.

180 C. Le Ninivin, A. Balland-Longeau, D. Demattei, C. Coutanceau, C. Lamy and J. M. Léger, Sulfonated Derivatives of Polyparaphenylene as Proton Conducting Membranes for Direct Methanol Fuel Cell Application, *J. Appl. Electrochem.*, 2004, **34**(11), 1159–1170, DOI: 10.1007/s10800-004-1708-y.

181 S. Wu, Z. Qiu, S. Zhang, X. Yang, F. Yang and Z. Li, The Direct Synthesis of Wholly Aromatic Poly(p-Phenylene)s Bearing Sulfobenzoyl Side Groups as Proton Exchange Membranes, *Polymer*, 2006, **47**(20), 6993–7000, DOI: 10.1016/j.polymer.2006.08.017.

182 C. Le Ninivin, A. Balland-Longeau, D. Demattei, P. Palmas, J. Saillard, C. Coutanceau, C. Lamy and J. M. Léger, Determination of the Physicochemical Characteristics and Electrical Performance of Postsulfonated and Grafted Sulfonated Derivatives of Poly(Para-Phenylene) as New Proton-Conducting Membranes for Direct Methanol Fuel Cell, *J. Appl. Polym. Sci.*, 2006, **101**(2), 944–952, DOI: 10.1002/app.24022.

183 S. Seesukphronrarak, K. Ohira, K. Kidena, N. Takimoto, C. S. Kuroda and A. Ohira, Synthesis and Properties of Sulfonated Copoly(p-Phenylene)s Containing Aliphatic Alkyl Pendant for Fuel Cell Applications, *Polymer*, 2010, **51**(3), 623–631, DOI: 10.1016/j.polymer.2009.12.023.

184 Y. Lim, H. Lee, S. Lee, H. Jang, M. A. Hossain, Y. Cho, T. Kim, Y. Hong and W. Kim, Synthesis and Properties of Sulfonated Poly(Phenylene Sulfone)s without Ether Linkage by Diels-Alder Reaction for PEMFC Application, *Electrochim. Acta*, 2014, **119**, 16–23, DOI: 10.1016/j.electacta.2013.11.190.

185 T. Ryu, S. C. Sutradhar, F. Ahmed, K. Choi, H. Yang, S. Yoon, S. Lee and W. Kim, Synthesis and Characterization of Sulfonated Mutiphenyl Conjugated Polyimide for PEMFC, *J. Ind. Eng. Chem.*, 2017, **49**, 99–104, DOI: 10.1016/j.jiec.2017.01.013.

186 J. Yoo, H. Jang, S. C. Sutradhar, J. Ha, K. Choi, T. Ryu, H. Yang, S. Yoon and W. Kim, Synthesis of Sulfonated Poly(Diketonephenylene)s Containing Dibenzoyl Moiety via Ni/Zn Catalyst, *Int. J. Hydrogen Energy*, 2017, **42**(3), 1766–1775, DOI: 10.1016/j.ijhydene.2016.09.068.

187 H. Jang, T. Ryu, S. C. Sutradhar, F. Ahmed, K. Choi, H. Yang, S. Yoon and W. Kim, Studies of Sulfonated Poly(Phenylene)-Block-Poly(Ethersulfone) for Proton Exchange Membrane Fuel Cell, *Int. J. Hydrogen Energy*, 2017, **42**(17), 12768–12776, DOI: 10.1016/j.ijhydene.2017.01.112.

188 S. C. Sutradhar, F. Ahmed, T. Ryu, J. Lei, S. Yoon, I. Choi, D. Kim, Y. Jin, W. Kim and A. Bisphenol, Based Carbon-Carbon Coupled Poly(Arylene)s from Dibenzoyl-Dichlorobenzene via Ni(II) Catalyzed and Condensation Polymerization for PEMFC, *Int. J. Hydrogen Energy*, 2019, **44**(38), 21090–21100, DOI: 10.1016/j.ijhydene.2018.12.132.

189 W. Dilthey, O. Trösken, K. Plum, W. Schommmer and H. Dierichs, Eigenfarbe Und Haloehromie Einiger Tieffarbiger, *Aromatiseher Fiinfringketone*, 1933, **1934**(1), 331–349.

190 J. K. Stille, F. W. Harris, R. O. Rakutis and H. Mukamal, Diels-Alder Polymerizations: Polymers Containing Controlled Aromatic Segments, *J. Polym. Sci., Part B: Polym. Lett.*, 1966, **4**(10), 791–793, DOI: 10.1002/pol.1966.110041023.

191 Z. B. Shifrina, M. S. Averina, A. L. Rusanov, M. Wagner and K. Müllen, Branched Polyphenylenes by Repetitive Diels-Alder Cycloaddition, *Macromolecules*, 2000, **33**(10), 3525–3529, DOI: 10.1021/ma991369f.

192 H. Mukamal, F. W. Harris and J. K. Stille, Diels-Alder Polymers. III. Polymers Containing Phenylated Phenylene Units, *J. Polym. Sci., Part A-1: Polym. Chem.*, 1967, **5**(11), 2721–2729, DOI: 10.1002/pol.1967.150051101.

193 J. Stille, R. Rakutis and H. Mukamal, Harris, F. Diels-Alder Polymerizations. IV. Polymers Containing Short Phenylene Blocks Connected by Alkylene Units, *Macromolecules*, 1968, **1**(5), 431–436, DOI: 10.1021/ma60005a01210.1021/ma60025a013.

194 J. K. Stille, F. W. Harris, H. Makamal, R. O. Rakutis, C. L. Schilling, G. K. Noren and J. A. Reed, The Diels-Alder Reaction in Polymer Synthesis, *Addition and Condensation Polymerization Processes*, American Chemical Society, Washington, DC., 1969, pp. 628–642.

195 J. K. Stille and G. K. Noren, Catenation and Kinetics of the Diels-Alder Step-Growth Reaction in the Synthesis of Phenylated Polyphenylenes, *Macromolecules*, 1972, **5**(1), 49–55, DOI: 10.1021/ma60025a013.

196 H. F. VanKerckhoven, Y. K. Gilliams and J. K. Stille, Poly (p-Phenylene). The Reaction of 5,5′-p-Phenylenebis-2-Pyrone with p-Diethynylbenzene, *Macromolecules*, 1972, **5**(5), 541–546, DOI: 10.1021/ma60029a002.

197 I. C.-Y. Hou, Y. Hu, A. Narita and K. Müllen, Diels–Alder Polymerization: A Versatile Synthetic Method toward Functional Polyphenylenes, Ladder Polymers and Graphene Nanoribbons, *Polym. J.*, 2018, **50**(1), 3–20, DOI: 10.1038/pj.2017.69.

198 B. Cherry, C. Fujimoto, C. Cornelius and T. Alam, Investigation of Domain Size in Polymer Membranes Using Double-Quantum-Filtered Spin Diffusion Magic Angle Spinning NMR, *Macromolecules*, 2005, **38**(4), 1201–1206, DOI: 10.1021/ma047885.

199 F. Wang, M. Hickner, Y. Seung, T. A. Zawodzinski and J. E. Mcgrath, Direct Polymerization of Sulfonated Poly(Arylene Ether Sulfone) Random (Statistical)

Copolymers: Candidates for New Proton Exchange Membranes, *J. Membr. Sci.*, 2002, **197**, 231–242, DOI: 10.1016/S0376-7388(01)00620-2.

200 M. Hickner, C. Fujimoto and C. Cornelius, Transport in Sulfonated Poly(Phenylene)s: Proton Conductivity, Permeability, and the State of Water, *Polymer*, 2006, **47**(11), 4238–4244, DOI: 10.1016/j.polymer.2006.02.034.

201 L. He, H. L. Smith, J. Majewski, C. H. Fujimoto, C. J. Cornelius and D. Perahia, Interfacial Effects on Water Penetration into Ultrathin Ionomer Films: An *in Situ* Study Using Neutron Reflectometry, *Macromolecules*, 2009, **42**(15), 5745–5751, DOI: 10.1021/ma900973f.

202 Z. Xie, C. Song, D. P. Wilkinson and J. Zhang, Catalyst Layers and Fabrication, *Proton Exchange Membrane Fuel Cells. Materials Properties and Performance*, CRC Press, Inc., Boca Raton, FL, 2010, pp. 61–105.

203 L. He, C. J. Cornelius and D. Perahia, Water Dynamics within a Highly Rigid Sulfonated Polyphenylene, *Eur. Polym. J.*, 2014, **56**(1), 168–173, DOI: 10.1016/j.eurpolymj.2014.03.035.

204 L. He, C. Fujimoto, C. Cornelius and D. Perahia, From Solutions to Membranes: Structure Studies of Sulfonated Polyphenylene Ionomers, *Macromolecules*, 2009, **42**(18), 7084–7090, DOI: 10.1021/ma900314g.

205 N. C. Osti, T. N. Etampawala, U. M. Shrestha, D. Aryal, M. Tyagi, S. O. Diallo, E. Mamontov, C. J. Cornelius and D. Perahia, Water Dynamics in Rigid Ionomer Networks, *J. Chem. Phys.*, 2016, **145**(22), 224901, DOI: 10.1063/1.4971209.

206 R. J. Stanis, M. A. Yaklin, C. J. Cornelius, T. Takatera, A. Umemoto, A. Ambrosini and C. Fujimoto, Evaluation of Hydrogen and Methanol Fuel Cell Performance of Sulfonated Diels Alder Poly(Phenylene) Membranes, *J. Power Sources*, 2010, **195**(1), 104–110, DOI: 10.1016/j.jpowsour.2009.06.082.

207 C. James, C. Cornelius and E. Marand, The Effect of Temperature and Humidity on the Oxygen Sorption in Diels-Alder Polyphenylenes, *Polymer*, 2009, **50**(14), 3220–3224, DOI: 10.1016/j.polymer.2009.05.004.

208 L. J. Abbott and A. L. Frischknecht, Nanoscale Structure and Morphology of Sulfonated Polyphenylenes via Atomistic Simulations, *Macromolecules*, 2017, **50**(3), 1184–1192, DOI: 10.1021/acs.macromol.6b02232.

209 T. D. Largier, D. Wang, J. Mueller and C. J. Cornelius, Improving Electrodialysis Based Water Desalination Using a Sulfonated Diels–Alder Poly(Phenylene), *J. Membr. Sci.*, 2017, **531**, 103–110, DOI: 10.1016/j.memsci.2017.03.001.

210 Y. Zhang, J. Li, L. Ma, W. Cai and H. Cheng, Recent Developments on Alternative Proton Exchange Membranes: Strategies for Systematic Performance Improvement, *Energy Technol.*, 2015, **3**(7), 675–691, DOI: 10.1002/ente.201500028.

211 L. Gubler, T. Nauser, F. D. Coms, Y.-H. Lai and C. S. Gittleman, Prospects for Durable Hydrocarbon-Based Fuel Cell Membranes, *J. Electrochem. Soc.*, 2018, **165**(6), F3100–F3103, DOI: 10.1149/2.0131806jes.

212 M. Adamski, *Synthetic Design and Development of Polymers for Energy Conversion Devices*, Simon Fraser University, 2019.

213 S. Xu, W. Yang, M. Adamski, K. Fraser and S. Holdcroft, Understanding the Role of Acid-Base Interactions Using Architecturally-Controlled, Pyridyl-Bearing Sulfonated Phenylated Polyphenylenes, *J. Mater. Chem. A*, 2020, **8**(45), 23866–23883, DOI: 10.1039/D0TA08203A.

214 S. M. Budy, D. Y. Son and X. Chang, Semi-Fluorinated Polyarylenes: Microwave-Assisted Synthesis and Structure–Property Relationships, *J. Polym. Sci.*, 2020, **58**(19), 2774–2783, DOI: 10.1002/pol.20200386.

215 Y. Zheng, U. Ash, R. P. Pandey, A. G. Ozioko, J. Ponce-gonza, M. Handl, T. Weissbach, J. R. Varcoe, S. Holdcroft, M. W. Liberatore, R. Hiesgen and D. R. Dekel, Water Uptake Study of Anion Exchange Membranes, *Macromolecules*, 2018, **51**(9), 3264–3278, DOI: 10.1021/acs.macromol.8b00034.

216 Calculations Were Based on a Chemical Formula of C60S4O12H41, a Density 1.17 g Cm3 and Using the NIST SLD Calculator, https://Www.Ncnr.Nist.Gov/Resources/Activation/.

217 Calculations Were Based on a Chemical Formula of C60H41, a Density 1.06 g Cm3 and Using the NIST SLD Calculator, https://Www.Ncnr.Nist.Gov/Resources/Activation/.

218 E. Balogun, M. Adamski and S. Holdcroft, Non-Fluorous, Hydrocarbon PEMFCs, Generating >1 W Cm-2 Power, *J. Electrochem. Soc.*, 2020, **167**(8), 084502, DOI: 10.1149/1945-7111/ab88bd.

219 A. Strong, B. Britton, D. Edwards, T. J. Peckham, H.-F. Lee, W. Y. Huang and S. Holdcroft, Alcohol-Soluble, Sulfonated Poly(Arylene Ether)s: Investigation of Hydrocarbon Ionomers for Proton Exchange Membrane Fuel Cell Catalyst Layers, *J. Electrochem. Soc.*, 2015, **162**(6), F513–F518, DOI: 10.1149/2.0251506jes.

220 T. Soboleva, X. Zhao, K. Malek, Z. Xie, T. Navessin and S. Holdcroft, On the Micro-, Meso-, and Macroporous Structures of Polymer Electrolyte Membrane Fuel Cell Catalyst Layers, *ACS Appl. Mater. Interfaces*, 2010, **2**(2), 375–384, DOI: 10.1021/am900600y.

221 H. Jang, T. Hong, J. Yoo, J. Pyo, J. Ha, C. Lee, K. Choi, T. Ryu, W. Kim and H. Jeon, The Sulfonated Poly(Phenylene) Membranes Containing Multi-Phenyl Rings Prepared by Nickel Catalyst, *J. Ind. Eng. Chem.*, 2016, **37**, 131–136, DOI: 10.1016/j.jiec.2016.03.016.

222 The Chemours Company, *NR211 and NR212: Ion Exchange Materials Product Bulletin P-11*, Texas, 2019.

223 S. Jang, Y. G. Yoon, Y. S. Lee and Y. W. Choi, One-Step Fabrication and Characterization of Reinforced Microcomposite Membranes for Polymer Electrolyte Membrane Fuel Cells, *J. Membr. Sci.*, 2018, **563**, 896–902, DOI: 10.1016/j.memsci.2018.06.060.

224 J. Miyake, M. Kusakabe, A. Tsutsumida and K. Miyatake, Remarkable Reinforcement Effect in Sulfonated Aromatic Polymers as Fuel Cell Membrane, *ACS Appl. Energy Mater.*, 2018, **1**(3), 1233–1238, DOI: 10.1021/acsaem.7b00349.

225 Y. Zhao, X. Li, W. W. Li, Z. Wang, S. Wang, X. Xie and V. Ramani, A High-Performance Membrane Electrode

Assembly for Polymer Electrolyte Membrane Fuel Cell with Poly(Arylene Ether Sulfone) Nanofibers as Effective Membrane Reinforcements, *J. Power Sources*, 2019, **444**, 227250, DOI: 10.1016/j.jpowsour.2019.227250.

226 E. Endoh, Highly Durable MEA for PEMFC Under High Temperature and Low Humidity Conditions, *ECS Trans.*, 2006, **3**(1), 9–18, DOI: 10.1149/1.2356118.

227 M. Danilczuk, F. D. Coms and S. Schlick, Visualizing Chemical Reactions and Crossover Processes in a Fuel Cell Inserted in the ESR Resonator: Detection by Spin Trapping of Oxygen Radicals, Nafion-Derived Fragments, and Hydrogen and Deuterium Atoms, *J. Phys. Chem. B*, 2009, **113**(23), 8031–8042, DOI: 10.1021/jp901597f.

228 L. Gubler, T. Nolte and T. Nauser, Antioxidant Strategies for Hydrocarbon-Based Membranes, *ECS Trans.*, 2018, **86**(13), 369–379, DOI: 10.1149/08613.0369ecst.

229 F. D. Coms, H. Liu and J. E. Owejan, Mitigation of Perfluorosulfonic Acid Membrane Chemical Degradation Using Cerium and Manganese Ions, *ECS Trans.*, 2008, **16**(2), 1735–1747, DOI: 10.1149/1.2982015.

230 T. Weissbach, T. Peckham and S. Holdcroft, CeO2, ZrO2 and YSZ as Mitigating Additives against Degradation of Proton Exchange Membranes by Free Radicals, *J. Membr. Sci.*, 2016, **498**, 94–104, DOI: 10.1016/j.memsci.2015.10.004.

231 S. Schlick, in *The Chemistry of Membranes Used in Fuel Cells: Degradation and Stabilization*, ed. Schlick, S., John Wiley & Sons, Hoboken, NJ., 2018, DOI: 10.1002/9781119196082.

232 J. Park and D. Kim, Effect of Cerium/18-Crown-6-Ether Coordination Complex OH d Quencher on the Properties of Sulfonated Poly (Ether Ether Ketone) Fuel Cell Electrolyte Membranes, *J. Membr. Sci.*, 2014, **469**, 238–244, DOI: 10.1016/j.memsci.2014.06.044.

233 H. Lee, M. Han, Y. W. Choi and B. Bae, Hydrocarbon-Based Polymer Electrolyte Cerium Composite Membranes for Improved Proton Exchange Membrane Fuel Cell Durability, *J. Power Sources*, 2015, **295**, 221–227, DOI: 10.1016/j.jpowsour.2015.07.001.

234 A. M. Baker, R. Mukundan, D. Spernjak, E. J. Judge, S. G. Advani, A. K. Prasad and R. L. Borup, Cerium Migration during PEM Fuel Cell Accelerated Stress Testing, *J. Electrochem. Soc.*, 2016, **163**(9), F1023–F1031, DOI: 10.1149/2.0181609jes.

235 M. Zaton, B. Prelot, N. Donzel, J. Roziere and D. J. Jones, Migration of Ce and Mn Ions in PEMFC and Its Impact on PFSA Membrane Degradation, *J. Electrochem. Soc.*, 2018, **165**(6), F3281–F3289, DOI: 10.1149/2.0311806jes.

236 B. Voit and A. Lederer, Hyperbranched and Highly Branched Polymer Architectures—Synthetic Strategies and Major Characterization Aspects, *Chem. Rev.*, 2009, **109**(11), 5924–5973, DOI: 10.1021/cr900068q.

237 K. Stumpe, H. Komber and B. I. Voit, Novel Branched Polyphenylenes Based on A2B3 and AB2AB Monomers via Diels-Alder Cycloaddition, *Macromol. Chem. Phys.*, 2006, **207**(20), 1825–1833, DOI: 10.1002/macp.200600422.

238 T. Suda, K. Yamazaki and H. Kawakami, Syntheses of Sulfonated Star-Hyperbranched Polyimides and Their Proton Exchange Membrane Properties, *J. Power Sources*, 2010, **195**(15), 4641–4646, DOI: 10.1016/j.jpowsour.2010.02.019.